JAERI-Research
2002-035

RE-EVALUATION OF NEUTRON NUCLEAR DATA FOR ^{242m}Am, ^{243}Am, ^{99}Tc AND ^{140}Ce

December 2002

Tsuneo NAKAGAWA, Osamu IWAMOTO and Akira HASEGAWA

日本原子力研究所
Japan Atomic Energy Research Institute

本レポートは，日本原子力研究所が不定期に公刊している研究報告書です。
入手の問合わせは，日本原子力研究所研究情報部研究情報課（〒319-1195　茨城県那珂郡東海村）あて，お申し越しください。なお，このほかに財団法人原子力弘済会資料センター（〒319-1195　茨城県那珂郡東海村日本原子力研究所内）で複写による実費頒布をおこなっております。

This report is issued irregularly.
Inquiries about availability of the reports should be addressed to Research Information Division, Department of Intellectual Resources, Japan Atomic Energy Research Institute, Tokai-mura, Naka-gun, Ibaraki-ken, 319-1195, Japan.

編集兼発行　　日本原子力研究所

Re-evaluation of Neutron Nuclear Data for ^{242m}Am, ^{243}Am, ^{99}Tc and ^{140}Ce

Tsuneo NAKAGAWA, Osamu IWAMOTO and Akira HASEGAWA

Department of Nuclear Energy System
Tokai Research Establishment
Japan Atomic Energy Research Institute
Tokai-mura, Naka-gun, Ibaraki-ken

(Received November 7,2002)

The evaluated nuclear data given in JENDL-3.2 were compared with other evaluated data sets and available experimental data, for important minor actinides of ^{242m}Am and ^{243}Am, and fission product nuclides of ^{99}Tc and ^{140}Ce. Since problems were found as a result of the comparison, the data of JENDL-3.2 were improved for these nuclides. It was found that the evaluated data of Maslov et al. were superior to the others. They were adopted for ^{242m}Am and ^{243}Am after further improvements. For ^{99}Tc and ^{140}Ce, resonance parameters and optical model parameters were improved. The cross sections of these two nuclides in the smooth part were re-calculated. The present results were given in the neutron energy range from 10^{-5} eV to 20 MeV in the ENDF-6 format, and adopted to JENDL-3.3.

Keywords: Nuclear Data, Evaluation, Americium-242m, Americium-243, Technetium-99, Cerium-140, Cross Sections, Resonance Parameters, Thermal Cross Sections, JENDL-3.3

^{242m}Am、^{243}Am、^{99}Tc および ^{140}Ce に対する中性子核データの再評価

日本原子力研究所東海研究所エネルギーシステム研究部
中川 庸雄・岩本 修・長谷川 明

(2002年11月7日 受理)

重要マイナーアクチニド核種である ^{242m}Am および ^{243}Am と核分裂生成物核種 ^{99}Tc および ^{140}Ce について、JENDL-3.2 に与えられている評価済核データを最近の測定データや評価済みデータと比較・検討を行った。その結果、データの問題点を抽出し、その改善を行った。^{242m}Am と ^{243}Am については Maslov et al.による最近の評価値が優れていることがわかり、それを更に改善して再評価値とした。^{99}Tc と ^{140}Ce については、共鳴パラメータや計算に使用する光学模型パラメータの改善などを行い、連続領域の断面積も再計算し、JENDL-3.2 のデータを改善した。データは 10^{-5} eV から 20 MeV で与え、ENDF-6 フォーマットで編集した。今回の結果は、JENDL-3.3 に採用された。

東海研究所：〒319-1195 茨城県那珂郡東海村白方白根 2–4

Contents

目　　次

1. Introduction

Importance of nuclear data for minor actinides (MA) and fission product (FP) nuclides is increasing. These data are highly needed for high burn-up reactors and nuclear transmutation technology. The evaluated data for important MA and FP nuclides are already given in JENDL-3.2. New measurements for the nuclear data of those nuclides have been made recently. In the case where discrepancies are found between those experimental data and evaluated data, we have to re-evaluate their nuclear data.

In the present work, the nuclear data of ^{242m}Am, ^{243}Am, ^{99}Tc and ^{140}Ce are investigated, for which new experimental data are available. The data of JENDL-3.2 are revised on the basis of these recent experimental data. The results of the present work were adopted to JENDL-3.3.

2. Americium-242m

2.1 Summary of Evaluated Data

There are several sets of evaluated data for ^{242m}Am. In the present work, the data of JENDL-3.2, ENDF/B-VI, JEFF-3 and new evaluation made by Maslov et al. [Ma97] are compared with each other and with experimental data.

The data of JENDL-3.2 were originally evaluated by Nakagawa and Igarasi [Na80] for JENDL-2, and revised by Nakagawa [Na89] for JENDL-3.2. Those of ENDF/B-VI were evaluated by Mann and Schenter [Ma77] around 1977. JEFF-3 adopted the data of JEF-2.2 which were based on KEDAK-4. The resonance parameters of JEFF-3 were reevaluated by Fröhner around 1989. The evaluation made by Maslov et al. [Ma97] under the ISTC project is the most recent one.

After comparison of evaluated data sets, we decided that the present evaluation for ^{242m}Am should be based on the evaluation of Maslov et al. as shown in the followings.

2.2 Cross Sections in the Resonance Region

(1) Thermal Cross Sections and Resolved Resonance Parameters

JENDL-3.2 gives resonance parameters for 48 levels up to 20 eV based on the experimental data of Browne et al. [Br84]. The resolved resonance region is from 10^{-5} eV to 20 eV. ENDF/B-VI adopted the parameters of Bowman et al. [Bo68a] for 6 levels, up to 3.55 eV. JEFF-3 is the same as JENDL-3.2. Recently, Maslov et al. reevaluated the resonance parameters using the fission cross section measured by Browne et al. [Br84] and expanded the upper

boundary of the resolved resonance region up to 43 eV. Concerning the resonance formula, JENDL-3.2 and ENDF/B-VI adopted the single level Breit-Wigner formula, and JEFF-3 and Maslov et al. the multi-level Breit-Wigner formula. JEFF-3 assumed a negative resonance at −0.627 eV. Therefore, the thermal cross sections calculated from JEFF-3 are larger than other evaluations.

From the considerations mentioned above, we concluded that the parameters of Maslov et al. are superior to the others, and adopted them for the present work. Their parameters give the almost the same cross section as JENDL-3.2 below 20 eV.

Table 2.1 shows the thermal cross sections. Those of evaluated data were calculated by using their resonance parameters. Experimental data reported after 1970 are listed there for comparison. Evaluated data for the fission cross section lie in the range from 6390 to 6874 barns. The value given by Maslov et al. (JENDL-3.3) is the lowest. On the other hand, the experimental data are more widely distributed from 5850 to 6950 barns. Especially, the most recent experiment by Kai et al. [Ka01a] gives the lowest value of 5850±250 barns.

For the capture cross section, there scarcely exist experimental data. Mughabghab [Mu84] recommended 2000±600 barns based on the old experimental data of Street et al. [St52] This value seems to have large uncertainty because they measured the ^{243}Am production from ^{242m}Am in a reactor. The evaluated data are much smaller than 2000 barns except JEFF-3 which gives 1806 barns. This large cross section of JEFF-3 at the thermal energy is due to the negative resonance at −0.627 eV.

The resonance integrals are compared in Table 2.2. The fission resonance integral measured by Zhuravlev et al. [Zh75] seems to be too large. The data of Dabbs et al. [Da83] is larger than that of Browne et al. [Br84]. Since the resonance parameters of Maslov et al. were based on the fission cross section of Browne et al., Maslov et al. and JENDL-3.3 are close to the resonance integral of Browne et al.

The fission cross section in the resolved resonance region is shown in Figs. 2.1(a) and 2.1(b). The data of JENDL-3.3 is the same as that of Maslov et al. Below 20 eV, JENDL-3.2 is also almost the same. The experimental data of Dabbs et al. are systematically large. JEFF-3 is also systematically larger than other evaluated data.

Around the upper boundary of the resolved resonance region, discrepancies of the evaluated data are large because of different boundary energies. In particular, the data of ENDF/B-VI is too large above 3.55 eV.

Figure 2.2 compares the fission cross section of JENDL-3.3 with the result of TOF experiment made by Kai et al. [Ka01a] which is the most recent one among the available

experimental data. JENDL-3.3 is in good agreement with the TOF experiment. The thermal cross section of Kai et al. shown by a solid symbol is smaller than the TOF experiment and other experimental data as shown in Table 2.1.

Figures 2.3 and 2.4 are comparison of evaluated data for the capture and the total cross sections. No experimental data exist for these quantities.

(2) Unresolved Resonance Parameters

Upper boundaries of the unresolved resonance region are 30 keV for JENDL-3.2, 50 keV for JEFF-3, 10 keV for ENDF/B-VI, and 27.2832 keV for Maslov et al. The energy of 27.2832 keV is the threshold energy of the inelastic scattering to the 4-th level.

The fission cross section in the energy range from 100 eV to 100 keV is shown in Fig. 2.5. The data of Dabbs et al. [Da83] and Bowman et al. [Ba68a] are systematically larger than the data of Browne et al. [Br84] Gerasimov et al. [Ge87] reported also large cross sections in this energy region which are in good agreement with ENDF/B-VI. However, we adopted the parameters of Maslov et al. which were consistent with the data of the resolved resonance region. The cross section of JENDL-3.3 is almost the same as JENDL-3.2 in this energy region.

The fission cross section was measured by Kai et al. [Ka01a] using Kyoto University Lead slowing-down Spectrometer (KULS). Their results are compared with the evaluated data in Fig. 2.6. The evaluated data are broadened with the same energy resolution as KULS. ENDF/B-VI above 3 eV is too large. Other evaluated data are sufficiently consistent with the measured values. This fact confirms that the evaluated data except ENDF/B-VI have no large problems below 10 keV except for around 10 eV.

2.3 Cross Sections above the Resonance Region

(1) Fission Cross Section

The fission cross section in the energy range from 100 keV to 20 MeV is shown in Fig. 2.7. ENDF/B-VI was based on the experimental data of Bowman et al. [Bo68a], but not in good agreement with recent experimental data. Evaluated data of Maslov et al. were calculated with the statistical model (the STAT code). This calculation reproduces the experimental data well, but not perfectly.

Above 27.2832 keV, JENDL-3.2 was adopted in the present work. to JENDL-3.3 since the data of JENDL-3.2 reproduce well the experimental data of Browne et al. and consistent with the most recent data of Fursov et al. [Fu94].

(2) Capture Cross Section

Figure 2.8 shows evaluated data of the capture cross section in the energy region from 10 keV to 20 MeV. No experimental data are available in this energy region. Maslov et al.'s evaluation which was based on the statistical model was adopted in the present work for JENDL-3.3. In the MeV region, the capture cross section of Maslov et al. was replaced with the direct and semi-direct capture cross section calculated with the DSD code developed by Kawano [Ka99].

(3) Inelastic Scattering Cross Section

The data of Maslov et al. was adopted in the present work. The evaluated data of the total inelastic scattering cross section are compared with each other in Fig. 2.9. The data of ENDF/B-VI is too small. The others exhibit almost the same tendency.

(4) (n,2n) and (n,3n) Reaction Cross Sections

The (n,2n) and (n,3n) reaction cross sections are shown in Fig. 2.10. Maslov's evaluation was adopted in the present work.

(5) Other Cross Sections and Comparison in the Whole Energy Region

Figures 2.11 and 2.12 show the total cross section and elastic scattering cross section above 100 keV, respectively.

Comparisons of total, elastic scattering, fission and capture cross sections are shown in Figs. 2.13 to 2.16. The cross sections in the resolved resonance region are averaged in suitable energy intervals. The evaluated data of total cross section show almost the same tendency except the data of ENDF/B-VI. The elastic scattering cross section of JEFF-3 has a tendency different from others. The difference in the resonance region is due to the negative resonance at −0.627 eV. Because of this resonance, JEFF-3 gives about 1000 barn larger cross section at 0.0253 eV than others.

2.4 Number of Prompt and Delayed Neutrons per Fission

Evaluated data for the number of prompt neutrons per fission (ν_p) are compared with experimental data of Jaffy and Lerner [Ja70], Kroshkin and Zamyatnin [Kr70], Howe et al. [Ho81], and Howe et al. [Ho83] Howe et al. [Ho81] measured total ν. The measurements of Howe et al.[Ho81, Ho83] were performed relatively to ν_p of ^{235}U. They were converted to the

data of ^{242m}Am using the ^{235}U data of JENDL-3.3. Figure 2.17 shows those data together with evaluated data.

The data of JENDL-3.2 are almost the same as ENDF/B-VI. JEFF-3 is the same as ENDF/B-VI. Maslov's evaluation was made on the basis of the data of Howe et al.[Ho81] and calculation with Madland-Nix model. In the present work, the data of Maslov et al. were adopted.

Evaluated data for the number of delayed neutrons per fission (ν_d) are shown in Fig. 2.18. Maslov et al. adopted the summation calculation by Brady and England [Br89]. The present work adopted JENDL-3.2 after changing the connection energies between the low energy part and the high energy one.

2.5 Other Data

(1) Angular distributions

The data of Maslov et al. were adopted.

(2) Energy distributions

For delayed neutron spectra from the fission, the calculation made by Brady and England [Br89] was adopted.

For the others, Maslov's evaluation was adopted. The interpolation method was changed to "unit-base interpolation" for the (n,2n), (n,3n) and inelastic scattering neutrons.

Figures 2.19 to 2.21 show the neutron spectra from the (n,2n), (n,3n) and inelastic scattering, respectively. Each line in the figures corresponds to a different incident energy. For comparison, the data of JENDL-3.2, ENDF/B-VI and JEFF-3 were shown in the second, third and forth figures, respectively. Since Maslov's evaluation considered the preequilibrium process, the shape of distributions is largely different from the other evaluations.

Figure 2.22 shows the fission neutron spectra in the same manner. Only one line is shown for JENDL-3.2 and JEFF-3 because they give an energy independent nuclear temperature for Maxwellian-type spectra. Maslov et al. considered multi-chance fission. Structure found in JENDL-3.3 comes from the multi-chance fission. The delayed neutron spectra are shown in Fig.2.23. The data of ENDF/B-VI and JEFF-3 are the same as JENDL-3.3.

3. Americium-243

3.1 Summary of Evaluated Data

The data of JENDL-3.2 were first evaluated by Kikuchi [Ki82] for JENDL-2, and partly revised by Nakagawa [Na89] for JENDL-3.2. The revised quantities at the last revision were the resolved resonance parameters and fission, capture and inelastic scattering cross sections.

According to the description given in the file, the data of UKNDL-2 were adopted for JEFF-3, and slightly revised. Therefore, they are relatively old data than other evaluations.

ENDF/B-VI evaluation was made in 1988 for the resonance parameters, and in 1996 for the data above 42 keV.

Maslov et al. [Ma96] made a new evaluation under the ISTC project. Their evaluation was based on the recent sophisticated evaluation method. In the present work, their evaluation was adopted after suitable modifications.

3.2 Cross Sections in the Resonance Region

(1) Thermal cross sections and resonance integrals

The cross-section data at 0.0253 eV are listed in Table 3.1. The rather old experimental data for the fission cross section are about 0.2 b. However much smaller values of about 0.08 b were reported by Wagemans et al. [Wa89] and Kobayashi et al. [Ko99] The present work adopted the data of Kobayashi et al. The other evaluations give smaller values than the experimental data.

For the capture cross section, no recent experimental data are available. The evaluated data are around the average value of Bak et al. [Ba67] and Gavrilov et al. [Ga76] The present work gives the smaller cross section than JENDL-3.2 because the resolved resonance parameters of Maslov's evaluation were adopted as described later.

Concerning the total cross section, there are two experimental data [Co59a, Be70]. All the evaluated data are in good agreement with the data of Berreth and Simpson [Be70].

Table 3.2 shows the resonance integrals. For the fission cross section, calculated values from the evaluated data are in the range from 6.4 to 7.6 b. On the other hand, experimental data are scattered largely from 3 to 17 b. The data of Knitter and Budtz-Jørgensen [Kn88] was measured in the energy range from 0.5 eV to 30 keV. The calculated value from JENDL-3.3 in this energy range is 2.3 b which is smaller than the data of Knitter and Budtz-Jørgensen. Therefore there is a possibility that the evaluated data are smaller than the correct value.

Concerning the resonance integral of capture cross section, the experimental data are

about 2200 b, whereas the evaluated data are about 1800 b. This discrepancy must be due to the resonance parameters of a few levels at low energies.

(2) Resolved resonance parameters

The resonance parameters given in JENDL-3.2 were based on those of JENDL-2 with modifications considering the data of Simpson et al. [Si74a] and Knitter and Budtz-Jørgensen. Since then, new analysis has not been reported.

Maslov et al. evaluated the resonance parameters up to 250 eV on the basis of the fission cross section measured by Seeger [Se70] and Knitter and Budtz-Jørgensen [Kn88], and the total cross section measured by Simpson et al. [Si74a] They considered the same experimental data as JENDL-3.2 evaluation, and added many small resonances and extended the upper boundary of the resolved resonance region from 215 eV to 250 eV.

We adopted the parameters of Maslov et al. for JENDL-3.3, and modified them slightly, since their parameters could not reproduce the most recent fission cross section at 0.0253 eV by Kobayashi et al. as shown in Table 3.1. A correction was made by adding a 1/v type background data for the fission cross section. Furthermore the fission cross section around 10 to 50 eV is too small comparing the data measured by Kobayashi et al. [Ko99] with slowing down spectrometer KULS at the Kyoto University. Maslov et al. assumed the fission width of 19 meV for the levels in this energy range which is smaller than measured fission width by Knitter and Budtz-Jørgensen. In the present evaluation, the fission widths of several levels were arbitrarily increased to reproduce better the data of Kobayashi et al.

Figure 3.1 (a) shows the fission cross section in the energy range from 0.01 to 10 eV. No energy dependent experimental data are available. The data at 0.0253 eV were already compared in Table 3.1.The cross section of JENDL-3.2 is too large and that of JEFF-3 too small at the thermal energy. Figure 3.1 (b) exhibits the fission cross section in the energy range from 80 to 95 eV. Since the experimental data of Seeger [Se70] are too large in this energy range, Maslov et al. analyzed their data after renormalization.

Comparison with the data of Kobayashi et al. [Ko99] is given in Fig. 3.2. Evaluated data are shown after broadened with energy resolution of the measurement. JENDL-3.3 is in good agreement with the experimental data.

Figure 3.3 shows the capture cross section below 10 eV. No experimental data are available except at the thermal energy. However, the evaluated data are in good agreement with each other. The total cross section is shown in Fig. 3.4. All the evaluated data represent well the data of Berreth and Simpson [Be70] and Simpson et al. [Si74a]

(3) Unresolved resonance parameters

The cross sections in the energy range from 250 eV to 42.3751 keV were represented with unresolved resonance parameters which were basically based on Maslov's evaluation. The unresolved resonance parameters of Maslov et al. give larger fission cross section than the experimental data of Kobayashi et al. [Ko99] Therefore the fission widths were slightly decreased below 10 keV.

The fission cross section of ^{243}Am in this energy region is shown in Fig. 3.2. Above about 300 eV, JENDL-3.3 is better than other evaluations. Above 10 keV, the experimental data of Kobayashi et al. are too small.

Figure 3.5 shows the neutron capture cross section of ^{243}Am in the energy range from 100 eV to 200 keV. Two sets of experimental data are available in this energy range: Wisshak and Käppeler [Wi83] and Weston and Todd [We85]. The data of Wisshak and Käppeler are systematically smaller than those of Weston and Todd. Maslov's data and JENDL-3.3 are in agreement with the data of Weston and Todd at the high energies.

3.3 Cross Sections above the Resonance Region

(1) Fission cross section

The fission cross section of ^{243}Am in the energy range from 1 keV to 20 MeV is shown in Figs. 3.6(a) and 3.6(b). The data of Seeger [Se70] existing below 10 keV were measured with underground nuclear explosion, and seem to be too large. The present evaluation of JENDL-3.3 is in good agreement with Knitter and Budtz-Jørgensen [Kn88] and Wisshak and Käppeler [Wi83]. JENDL-3.2 was too small in the energy range below 100 keV.

There are many sets of experimental data above 100 keV. Behrens and Browne [Be81] and Goverdovskii et al. [Go90] measured the fission cross section relative to the ^{235}U fission cross section. In the figure, their data are converted to the cross section by using the ^{235}U fission cross section of JENDL-3.3. Both sets of data are larger than other experimental data as shown in Fig. 3.6 (b).

The evaluated data of Maslov et al. is a result of a statistical model calculation. It represents well the tendency of the experimental data. However, we adopted the JENDL-3.2 data above 500 keV which represent better the measured data.

(2) Capture cross section

The capture cross section from 100 eV to 20 MeV is shown in Fig. 3.7. For JENDL-3.3, the data of Maslov et al. was adopted up to about 5 MeV. Above a several MeV, the direct and semi-direct process is dominant. Maslov et al. gave a constant cross section of 1 mb in this energy region. The cross section in this region was replaced with the direct and semi-direct capture cross section calculated with the DSD code [Ka99]. JENDL-3.2 which was a result of a statistical model calculation was too small above a few MeV.

(3) Inelastic scattering cross section

Total inelastic scattering cross sections are compared in Fig. 3.8. They are almost the same except JEFF-3. The data of Maslov et al. was adopted for JENDL-3.3.

(4) (n,2n) and (n,3n) reaction cross sections

These cross sections are compared in Fig. 3.9. JENDL-3.2 was based on a very simple evaporation model so that the (n,3n) reaction cross section was too large. The data of Maslov et al. was adopted for JENDL-3.3.

(5) Other cross sections and comparison in the whole energy region

The total cross section above 100 keV is shown in Fig. 3.10. The available evaluated data are almost the same as each other except JEFF-3. The data of Maslov et al. was adopted for JENDL-3.3. Figure 3.11 shows the elastic scattering cross section. JENDL-3.3 was obtained by subtracting a sum of partial cross sections from the total. JENDL-3.3 is slightly different from the data of Maslov et al. because of different fission cross sections.

The total, elastic scattering, fission and capture cross sections in the whole energy range from thermal to 20 MeV are shown in Figs. 3.12 to 3.15. The cross sections from 0.32242 eV to upper boundaries of the resolved resonance region are presented using average values in suitable energy intervals. Large discrepancies are found in the fission cross section below a few hundred keV and the capture cross section in the MeV region.

3.4 Number of Prompt and Delayed Neutrons per Fission

(1) Prompt neutrons

Khokhlov et al. [Kh94] measured the number of prompt neutrons per fission in the energy range from 0.5 to 10 MeV, and obtained the following result:

$$\nu_p(E) = (3.207 \pm 0.12) + (0.154 \pm 0.005)E \qquad (E \text{ in MeV})$$

The numbers of neutrons calculated from this equation are given in EXFOR.

In the present work, the evaluated data of Maslov et al. was adopted. They calculated ν_p with Madland-Nix model adjusting parameters to reproduce the data of Khokhlov et al. Figure 3.16 compares evaluated data and experimental data of ν_p. JENDL-3.2 was estimated from the systematic trend and a neutron separation energy as 3.2 + 0.16E(MeV). Compared with the data of Khoklov et al., this estimation was very good.

(2) Delayed neutrons

The number of delayed neutrons is shown in Fig. 3.17. Experimental data were reported by Saleh et al. [Sa97] and Charlton et al. [Ch97]; 0.0084±0.0004 [Sa97] at the thermal energy, and 0.0086±0.0005 [Ch97] in a fast reactor spectrum. The present work adopted the average value of 0.0085 in the lower energy region, and 0.00477 calculated by Brady and England [Br89] in the higher energy region. These two were connected in the energy range from 6 to 8 MeV. JENDL-3.2 was based on Tuttle's systematics.

As the decay constants and fractions of 6 temporal groups, the data of Saleh et al. were adopted for JENDL-3.3.

3.5 Other Data

(1) Angular distributions

The evaluated data of Maslov et al. were adopted for all angular distributions of emitted neutrons.

(2) Energy distributions

For the neutrons emitted from (n,2n), (n,3n), inelastic scattering and fission, the data of Maslov et al. were adopted. For the energy distributions of delayed neutrons adopted are those calculated by Brady and England [Br89].

Figures 3.18 to 3.20 show the energy distributions of (n,2n), (n,3n) and inelastic scattering, respectively. Those of prompt neutrons and delayed neutrons by fission are shown in Figs. 3.21 and 3.22.

4. Technetium-99

4.1 Summary of Evaluated Data

The data of ^{99}Tc given in JENDL-3.2 were evaluated by the Fission Product Nuclide Data Working Group of Japanese Nuclear Data Committee [Ka92, Ka01b]. Their evaluation was completed in 1990 [Ka92], and after then, the resonance parameters were revised in 1994 [Ka01b].

The resonance parameters of ENDF/B-VI were revised in 2001 [Oh00]. The other data of ENDF/B-VI were old ones evaluated in 1970's. JEFF-3 adopted the data of JENDL-3.2.

Concerning experimental data, new data after the JENDL-3.2 evaluation are available for the resonance parameters and capture cross section. In the present work, the data of JENDL-3.2 were revised by considering these recent experimental data.

4.2 Thermal Cross Sections and Resonance Integral

Experimental data of thermal cross sections and values calculated from evaluated data are compared in Table 4.1. The most recent experiment was made by Harada et al. [Ha95] Their result of 22.9±1.3 b is slightly larger than JENDL-3.2. In the present evaluation, the value of Harada et al. was adopted, and the resonance parameters were adjusted so as to reproduce this value. The calculated capture cross section from the present evaluation is 22.77 b at 0.0253 eV.

The total cross section of the present evaluation is 27.33 b which is larger than JENDL-3.2, but just between two available experimental data [Pa58, Wa70].

The data of capture resonance integral are shown in Table 4.2. The previous evaluation gave 312 b which were smaller than experimental data of Watanabe and Reeder and Harada et al. The data of other two experiments are too small and therefore are not acceptable. The resonance integral calculated from revised resonance parameters is 324 b which is still smaller than the experimental data.

4.3 Resonance Parameters

(1) Resolved resonance parameters

After JENDL-3.2 evaluation [Ka01b] was performed, three papers have been published; Gunsing et al. [Gu97], Raepsaet et al. [Ra97] and Gunsing et al. [Gu00] These three are the experiments performed at IRMM using GELINA, and analyses with the REFIT code. The reference of [Gu00] is a final report of [Gu97]. Gunsing et al. measured transmission in the energy range from 3 eV to 150 keV, and obtained the resonance parameters for 659 levels below

10 keV. Raepsaet et al. [Ra97] measured the capture cross section, and analyzed resonance parameters for 33 levels from 14 to 380 eV. However this is a preliminary analysis. Since the capture cross section was also measured up to 150 keV, a combined analysis of the transmission and the capture will be made in the future [Gu00].

The present evaluation adopted the results of Gunsing et al. [Gu00] Their parameters were given for the Reich-Moore multi-level formula. However we adopted the multi-level Breit-Wigner formula, since the large discrepancies were not found among the results of both formulae.

The parameters of a level at −15 eV (a negative resonance) were slightly adjusted so as to reproduce well the thermal capture cross section of 22.9±1.3 b [Ha95]

The upper boundary of the resolved resonance region was set at 6 keV, because the average cross sections calculated from the parameters become smaller than experimental data above several keV. Small resonances might be missed at the high energies. In particular, the number of p-wave resonances deceases above about 6 keV.

The scattering radius obtained by Gunsing et al. is 7.17±0.13 fm. This value is considerably larger than the recommendation of Mughabghab et al. [Mu81] of 6.0±0.5 fm. The elastic scattering cross sections obtained from the 7.17 fm are fairly larger than the cross sections in the unresolved resonance region. We adopted the scattering radius of 6.7 fm in the present evaluation so that the average elastic scattering cross section in the resolved and unresolved resonance regions are almost the same.

Figure 4.1 shows the total cross section below 100 eV. The present result (JENDL-3.3) is larger than JENDL-3.2. In this fugure, the data of Watanabe and Reeder is given at 0.0253 eV. Their energy dependent data and those of Gunsing et al. cannot be shown in the figure because thay are not in EXFOR database.

The capture cross section is shown in Fig. 4.2. The most recent experimental data are those of Kobayashi et al. [Ko01] which were measured at the Kyoto University by means of the TOF method with 46 MeV LINAC. Their data were normalized to the thermal cross section of Harada et al.

(2) Unresolved resonance parameters

In the present evaluation, as will be described in the next section, the optical model parameters (OMP) were revised. Therefore, the cross sections in the unresolved resonance region were changed. The unresolved resonance parameters were reanalyzed with the ASREP code [Ki99] to reproduce the total and capture cross sections calculated with the CATHSY code

[Ig91] and the new OMP.

Figure 4.3 shows the total and capture cross sections to be fitted and the cross sections calculated from obtained unresolved resonance parameters. Both are in very good agreement with each other. The scattering radius obtained in the analyses is 6.15 fm.

4.4 Cross Sections above the Resonance Region

4.4.1 Total Cross Section and Optical Model Parameters

As shown in Figs. 4.4 and 4.5, the total cross section given in JENDL-3.2 was not in good agreement with experimental data of Foster and Glasgow [Fo71]. At the energies below 150 keV, the total cross section measured by Gunsing et al. [Gu00] is about 9 b which is shown in the figure of Ref. [Gu00]. Therefore the data of JENDL-3.2 seem to be smaller than the correct value.

The optical potential parameters were re-adjusted so as to reproduce the total cross section by using the TOTAL code [Ig*1]. The new OMP's are listed in Table 4.3 together with the parameters used in JENDL-3.2 evaluation. The total cross section calculated from the new parameters is shown in Figs. 4.4 and 4.5 with solid lines. The present result could reproduce well the data of Foster and Glasgow.

4.4.2 Threshold Reaction Cross Sections

The cross sections of (n,2n), (n,3n), (n,p), (n,α), (n,np), (n,nα), (n,nd), (n,nt), (n,d), (n,t) and (n,^{3}He) reactions given in JENDL-3.2 were calculated with the PEGASUS code [Na99]. Those of the (n,2n), (n,p) and (n,α) reactions were normalized to experimental data or sytematics at 14.5 MeV.

JEFF-3 gives the same cross sections as JENDL-3.2, and ENDF/B-VI.8 only the (n,2n) reaction cross section.

(1) (n,2n) reaction cross section

For JENDL-3.2, the calculated values with the PEGASUS code were normalized to recommendation of Bychkov et al. [By80] which was based on the experimental data of Qaim [Qa73]. Figure 4.6 shows the evaluated data and experimental data of the ^{99}Tc(n,2n) reaction cross section. No experimental data other than Ref.[Qa73] are available. Therefore, we adopted the data of JENDL-3.2 for JENDL-3.3.

(2) (n,p) reaction cross section

Currently available cross-section data of this reaction are shown in Fig. 4.7. ENDF/B-VI.8 does not give this reaction data. JENDL-3.2 is in agreement with the experimental data of Qaim [Qa73] and Ikeda et al. [Ik94]. Therefore JENDL-3.2 was adopted in the present work.

(3) (n,α) reaction cross section

Figure 4.8 shows the (n,α) reaction cross section. JENDL-3.2 is in agreement with the experimental data of Qaim [Qa73] and Goldstein [Go66]. However, the most recent experimental data of Ikeda et al.[Ik94] are smaller then JENDL-3.2. Therefore, in the present work, the data of JENDL-3.2 were renormalized to the data of Ikeda et al.

(4) (n,3n), (n,np), (n,nα), (n,nd) and (n,nt) reaction cross sections

These data of JENDL-3.2 are shown in Fig. 4.9. Experimental data are available only for the (n,nα) reaction cross section. JENDL-3.2 is smaller than these experimental data [Qa73, Ik94]. For JENDL-3.3 (solid line), JENDL-3.2 was renormalized to the data of Ikeda et al. The data of the other reactions adopted to JENDL-3.3 are the same as JENDL-3.2.

(5) (n,d), (n,t) and (n,^{3}He) reaction cross sections

JENDL-3.2 data of these reactions are given in Fig. 4.10. They were adopted to JENDL-3.3 without any modifications. Qaim [Qa73] measured the (n,^{3}He) and (n,2p) reaction cross sections, and reported that they were less than 7 μb and less than 14 μb at 14.7 MeV, respectively. However, we did not modified the (n,^{3}He) reaction cross section and did not adopt the (n,2p) cross section, because they have large uncertainties.

4.4.3 Inelastic Scattering Cross Sections

The excited levels considered in the calculation are listed in Table 4.4. They were adopted from Table of Isotopes [Fi98] and RIPL-1 [IA98] The direct inelastic scattering process was not considered in the JENDL-3.2 evaluation. In the present work, it was calculated with the DWUCKY code [Ya88, Ku*1] to the nine levels marked with "*" in Table 4.4.The deformation parameters, β, were determined from the recommendation of Raman et al. [Ra87] The average value of β's was determined as 0.203 from neighboring even-even nuclides (^{98}Mo, ^{100}Mo, ^{98}Ru and ^{100}Ru). This value was used as an input data of levels with the angular momentum transfer =

2. The DWUCKY code calculates the effective β value of each level from this input data based on the weak-coupling model.

Figure 4.11 shows the direct inelastic scattering cross sections. These values were used as the competing cross sections in the statistical model calculation with the CASTHY code. The inelastic scattering cross sections were obtained as the sum of these direct cross sections and the results of CASTHY calculation. The total inelastic scattering cross section is compared with other evaluated data libraries in Fig. 4.12.

4.4.4 Capture, Total and Elastic Scattering Cross Sections

The capture and total cross sections were calculated with the CASTHY code. The parameters used are listed in Tables 4.3 and 4.4. The level density parameters for the Gilbert-Cameron formula are the same as those used in the JENDL-3.2 evaluation. The gamma-ray strength function of 8.01×10^{-3} was determined by the CASTHY code so as to reproduce the capture cross section of 620 mb at 50 keV.

The capture cross section is shown in Figs 4.13 and 4.14. The recent experimental data were reported by Kobayashi et al. [Ko01] and Igashira et al. [Ig01] Kobayashi et al. measured the cross sections from 0.01 eV to 40 keV, and normalized them to 22.9 b [Ha95] at 0.0253 eV. Igashira et al. used neutrons from the ^{7}Li(p,n) reaction and the TOF method, and obtained the cross sections from 12 to 540 keV.

The calculation with the CASTHY code reproduces well the data of Macklin [Ma82] and Kobayashi et al. below 1 MeV. The data of Igashira et al. are larger than the present calculation in the tens keV region. In the energy region above 1 MeV, the calculation was too large. Therefore, it was modified so as to reproduce the experimental data above 1 MeV.

Above several MeV, the direct/semi-direct capture is dominant. In the JENDL-3.2 evaluation, this contribution was estimated with a simple formula recommended by Benzi and Reffo [Be69], and normalized to 1 mb at 14 MeV. This formula was used again in the present work, but normalized to 9±2 mb at 14.7 MeV which was the measured data by Qaim [Qa73].

The Maxwellian-averaged capture cross sections at kT=30 keV are compared in Table 4.5. The present result is larger than JENDL-3.2 and recommendation of Bao et al. [Ba00]. Recently Gunsing et al. [Gu01] reported the Malwellian-averaged cross section based on the measured data at GELINA. Their result at kT=30 keV is 0.933 b which is quite larger than others.

The evaluated data for the total, elastic scattering and capture cross sections are compared with each other in Figs. 4.15, 4.16 and 4.17, respectively, in the energy region from the thermal to 20 MeV.

4.5 Other Data

The angular distributions of elastically scattered neutrons were adopted from the CASTHY calculation. Those of inelastic scattering neutrons were sum of the CASTHY and DWUCKY calculations.

The energy distributions of neutrons are the same as JENDL-3.2 which were calculated with the PEGASUS code. The interpolation method of neutron spectra was changed to "unit base interpolation."

5. Cerium-140

5.1 Summary of Evaluated Data

The evaluated data given in JENDL-3.2 was partly revised [Ka01b] after the evaluation for JENDL-3.1 [Ka92]. ENDF/B-VI and JEFF-3 have also the data for this nuclide. The data of JEFF-3 are the same as JEF-2.2. According to the description given in the data file, JEFF-3 adopted the data of ENDF/B-V and then revised the resonance parameters and added the charged-particle emission cross sections from REAC-ECN-4. ENDF/B-VI is essentially the same as ENDF/B-V.

The neutron number of ^{140}Ce is a magic number of 82. Therefore the capture cross section is small, and there are small number of resonances. There are relatively many experimental data. By the reactions of (n,2n), (n,α), etc., radioactive nuclides are produced. Therefore, many experimentalists measured such radioactive nuclide production cross sections.

5.2 Thermal Cross Sections and Resonance Integral

Thermal cross sections are listed in Table 5.1. The capture and the elastic scattering cross sections of JENDL-3.2 are in good agreement with the recommendation of Mughabghab et al. [Mu81]. No recent experimental data have been reported.

Table 5.2 is a list of the data of capture resonance integral. The resonance integral calculated from JENDL-3.2 seems to be too small. The resonance parameters are revised as described in the next section so as to improve this value. JENDL-3.3 gives the capture resonance integral of 0.344 b. However it is still smaller than the experimental data of about 0.47 b.

5.3 Resolved Resonance Parameters

The resolved resonance region of JENDL-3.2 is up to 200 keV. The parameters of JENDL-2 determined on the basis of the data of Hacken et al. [Ha74], Camarda [Ca78] and Musgrove et al. [Mu79] were revised based on the data of Ohkubo et al. [Oh85] for JENDL-3.2.

ENDF/B-VI does not give the resonance parameters. The parameters of JEFF-3 were based on the data of Musgrove et al. [Mu79]

The total and capture cross sections are shown in Figs. 5.1 and 5.2, respectively.

The resonance parameters were reported by Ohkubo et al. [Oh93] after the JENDL-3.2 evaluation. They superseded the previous results of Ref. [Oh85]. In the present work, their parameters were adopted to 15 levels between 2.5 and 55 keV. The new parameters are almost the same as previous ones.

JENDL-3.2 assumed a negative resonance at −64 eV which was based on the recommendation of Mughabghab et al. By the effects of this negative level, the capture cross section rapidly decreases with increasing energies. Since average spacing of s-wave resonances is about 3.2 keV [Mu81], the position of the first negative resonance might be around -0.7 keV. In this work, a negative resonance was assumed at −700 eV. The neutron width of this resonance was adjusted so as to give the elastic scattering cross section of about 2.8 b [Mu81], and the radiative capture width of 0.035 eV was assumed.

$E = -700$ eV, $\Gamma_n = 2$ eV, $\Gamma_\gamma = 0.035$ eV.

In order to reproduce the capture cross section at 0.0253 eV, we needed background cross sections in a 1/v form. Above 60 keV, a background cross section given in JENDL-3.2 to compensate level missing was kept.

Harnood et al. [Ha00] measured recently the capture cross section in the resolved resonance region and revealed that the data of JENDL-3.2 was too small by about 30%. This underestimation was caused by the data of Musgrove et al. adopted to JENDL-3.2 which was too small. For JENDL-3.3, the capture widths of all the resonances were increased by 40% so as to agree with the data of Harnood et al.

It is also seen by comparison of Maxwellian averaged capture cross section around 30 keV that the cross section calculated from JENDL-3.2 resonance parameters is too small. Table 5.3 compares them. JENDL-3.2 is about 30% smaller than the data of Käppeler et al. [Ka96] The present results are better than JENDL-3.2.

Improved cross sections are shown in Figs. 5.1 and 5.2 with solid lines.

5.4 Cross Sections above the Resonance Region

5.4.1 Total Cross Section and Optical Model Parameters

The total cross section was measured by Camarda et al. [Ca84]. The optical model parameters used for the JENDL-3.2 evaluation were slightly improved to reproduce the data of Camarda et al. The potential parameters are listed in Table 5.4. The calculated total cross section is compared with other evaluated data and the experimental data in Fig. 5.3. The present calculation reproduces well the data of Camarda et al. The calculated total cross section was adopted for JENDL-3.3 above 200 keV.

5.4.2 Threshold Reaction Cross Sections

(1) (n,2n) reaction cross section

There are many experimental data for this reaction. Figure 5.4 shows the total (n,2n) reaction cross section. No data are given in ENDF/B-VI and JEFF-3 for this reaction. The recent measurements were performed by Kasugai et al. [Ka01c], Filatenkov et al.[Fi97,Fi99], Molla et al.[Mo97] and Kong et al.[Ko95]. They are smaller than JENDL-3.2. Therefore, the data of JENDL-3.2 was decreased in the present work by multiplying a factor of 0.95 so as to reproduce well the data of Filatenkov et al. which are nearly average of the recent data. The result is shown with a solid line in Fig. 5.4. The data after 1990 are shown with their error-bars. The present data for JENDL-3.3 is consistent with the upper limit of the data of Kasugai et al.

(2) (n,p) reaction cross section

Evaluated data are given in JENDL-3.2 and JEFF-3. Both are almost the same as each other.

Experimental data exist around 14 to 15 MeV. The recent experimental data by Filatenkov et al. [Fi97, Fi99], Kasugai et al. [Ka01c] and Teng Dan et al.[Te85] are in good agreement with each other. JENDL-3.2 reproduces these experimental data as seen in Fig. 5.5. The present work adopted the data of JENDL-3.2.

(3) Other threshold reactions

Figure 5.6 shows the cross sections of (n,3n), (n,nα), (n,np) and (n,nd) reactions. Only JENDL-3.2 gives those cross sections. Figure 5.7 is a graph of the (n,α), (n,d), (n,t), (n,^{3}He) and (n,2p) reaction cross sections. JENDL-3.2 does not give the data for (n,^{3}He) and (n,2p) reactions, because their cross sections calculated with the PEGASUS were smaller than 0.001 mb.

In the present work, the data of JENDL-3.2 for these reactions were adopted without any modifications.

5.4.3 Inelastic Scattering Cross Sections

JENDL-3.2 considered the level scheme of ^{140}Ce up to 3.25 MeV. The direct inelastic process was considered to the 2+ and 3– levels at 1.596 MeV and 2.464 MeV, respectively.

In the present work, twenty-three levels up to 3.3951 MeV listed in Table 5.4 were taken into consideration on the basis of Table of Isotopes 8th edition [Fi98], and those above 3.4246 MeV were assumed to be overlapping. The direct inelastic scattering cross sections were assumed to be the same as JENDL-3.2 calculated with the DWUCK code.

The present result is shown in Fig 5.8 together with other evaluated data. The data of ENDF/B-VI and JEFF-3 are the same each other. The shape of ENDF/B-VI and JEFF-3 seems to be inadequate.

5.4.4 Capture, Total and Elastic Scattering Cross Sections

The capture cross section was calculated with the CASTHY code by adopting the parameters given in Tables 5.4 and 5.5. The gamma-ray strength function of 5.73×10^{-6} was determined so as to reproduce the capture cross section of 4.7 mb at 500 keV which was a slightly large cross section than Harnood et al.

Bergqvist et al. [Be78] measured the direct capture cross section at energies from 6.2 to 11 MeV. They are about 2 times larger than JENDL-3.2 which was calculated from a simple sistematics of Benzi and Reffo [Be69]. Therefore, the direct capture cross section was adopted after multiplying a factor of 2.

The capture cross section is shown in Fig. 5.9. Below 200 keV, in the resonance region, the average cross section is in good agreement with the data of Harnood et al. Above 200 keV, the present evaluation is slightly larger than JENDL-3.2.

The elastic scattering cross section above 200 keV was obtained by subtracting sum of partial cross sections from the total. The total, elastic scattering and capture cross sections in the whole energy range from thermal to 20 MeV are shown in Figs. 5.10, 5.11 and 5.12.

5.5 Other Data

The angular distributions of elastically scattered neutrons were adopted from the CASTHY calculation. Those of inelastic scattering neutrons for the levels at 1.5962 and 2.4641

MeV were sum of the CASTHY and DWUCKY calculations.

The energy distributions of neutrons are the same as JENDL-3.2 which were calculated with the PEGASUS code. The interpolation method was changed to "unit base interpolation."

6. Conclusions

Improvement of JENDL-3.2 data was made for ^{242m}Am, ^{243}Am, ^{99}Tc and ^{140}Ce. Almost all data of JENDL-3.2 for these nuclides were replaced with improved data. The data were compiled in the ENDF-6 format and adopted to JENDL-3.3.

Acknowledgements

The authors thank Dr. M.Ishikawa of JNC for supporting the present work, and Drs. M.Igashira of Tokyo Institute of Technology, K.Kobayashi of Kyoto University and T.Kai of JAERI for permitting us to use their recent experimental data.

References

Al67) Alstad J., Jahnsen T., Pappas A.C.: *J. Inorg. Nucl. Chem.*, **29**, 2155 (1967), EXFOR20044.

Al73) Alian A., Born H-J., Kim J.I.: *J. Radioanal. Chem.*, **15**, 535 (1973), EXFOR 20644.

An79) Anand R.P., Jhingan M.L., Bhattachrya D., Kondaiah E.: *Il Nuovo Cimento*, **50A**, 247 (1979), EXFOR30390.

As79) Asghar M., Caïtucoli F., Perrin P., Barreau G., Leroux B.: *Annals Nucl. Energy*, **6**, 561 (1979).

Ba67) Bak M.A., Krivokhatskii A.S., Petrzhak K.A., Petrov Yu.G., Romanov Yu.F., Shlyamin É.A.: *Sov. At. Energy*, **23**, 1059 (1967), EXFOR40062.

Ba71) Bari A.: private communication to EXFOR (1971), EXFOR10431.

Ba82) Bari A.: *J. Radioanal. Chem.*, **75**, 189 (1982), EXFOR12872.

Ba00) Bao Z.Y., Beer H., Käppeler F., Voss F., Wisshak K.: *At. Data Nucl. Data Tables*, **76**, 70 (2000).

Be69) Benzi V., Reffo G.: *CCDN-NW*/10 (1969).

Be70) Berreth J.R., Simpson F.B.: "Total neutron cross section of ^{243}Am from 0.01 to 25 eV," *IN*-1407, p.66 (1970), EXFOR10272.

Be76) Belanova T.S., Kolesov A.G., Poruchikov V.A., Timofeev G.A., Kalebin S.M., Artamonov V.S., Ivanov R.N.: *Sov. At. Energy*, **40**, 368 (1976), EXFOR40280.

Be78) Bergqvist I., Pålsson B., Nillson L., Lindholm A., Drake D.M., Arthur E., McDaniels D.K., Varghese P.: *Nucl. Phys.*, **A295**, 256 (1978), EXFOR21295.

Be81) Behrens J.W., Browne J.C.: *Nucl. Sci. Eng.*, **77**, 444 (1981), EXFOR10652.

Bo68a) Bowman C.D., Auchampaugh G.F., Fultz S.C., Hoff R.W.: *Phys. Rev.*, **166**, 1219 (1968), EXFOR12572.

Bo68b) Bormann M., Behrend A., Riehle I., Vogel O.: *Nucl. Phys.*, **A115**, 309 (1968) [in German], EXFOR20834.

Br84) Browne J.C., White R.M., Howe R.E., Landrum J.H., Dougan R.J., Dupzyk R.J.: *Phys. Rev.*, **C29**, 2188 (1984), EXFOR10805.

Br89) Brady M.C., England T.R.: *Nucl. Sci. Eng.*, **103**, 129 (1989).

Bu61) Butler D.K., Sjoblom R.K.: *Phys. Rev.*, **124**, 1129 (1961), EXFOR12543.

By80) Bychkov V.M., Manokhin V.N., Pashchenko A.B., Plyaskin V.I.: "Cross Sections for (n,p), (n,α) and (n,2n) Threshold Reactions," *INDC(CCP)*-146/LJ (1980).

Ca78) Camarda H.S.: *Phys. Rev.*, **C18**, 1254 (1978).

Ca84) Camarda H.S., Phillips T.W., White R.M.: *Phys. Rev.*, **C29**, 2106 (1984), EXFOR12891.

Ch73) Chou J-C., Werle H.: *J. Nucl. Energy*, **27**, 811 (1973), EXFOR20352.

Ch97) Charlton W., Parish T., Raman S, Shinohara N., Andoh M: *Proc. International Conf. Nucl. Data for Sci. Technol.*, Trieste, Italy, 19-24 May 1997, Part I, p.491 (1997).

Co59a) Coté R.E., Bollinger L.M., Barnes R.E. Diamond H.: *Phys. Rev.*, **114**, 505 (1959), EXFOR12539.

Co59b) Coleman R.F., Hawker B.E., O'Connor L.P., Perkin J.L.: *Proc. Phys. Society*, **73**, 215 (1959), EXFOR21440.

Cs68) Csikai J., Fominich V.I., Latakos T.: *Acta Phys. Hangarica*, **24**, 233 (1968), EXFOR30040.

Cu67) Cuzzocrea P., Notarrigo S., Perillo E.: *Il Nuovo Cimento*, **52B**, 476 (1967), EXFOR21289.

Da83) Dabbs J.W., Bemis C.E. Jr., Raman S., Dougan R.J., Hoff R.W.: *Nucl. Sci. Eng.*, **84**, 1 (1983), EXFOR12808.

Di68) Dilg W., Vonach H., Winkler G., Hille P.: *Nucl. Phys.*, **A118**, 9 (1968) [in German], EXFOR20802.

Fi97) Filatenkov A.A., Chuvaev S.V., Jakovlev V.A., Malyshenkov A.V., Vasiljev S.K.: *Proc. International Conf. Nucl. Data for Sci. Technol.*, Trieste, Italy, 19-24 May 1997, Part I, p.598 (1997).

Fi98) Firestone R.B.: *Table of Isotopes, Eighth Edition, 1998 Update*, A Wiley- Interscience Publication (1998).

Fi99) Filatenkov A.A., Chuvaev S.V., Yakovlev V.A., Malyshenkv A.V., Vasil'ev S.K.: "Systematic Measurements of Cross-Sections at Neutron Energies 13.4 – 14.9 MeV," *RI*-252 (1999), EXFOR41298, 41240.

Fo67) Fomushkin É.F., Gutnikova E.K., Zamyatnin Yu.S., Maslennikov B.K., Belov V.N., Surin V.M., Nasyrov F., Pashkin N.F.: *Sov. J. Nucl. Phys.*, **5**, 689 (1967), EXFOR40779.

Fo68) Folger R.L., Smith J.A., Brown L.C., Overman R.F., Holcomb H.P.: *Proc. Conf. Neutron Cross Sections and Technol.*, Washington, D.C., USA, 4 – 7 May 1968, Vol.2, 1279 (1968), EXFOR12534.

Fo71) Foster D.G. Jr., Glasgow D.W.: *Phys. Rev.*, **C3**, 576 (1971), EXFOR10047.

Fo81) Fomushkin É.F., Novoselov G.F., Vinogradov Yu.I., Gavrilov V.V., In'kov V.I., Maslennikov B.K., Polynov V.N., Surin V.M., Shvetsov A.M.: *Sov. J. Nucl. Phys.*, **33**, 324 (1981), EXFOR41173.

Fo84) Fomushkin Eh., Novoselov G.F., Vinogradov Yu.I., Gavrilov V.V., Maslennikov B.K., Polynov V.N., Surin V.M., Shvetsov A.M.: *INDC(CCP)*-281/L, p.23 (1988), EXFOR40856.

Fu86) Fursov B.I., Baranov E.Yu., Klemyshev M.P., Samylin B.F., Smirenkin G.N., Turchin Yu.M.: *Sov. At. Energy*, **59**, 899 (1986), EXFOR40837.

Fu94) Fursov B.I., Samylin B.F., Smirenkin G.N., Polynov V.N.: *Proc. Int. Conf. Nucl. Data for Science and Technol., Gatlinburg*, Tenn. USA, 9 – 13 May 1994, Vol. 1, p.269 (1994), EXFOR41303.

Ga76) Gavrilov V.D., Gonchrov V.A., Ivanenko V.V., Kustov V.N., Smirnov V.P.: *Sov. At. Energy*, **41**, 808 (1976), EXFOR40467.

Ge87) Gerasimov V.F., Danichev V.V., Dement'ev V.N., Zenkevich V.S., Mozolev G.V.: *Proc 1st International Conf. Neutron Phys.*, Kiev, USSR, 14 – 18 Sep. 1987, Vol. 3, p.84 (1987), EXFOR40993.

Go65) Golchert N.W., Gardner D.G., Sedlet J.: *Nucl. Phys.*, **73**, 349 (1965), EXFOR 11289.

Go66) Goldstein G.: *J. Inorg. Nucl. Chem.*, **28**, 676 (1966), EXFOR13029.

Go90) Goverdovskii A.A., Gordyushin A.K., Kuz'minov B.D., Mitrofanov V.F., Sergachev A.I., Solov'ev S.M., Kuz'mina T.E.: *Sov. At. Energy*, **67**, 524 (1990), EXFOR41058.

Go99) Golovnya V.Ya., Bozhko V.P., Oleynik S.N., Shpakov V.P., Kalinin V.A.: *JINR-E3*-419, p.293 (1999), EXFOR41361.

Gu97) Gunsing F., Brusegan A., Leprêtre A., Mounier C., Raepsaet C.: *Proc. International Conf. Nucl. Data for Sci. Technol.*, Trieste, Italy, 19-24 May 1997, Part II, p.1293 (1997).

Gu00) Gunsing F., Leprêtre A., Mounier C., Raepsaet C., Brusegan A., Macavero E.: *Phys., Rev.*, **C61**, 054608 (2000).

Gu01) Gunsing F., Leprêtre A., Mounier C., Raepsaet C., Bastian C., Corvi F., Gonzalez J.: *Nucl. Phys.*, **A688**, 496c (2001).

Ha59) Harvey J.: private communication to EXFOR (1959), EXFOR 11940.

Ha71) Havlik E.: *Acta Physica Austraca*, **34**, 209 (1971), EXFOR20509.

Ha74) Hacken G., Liou H.I., Makofske W.J., Rahn F., Rainwater J.: *USNDC*-11, p.68 (1974).

Ha95) Harada H., Nakamura S., Katoh T., Ogata Y.: *J. Nucl. Sci. Technol.*, **32**, 395 (1995).

Ha00) Harnood S., Igashira M., Matsumoto T., Mizuno S., Ohsaki T.: *J. Nucl. Sci. Eng.*, **37**, 740 (2000).

He78) Heft R.E.: 78Mayag, 495 (1978), EXFOR12866.

Ho81) Howe R.E., Browne J.C., Dougan R.J., Dupzyk R.J., Landrum J.H.: *Nucl. Sci. Eng.*, **77**, 454 (1981).

Ho83) Howe R.E., White R.M., Browne J.C., Landrum J.H., Dougan R.J., Lougheed R.W., Dupzyk R.J.: *Nucl. Phys.*, **A407**,193 (1983), EXFOR 12851.

Hu50) Hughes D.J., Sherman D.: *Phys. Rev.*, **78**, 632 (1950), EXFOR11596.

IA98) IAEA; "Handbook for Calculations of Nuclear Reaction Data, Reference Input Parameter Library," *IAEA-TECDOC*-1034 (1998).

Ig*1) Igasasi S., Kawai M., Nakagawa T.: private comm.unication.

Ig91) Igarasi S. and Fukahori T.: "Program CASTHY - Statistical Model Calculation for Neutron Cross Sections and Gamma Ray Spectrum -," JAERI 1321 (1991).

Ig01) Igashira M., et al.: private comm.unication (2001).

Ik94) Ikeda Y., Cheng E.T., Konno C., Maekawa H.: *Nucl. Sci. Eng.*, **116**, 28 (1994).

Ja70) Jaffey A.H., Lerner J.L.: *Nucl. Phys.*, **A145**, 1 (1970), EXFOR 10125.

Ka49) Katcoff S., Leary J., Walsh K., Elmer R., Goldsmith S., Hall L., Newbury E., Povelites J., Waddell J.: *J. Chem. Phys.*, **17**, 421 (1949), EXFOR12053.

Ka87) Kanda K., Imaruoka H., Terayama H., Karino Y., Hirakawa N.: *J. Nucl. Sci. Technol.*, **24**, 423 (1987), EXFOR22044.

Ka92) Kawai M., Iijima S., Nakagawa T., Nakajima Y., Sugi T., Watanabe T., Matsunobu H., Sasaki M., Zukeran A.: *J. Nucl. Sci. Technol.*, **29**, 195 (1992).

Ka96) Käppeler F., Toukan K.A., Schumann M., Mengoni A.: *Phys. Rev.*, **C53**, 1397 (1996).

Ka99) Kawano T.: DSD code, private communication (1999).

Ka01a) Kai T., Kobayashi K., Yamamoto S., Cho H.-J., Fujita Y., Kimura I., Ohkawachi Y., Wakabayashi T.: *Annals Nucl. Energy*, **28**, 723 (2001).

Ka01b) Kawai M., Nakagawa T., Watanabe T., Nakajima Y., Zukeran A., Matsunobu H., Sugi T., Chiba S.: *J. Nucl. Sci. Technol.*, **38**, 261 (2001).

Ka01c) Kasugai Y., Ikeda Y., Uno Y., Yamamoto H., Kawade K.: "Activation Cross Section Measuremet at Neutron Energy from 13.3 to 14.9 MeV using FNS Facility," JAERI-Research 2001-025 (2001), EXFOR22393.

Kh94) Khokhlov Yu.K., Ivanin I.A., In'kov V.I., Vinogradov Yu.I., Danilin L.D., Polynov B.N.: *Proc. Int. Conf. Nucl. Data for Science and Technol., Gatlinburg*, Tenn. USA, 9 – 13 May 1994, Vol. 1, p.272 (1994).

Ki82) Kikuchi Y.: "Evaluation of Neutron Nuclear Data for ^{241}Am and ^{243}Am," *JAERI-M* 82-096 (1982).

Ki99) Kikuchi Y., Nakagawa T., Nakajima Y.: "ASREP: A Computer Program for Automatic Search of Unresolved Resonance Parameters," *JAERI-Data/Code* 99-025 (1999) in Japanese.

Kn88) Knitter H-H. Budtz-Jørgensen C.: *Nucl. Sci. Eng.*, **99**, 1 (1988), EXFOR22032.

Ko53) Koehler W.C., Wollan E.O.: *Phys. Rev.*, **91**, 597 (1953).

Ko95) Kong Xiangzhong, Wang Yongchang, Yang Jingkang, Yuan Junqian: *INDC(CPR)*-036/L, p.5 (1995), EXFOR31485.

Ko99) Kobayashi K., Kai T., Yamamoto S., Cho H.-J, Fujita Y., Kimura I., Shinohara N.: *J. Nucl. Sci. Technol.*, **36**, 20 (1999).

Ko01) Kobayashi K., Lee S., Yamamoto S., Yoshimoto T., Fujita Y., Kim G., Lee Y., Chang J.: *Proc. International Conf. Nucl. Data Sci. Technol.*, Tsukuba, Japan, Oct. 7 – 12, 2001, Vol. 1, p.214 (2002).

Kr70) Kroshkin N.I., Zamyatnin Yu.S.: *Sov. At. Energy*, **29**, 790 (1970), EXFOR 40064.

Ku*1) Kunz P.D.: DWUCK , unpublished.

La64) Lantz P.M., Baldock C.R., Idom L.E.: *Nucl. Sci. Eng.*, **20**, 302 (1964).

Li77) Little R.C., Block R.C: *Trans. Am. Nucl. Soc.*, **26**, 574 (1977), EXFOR10671.

Lu70a) Lu W-D., RanaKumar N., Fink R.W.: *Phys. Rev.*, **C1**, 350 (1970), EXFOR 10497.

Lu70b) Lu W-D., RanaKumar N., Fink R.W.: *Phys. Rev.*, **C1**, 358 (1970), EXFOR 10145.

Lu77) Lucas M., Hegemann R., Naudet R., Renson C., Chevalier C.: Proc. Meeting Technical Committee on Natural Fission Reactors, Paris, 19 – 21 Dec. 1977, Vol. 1, 431 (1978), EXFOR 21563.

Ma57) Macklin R.L.. Lazar N.H., Lyon W.S.: *Phys. Rev.*, **107**, 504 (1957), EXFOR 11399.

Ma77) Mann F.M., Schenter R.E.: "HEDL Evaluation of Actinide Cross Sections for ENDF/B-V," *HEDL TME* 77-54 (1977)

Ma82) Macklin R.L.: *Nucl. Sci. Eng.*, **81**, 520 (1982), EXFOR12753.

Ma96) Maslov V.M., Sukhovitskij E.Sh, Porodzinskij Yu.V., Klepatskij A.B., Morogovskij G.B.: "Evaluation of Neutron Data for Americium-243," *INDC(BLR)*-006 (1996).

Ma97) Maslov V.M., Sukhovitskij E.Sh, Porodzinskij Yu.V., Morogovskij G.B.: "Evaluation of Neutron Data for Americium-242m," *INDC(BLR)*-7 (1997).

Mo97) Molla N.I., Miah R.U., Basunia S., Hossain S.M., Rahman M.: *Proc. International Conf. Nucl. Data for Sci. Technol.*, Trieste, Italy, 19-24 May 1997, Vol.1, p.517 (1997), EXFOR31491.

Mu79) Musgrove A.R.de L., Allen B.J., Macklin R.L.: *Aust. J. Phys.*, **32**, 213 (1979), EXFOR30361.

Mu81) Mughabghab S.F., Divadeenam M., Holden N.E.: "Neutron Cross Sections, Vol.1, Neutron Resonance Parameters and Thermal Cross Sections, Part A, Z=1-60," Academic Press, New York (1981).

Mu84) Mughabghab S.F.: "Neutron Cross Sections, Vol.1, Neutron Resonance Parameters and Thermal Cross Sections, Part B, Z=61-100," Academic Press, New York (1984).

Na80) Nakagawa T., Igarashi S.: "Evaluation of Neutron Nuclear Data for ^{242m}Am and ^{242g}Am," *JAERI-M* 8903 (1980) [in Japanese].

Na89) Nakagawa T.: "Evaluation of Nuclear Data for Americium Isotopes," JAERI-M 89-008 (1989).

Na99) Nakagawa T., Iijima S., Sugi T., Nishigori T.: "PEGASUS: A Preequilibrium and Multi-step Evaporation Code for Neutron Cross Section Calculation," *JAERI-Data/Code* 99-031 (1999).

Ne59) Newson H.W., Block R.C., Nichols P.F., Taylor A., Furr A.K., Merzbacher E.: *Annals Phys.*, **8**, 211 (1959), EXFOR11452.

Oh85) Ohkubo M., Mizumoto M., Nakajima Y., Sugimoto M., Furuta Y., Kawarasaki Y.: *Proc. Int. Conf. Nucl. Data for Basic and Applied Science*, Santa Fe, USA, 13-17 May 1985, Vol.2, p.1623 (1986).

Oh93) Ohkubo M., Mizumoto M., Nakajima Y.: "Neutron Transmission Measurements on ^{121}Sb, ^{123}Sb, ^{140}Ce and ^{142}Ce in the Resonance Region," *JAERI-M* 93-012 (1993), EXFOR21926.

Oh00) Oh S-Y., Chang J., Mughabghab S.: "Neutron Cross Section Evaluations of Fission Products Below the Fast Energy Region," *BNL-NCS*-67469 (2000).

Ov74) Ovechkin V.V., Rau D.F., Rudenko V.S.: *Proc. 2nd National Soviet Conf. Neutron Phys.*, Kiev, USSR, 28 May – 1 June 1973, Vol. 2, p.131 (1974), EXFOR40295.

Pa58) Pattenden N.J.: *Proc. 2nd UN Conf. Peaceful Uses of At. Energy*, Geneva, 1 – 13 Sep. 1958, Vol.16, p.44 (1958), EXFOR21325.

Po52) Pomerance H.: *Phys. Rev*,, **88**, 412 (1952), EXFOR11507.

Qa73) Qaim S.M.: *J. Inorg. Nucl. Chem.*, **35**, 3669 (1973), EXFOR20350.

Qa74) Qaim S.M.: *Nucl. Phys.*, **A224**, 319 (1974), EXFOR20541.

Qa76) Qaim S.M.: *Radiochem. Radioanal. Letters*, **25**, 335 (1976), EXFOR20716.

Ra87) Raman S., Malarkey C.H., Milner W.T., Nestor C.W., Jr., Stelson P.H.: *At. Data Nucl. Data Tables*, **36**, 1 (1987).

Ra97) Raepsaet C., Bastian C., Corvi F., Gunsing F., Leprêtre: *Proc. International Conf. Nucl. Data for Sci. Technol.*, Trieste, Italy, 19-24 May 1997, Part II, p.1289 (1997).

Ri68) Ricabarra G.H., Turjanski R., Ricabarra M.D.: *Proc. International Conf. Nuclear Data for Reactors*, Helsinki, June 15 – 19, 1970, Vol. II, p.589 (1970). [in French], EXFOR39129.

Sa97) Saleh H.H., Parish T.A., Raman S., Shinohara N.: *Nucl. Sci. Eng.*, **125**, 51 (1997).

Se67) Seeger P.A., Hemmendinger A., Diven B.C.: *Nucl. Phys.*, **A96**, 605 (1967), EXFOR12558.

Se70) Seeger P.A.: *LA*-4420, p.138 (1970), EXFOR10063.

Sh91) Shigin V.A.: *Sov. J. Nucl. Phys.*, **53**, 409 (1991), EXFOR41108.

Si74a) Simpson O.D., Simpson F.B., Harvey J.A., Slaughter G.G., Benjamin R.W., Ahlfeld C.E.: *Nucl. Sci. Eng.*, **55**, 273 (1974), EXFOR10204.

Si74b) Siddappa K., Sriramachandra Murty M., Rama Rao J.: *Annals Phys.*, **83**, 355 (1974), EXFOR30502.

So78) Sothras S.L., Salaita G.N.: *J. Inorg. Nucl. Chem.*, **40**, 585 (1978), EXFOR 10751.

St52) Street K. Jr., Chiorso A., Thompson S.G.: *Phys. Rev.*, **85**, 135 (1952), EXFOR 12583.

St72) Steinnes E.: *J. Inorg. Nucl. Chem.*, **34**, 2699 (1972), EXFOR20188.

Ta60) Tattersall R.B., Rose H., Pattenden S.K., Jowitt D.: *J. Nucl. Energy*, **A12**, 32 (1960), EXFOR20638.

Te85) Teng Dan, Zhao Wenrong, Fan Peiguo, Lu Hanlin: *Chinese J. Nucl. Phys.*, **7**, 307 (1985), EXFOR30777.

Tr87) Trofimov Yu.N: *Proc 1st International Conf. Neutron Phys.*, Kiev, USSR, 14 – 18 Sep. 1987, Vol.3, p.331 (1987), EXFOR41001.

Tr89) Trofimov Yu.N.: *Yadernye Konstanty*, **4** (*INDC(CCP)*-311/G), p.36 (1989) [in Russian], EXFOR 41050.

Va74) Van der Linden R., De Corte F., Hoste J.: *J. Radianal. Chem.*, **20**, 695 (1974), EXFOR20645.

Ve70) Vertebnyj V., et al.: *Proc. International Conf. Nuclear Data for Reactors*, Helsinki, June 15 – 19, 1970, Vol. I, p.651 (1970). [in Russian]

Wa70) Watanabe T., Reeder S.D.: *Nucl. Sci. Eng.*, **41**, 188 (1970), EXFOR10265.

Wa89) Wagemans C., Schillebeeckx P., Bocquet J.P.: *Nucl. Sci. Eng,*, **101**, 293 (1989).

We85) Weston L.W., Todd J.H.: *Nucl. Sci. Eng.*, **91**, 444 (1985), EXFOR12951.

Wi60) Wille R.G., Fink R.W.: *Phys. Rev.*, **118**, 242 (1960), EXFOR12033.

Wi83) Wisshak K., Käppeler F.: *Nucl. Sci. Eng.*, **85**, 251 (1983), EXFOR21863.

Xi90) Xia Yijun, Wang Chunhao, Yang Jinfu, Yang Zhihua, Liu Mantian: *Chinese J. Nucl. Phys.*, **12**, 261 (1990). EXFOR32536.

Ya88) Yamamuro N.: "A Nuclear Cross Section Calculation System with Simpilified Input-Format Version I (SINCROS-I)," *JAERI-M* 88-140 (1988) [in Japanese].

Zh75) Zhuravlev K.D., Kroshkin N.I., Chetverikov A.P.: *Sov. At. Energy*, **39**, 907 (1976).

Table 2.1 Thermal cross sections (b) of ^{242m}Am

a) Fission		
	Present (JENDL-3.3)	6390
	JENDL-3.2	6409
	ENDF/B-VI	6620
	JEFF-3	6874
	Maslov et al.	6390
	Mughabghab [Mu84]	6950±280
	Zhuravlev et al. [Zh75]	6080±500
	Dabbs et al. [Da83]	6950±250
	Browne et al. [Br84]	6328±0.5%
	Kai et al. [Ka01a]	5850±250
b) Capture		
	Present (JENDL-3.3)	1229
	JENDL-3.2	1254
	ENDF/B-VI	1342
	JEFF-3	1806
	Maslov et al.	1229
	Mughabghab [Mu84]	2000±600
c) Elastic scattering		
	Present (JENDL-3.3)	5.25
	JENDL-3.2	5.67
	ENDF/B-VI	5.84
	JEFF-3	13.72
	Maslov et al.	5.25
d) Total		
	Present (JENDL-3.3)	7625
	JENDL-3.2	7669
	ENDF/B-VI	7968
	JEFF-3	8694
	Maslov et al.	7625

Table 2.2 Resonance integrals (b) of ^{242m}Am fission and capture cross sections

a) Fission			
	Present (JENDL-3.3)	1540	
	JENDL-3.2	1560	
	ENDF/B-VI	1890	
	JEFF-3	1640	
	Maslov et al.	1540	
	Mughabghab [Mu84]	1800±65	
	Zhuravlev et al. [Zh75]	2260±200	
	Dabbs et al. [Da83]	1800±65	0.5 eV – 20 MeV
	Browne et al. [Br84]	1553±78	0.5 eV – 20 MeV
b) Capture			
	Present (JENDL-3.3)	240	
	JENDL-3.2	246	
	ENDF/B-VI	287	
	JEFF-3	262	
	Maslov et al.	240	

Table 3.1 Thermal cross sections (b) of ^{243}Am

a) Fission			
	Present (JENDL-3.3)	0.0813	
	JENDL-3.2	0.116	
	ENDF/B-VI	0.0739	
	JEFF-3	0.0496	
	Maslov et al.	0.0638	
	Mughabghab [Mu84]	0.1983±0.0043	
	Zhuravlev et al. [Zh75]	0	
	Gavrilov et al. [Ga76]	0.20±0.11	
	Asghar et al. [As79]	0.1983±0.0042 (rel. to 582.2 b of ^{235}U)	
	Wagemans et al. [Wa89]	0.074±0.004	
	Kobayashi et al. [Ko99]	0.0813±0.0025	
b) Capture			
	Present (JENDL-3.3)	76.71	
	JENDL-3.2	78.50	
	ENDF/B-VI	75.08	
	JEFF-3	75.94	
	Maslov et al.	76.71	
	Bak et al. [Ba67]	73±6	
	Folger et al. [Fo68]	78	(absorption cross section)
	Gavrilov et al. [Ga76]	83±6	
c) Elastic scattering			
	Present (JENDL-3.3)	7.46	
	JENDL-3.2	7.48	
	ENDF/B-VI	8.54	
	JEFF-3	7.11	
	Maslov et al.	7.46	
d) Total			
	Present (JENDL-3.3)	84.25	
	JENDL-3.2	86.10	
	ENDF/B-VI	83.69	
	JEFF-3	83.11	
	Maslov et al.	84.23	
	Coté et al. [Co59a]	190	
	Berreth and Simpson [Be70]	85±4	

Table 3.2 Resonance integrals (b) ^{243}Am fission and capture cross sections

a) Fission			
	Present (JENDL-3.3)	7.48	
	Present (JENDL-3.3)	2.26 (0.5 eV – 30 keV)	
	JENDL-3.2	7.59	
	ENDF/B-VI	7.55	
	JEFF-3	6.52	
	Maslov et al.	6.37	
	Zhuravlev et al. [Zh75]	9±1	
	Gavrilov et al. [Ga76]	17.1±1.3	
	Knitter and Budtz-Jørgensen [Kn88]	3.05±0.15	(0.5 eV – 30 keV)
b) Capture			
	Present (JENDL-3.3)	1790	
	JENDL-3.2	1820	
	ENDF/B-VI	1820	
	JEFF-3	1810	
	Maslov et al.	1790	
	Mughabghab [Mu84]	1820±70	
	Bak et al. [Ba67]	2300±200	
	Folger et al. [Fo68]	2250	(absorption)
	Gavrilov et al. [Ga76]	2200±150	

Table 4.1 Thermal cross sections (b) of ^{99}Tc

a) Capture			
	Present (JENDL-3.3)	22.77	
	JENDL-3.2	19.64	
	ENDF/B-VI.8	20.01	
	JEFF-3	19.64	
	Mughabghab et al. [Mu81]	20±1	
	Pattenden [Pa58]	24.8±2.0	
	Tattersall et al. [Ta60]	16±7	
	Ovechkin et al. [Ov74]	24±4	
	Lucas et al. [Lu77]	20±2	
	Harada et al. [Ha95]	22.9±1.3	activation method
b) Elastic scattering			
	Present (JENDL-3.3)	4.562	
	JENDL-3.2	3.422	
	ENDF/B-VI.8	5.776	
	JEFF-3	3.422	
c) Total			
	Present (JENDL-3.3)	27.33	
	JENDL-3.2	23.06	
	ENDF/B-VI.8	25.78	
	JEFF-3	23.06	
	Pattenden [Pa58]	30±2	
	Watanabe and Reeder[Wa70]	24.7±1.7	

Table 4.2 Resonance integral (b) of ^{99}Tc capture cross section

Present (JENDL-3.3)	324	
JENDL-3.2	312	
ENDF/B-VI.8	312	
JEFF-3	312	
Mughabghab [Mu81]	340±20	
Tattersall et al. [Ta60]	60±20	cut-off energy=0.67 eV
Watanabe and Reeder [Wa70]	340±20	
Lucas et al. [Lu77]	186±16	non 1/v only
Harada et al. [Ha95]	398±38	activation method

Table 4.3 Optical potential parameters for n + ^{99}Tc Reaction

For JENDL-3.2 evaluation

Potential shape: Derivative Woods-Saxon for imaginary part

Depth (MeV)	Radius (fm)	Diffuseness (fm)
V=47.5	5.972	0.62
Ws= 9.74	6.594	0.35
Vso= 7.0	5.97	0.62

For the present evaluation

Potential shape: Derivative Woods-Saxon for imaginary part

Depth (MeV)	Radius (fm)	Diffuseness (fm)
V=45.5 – 0.48*En	1.350*A**(1/3)	0.60
Ws= 6.79+0.83*E	1.330*A**(1/3)	0.40
Vso= 7.0	1.350*A**(1/3)	0.60

A: mass number

Table 4.4 Parameters used in CASTHY calculation for ^{99}Tc data

a) Level density parameters

Nuclide	a(1/MeV)	T(MeV)	C(1/MeV)	Ex(MeV)	Pairing (MeV)
^{99}Tc	16.0	0.655	2.973	5.984	1.290
^{100}Tc	16.37	0.585	11.89	3.635	0.0

b) Gamma-ray strength function

8.01×10^{-3}: adjusted to reproduce the capture cross section of about 620 mb at 50 keV

c) Excited levels

No.	Energy(MeV)	Spin-parity		
0	0.0	9/2	+	
1	0.1405	7/2	+	*
2	0.1427	1/2	−	
3	0.1811	5/2	+	*
4	0.5091	3/2	−	
5	0.5344	3/2	+	
6	0.5369	5/2	+	
7	0.6125	5/2	−	*
8	0.6254	9/2	+	*
9	0.6715	3/2	−	
10	0.7198	7/2	+	*
11	0.7267	11/2	+	*
12	0.7617	5/2	+	*
13	0.7619	13/2	+	*
14	0.9206	1/2	+	
15	0.9861	7/2	−	*
16	1.0041	3/2	−	
17	1.0175			continuum

Table 4.5 Maxwellian-averaged ^{99}Tc capture cross section (b) at kT=30 keV

Present (JENDL-3.3)	0.806
JENDL-3.2	0.786
ENDF/B-VI.8	0.805
JEFF-3	0.786
Bao et al. [Ba00]*	0.781±0.050
Gunsing et al.[Gu01]	0.933

*) recommended value

Table 5.1 Thermal cross sections (b) of ^{140}Ce

a) Capture		
Present (JENDL-3.3)	0.570	
JENDL-3.2	0.570	
ENDF/B-VI	0.505	
JEFF-3	0.574	
Mughabghab et al. [Mu81]	0.57±0.04	
Katcoff et al. [Ka49]	0.31±0.07	Maxwell av.
Hughes and Sherman [Hu50]	0.24	Maxwell av.
Pomerance [Po52]	0.63±10%	Maxwell av.
Alstad et al. [Al67]	0.54±0.02	Maxwell av.
Lantz et al. [La64]	0.59±0.06	Activation method
Alian et al. [Al73]	0.68	Maxwell av.
b) Elastic scattering		
Present (JENDL-3.3)	2.883	
JENDL-3.2	2.830	
ENDF/B-VI	4.93	
JEFF-3	3.264	
Mughabghab et al. [Mu81]	2.83±0.11	
Koehler and Wollan [Ko53]	2.8±0.1	
Vertebnyj et al. [Ve70]	4.0±0.2	
c) Total		
Present (JENDL-3.3)	3.453	
JENDL-3.2	3.400	
ENDF/B-VI	5.50	
JEFF-3	3.838	

Table 5.2 Resonance integral (b) of ^{140}Ce capture cross section

Present (JENDL-3.3)	0.344	
JENDL-3.2	0.278	
ENDF/B-VI	0.446	
JEFF-3	0.336	
Mughabghab [Mu81]	0.47±0.05	
Lantz et al. [La64]	0.48±0.05	activation
Alstad et al. [Al67]	0.49±0.05	E=0.4 eV – 1.0 MeV
Ricabarra et al. [Ri68]	0.25±0.03	
Steinnes [St72]	0.48±0.05	Cut-off=0.5 eV
Alian et al. [Al73]	0.66	Cut-off=0.5 eV
Van der Linden et al. [Va74]	0.43±0.02	
Heft [He78]	0.483±0.005	Cut-off=0.5 eV

Table 5.3 Maxwellian averaged ^{140}Ce capture cross section (mb)

References	kT=25 keV	kT=30 keV
Present (JENDL-3.3)	11.0	10.0
JENDL-3.2	8.11	7.46
ENDF/B-VI	24.8	22.9
JEFF-3	18.9	18.5
Xia et al. [Xi90]	15.33±1.0[a]	
Käppeler et al. [Ka96]	12.0±0.4	11.0±0.4
Bao et al. [Ba00]*		11.0±0.4

*) recommended value
a) at 24 keV

Table 5.4 Optical potential parameters for n + ^{140}Ce Reaction

For JENDL-3.2 evaluation

Potential shape: Derivative Woods-Saxon for imaginary part

Depth (MeV)	Radius (fm)	Diffuseness (fm)
V= 41.8	6.89	0.62
Ws= 2.95+0.789*En	7.098	0.35
Vso= 7.0	6.89	0.62

For the present evaluation

Potential shape: Derivative Woods-Saxon for imaginary part

Depth (MeV)	Radius (fm)	Diffuseness (fm)
V=45.36 – 0.342*En	1.307*A**(1/3)	0.62
Ws= 9.763+0.4167*En	1.280*A**(1/3)	0.35
Vso= 7.0	1.307*A**(1/3)	0.62

A: Mass number

Table 5.5 Parameters used in CASTHY calculation for ^{140}Ce data

a) Level density parameters

Nuclide	a(1/MeV)	T(MeV)	C(1/MeV)	Ex(MeV)	Pairing
^{140}Ce	14.13	0.6541	0.3376	5.852	2.020
^{141}Ce	17.14	0.5150	0.7134	3.957	1.170

b) Gamma-ray strength function

5.73×10^{-6}: Adjusted to reproduce the capture cross section of 4.7 mb at 500 keV

c) Excited levels

No.	Energy(MeV)	Spin-parity		
0	0.0	0	+	
1	1.5962	2	+	*
2	1.9033	0	+	
3	2.0833	4	+	
4	2.1079	6	+	
5	2.3479	2	+	
6	2.3498	5	+	
7	2.4120	3	+	
8	2.4641	3	−	*
9	2.4809	4	+	
10	2.5158	4	+	
11	2.5214	2	+	
12	2.5473	1	+	
13	2.6289	6	+	
14	2.8997	2	+	
15	3.0011	2	+	
16	3.0168	0	+	
17	3.040	3	−	
18	3.1186	2	+	
19	3.226	0	+	
20	3.3204	2	+	
21	3.331	4	+	
22	3.3947	4	−	
23	3.3951	4	+	
	3.4246			continuum

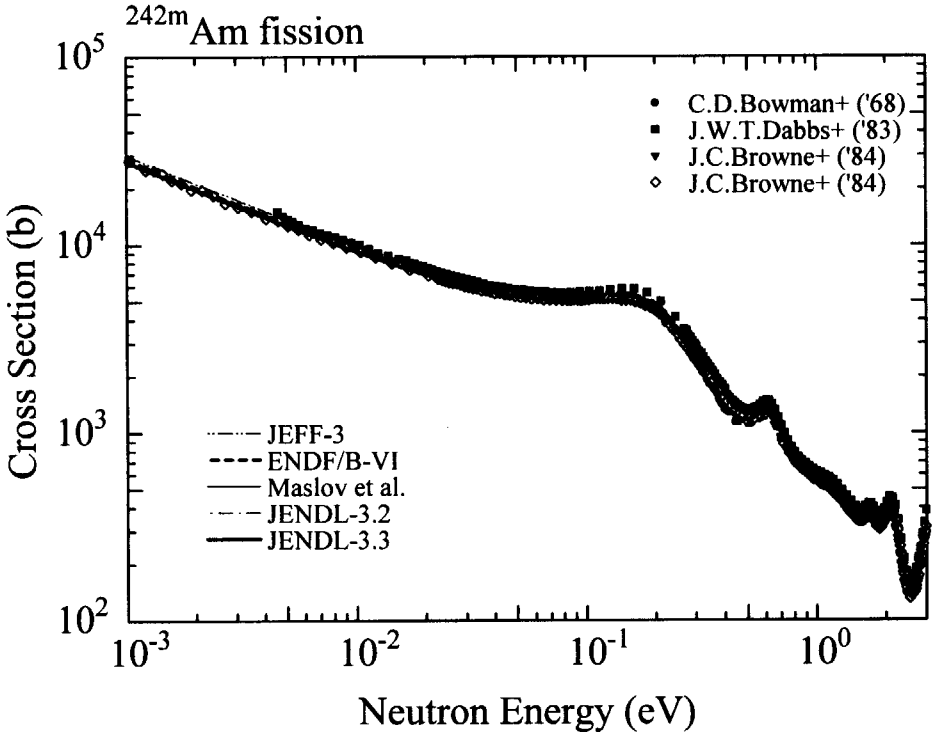

Fig. 2.1(a) ^{242m}Am fission cross section (0.001 – 3 eV)
Experimental data: Bowman+('68)[Bo68a], Dabbs+('83)[Da83], Browne+('84)[Br84]

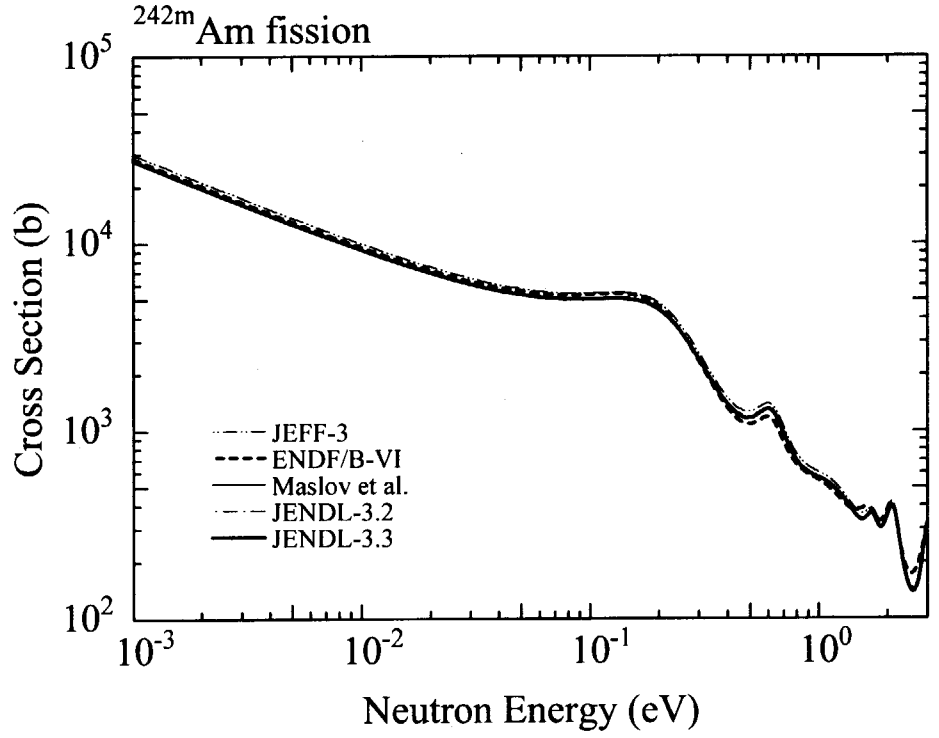

Fig. 2.1(a)-2 ^{242m}Am fission cross section (0.001 – 3 eV, Evaluated data only)

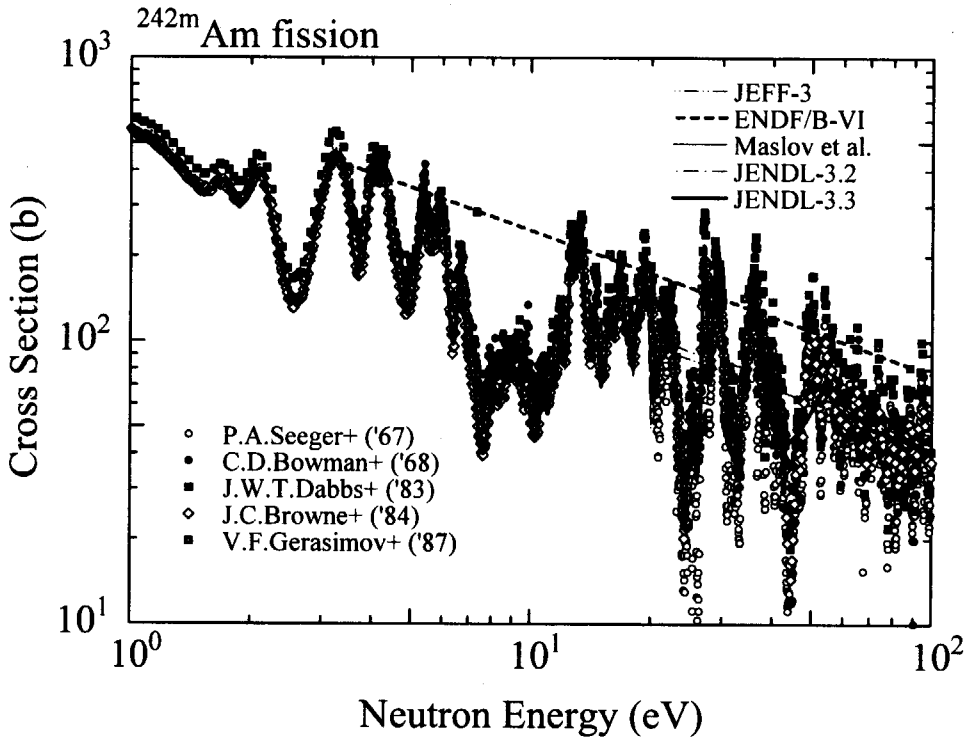

Fig. 2.1(b)-1 ^{242m}Am fission cross section (1 – 100 eV)
Experimental data: Seeger+('67)[Se67], Bowman+('68)[Bo68a], Dabbs+('83)[Da83], Browne+('84)[Br84], Gerasimov+('87)[Ge87]

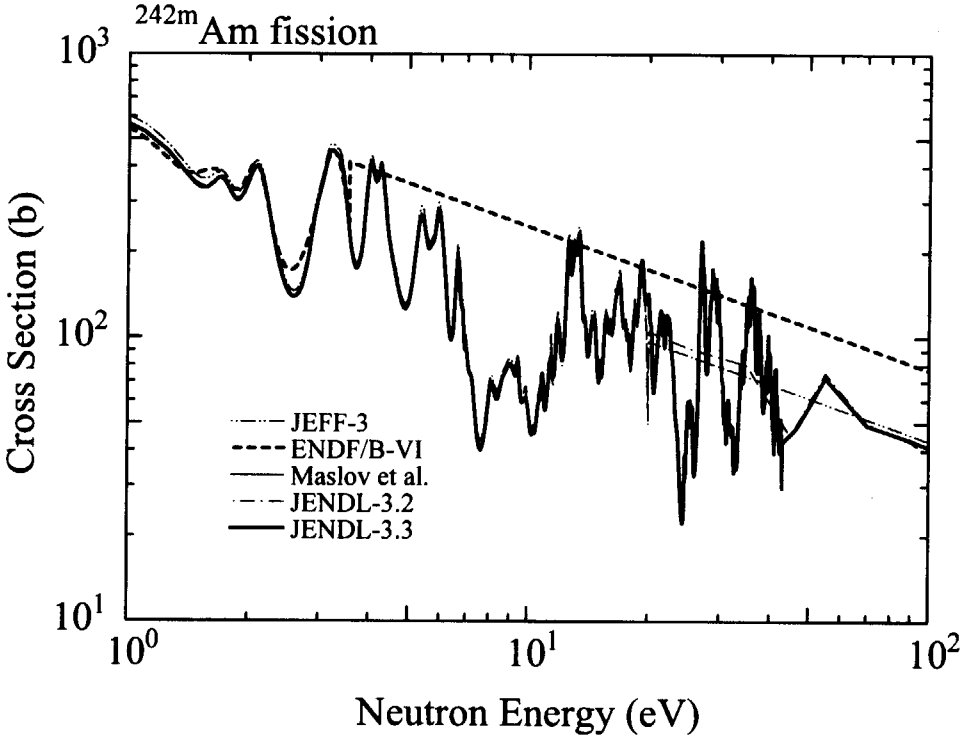

Fig. 2.1(b)-2 ^{242m}Am fission cross section (1 – 100 eV, Evaluated data only)

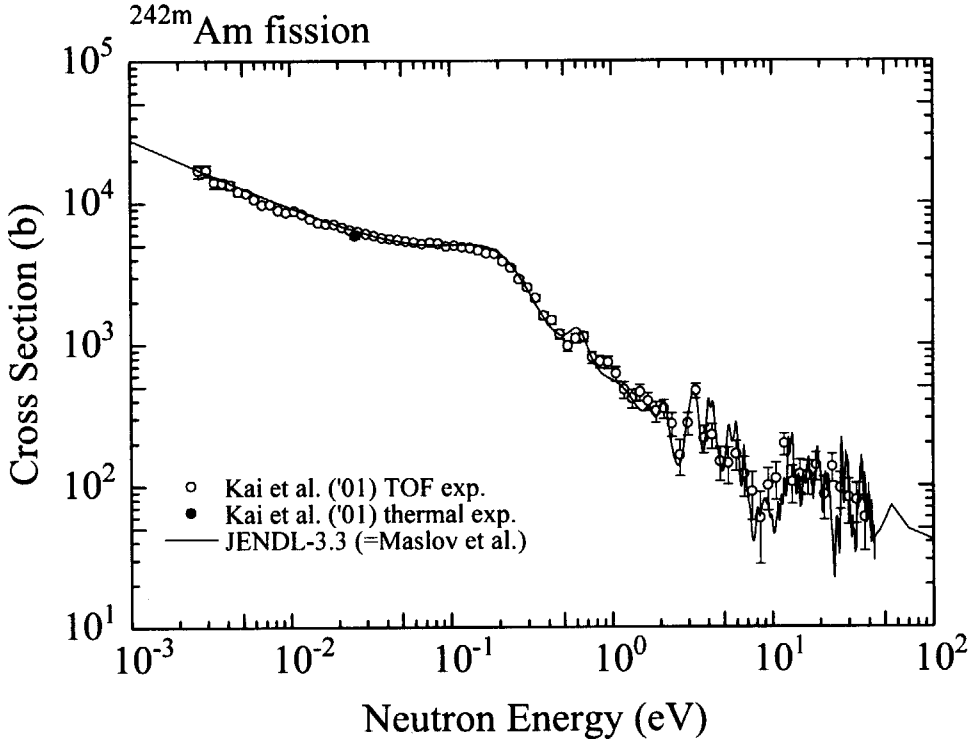

Fig. 2.2 ^{242m}Am fission cross section (comparison with TOF measurement by Kai et al. [Ka01a]

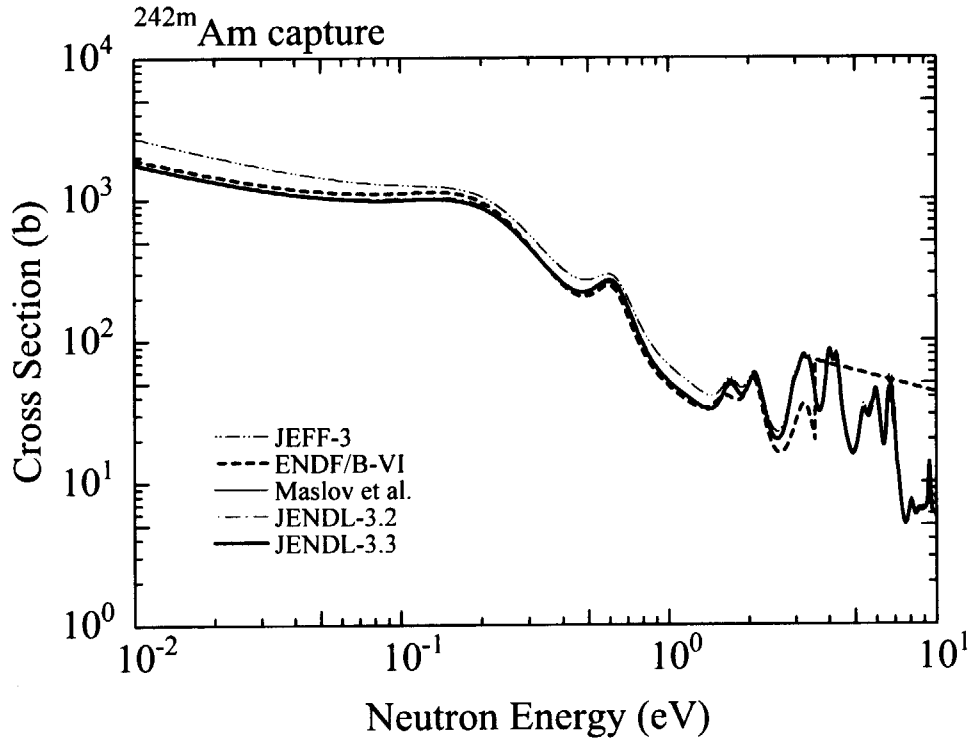

Fig. 2.3 ^{242m}Am capture cross section (0.01 – 10 eV)

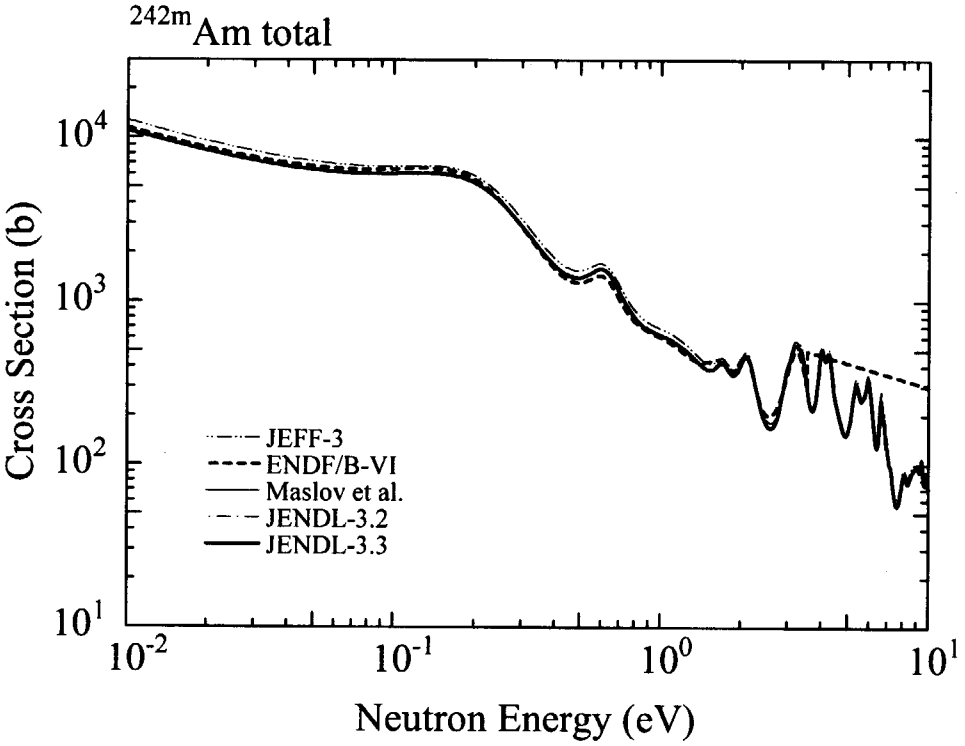

Fig. 2.4 ^{242m}Am total cross section (0.01 – 10 eV)

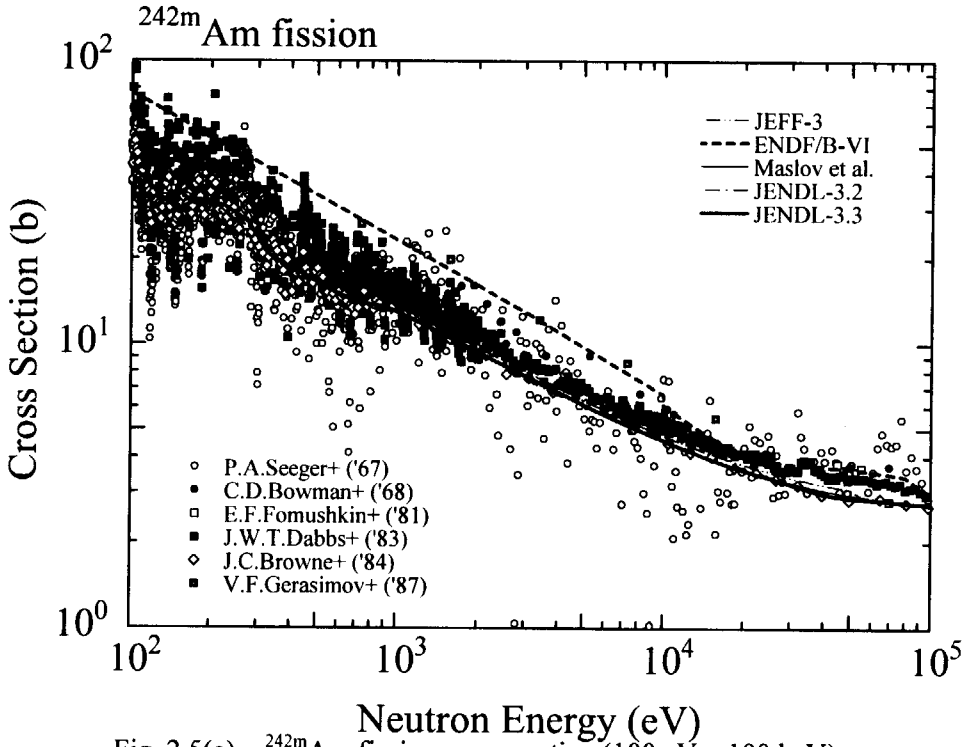

Fig. 2.5(a) ^{242m}Am fission cross section (100 eV – 100 keV)

Experimental data: Seeger+(67)[Se67], Bowman+('68)[Bo68a], Fomushkin+('81)[Fo81] Dabbs+('83)[Da83], Browne+('84)[Br84], Gerasimov+('87)[Ge87]

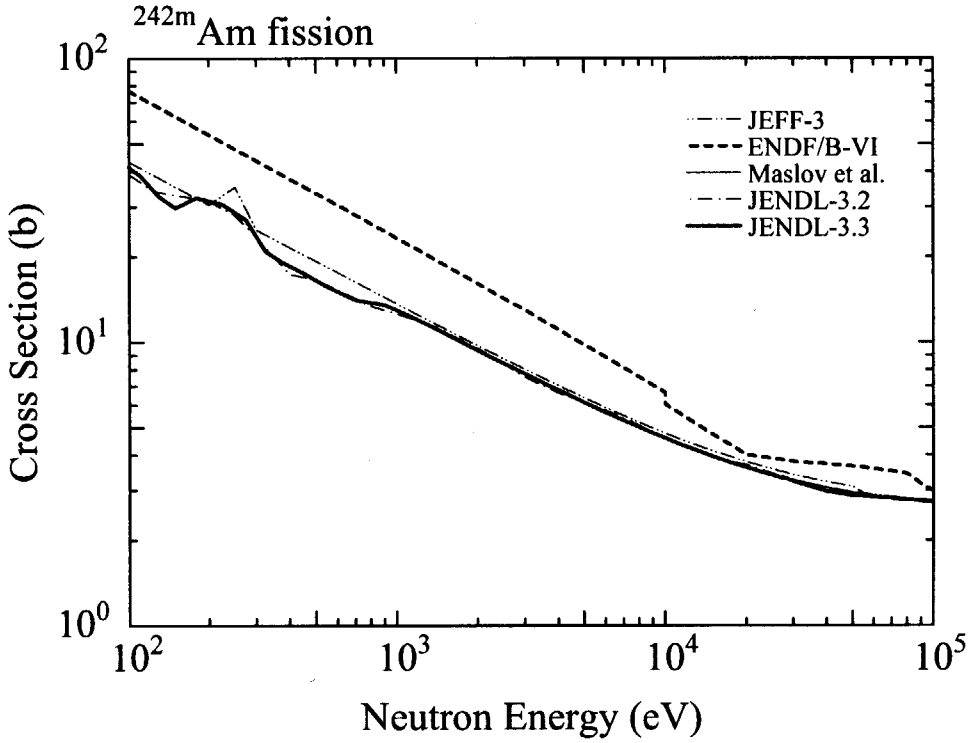

Fig. 2.5(b) ^{242m}Am fission cross section (100 eV – 100 keV, Evaluated data only)

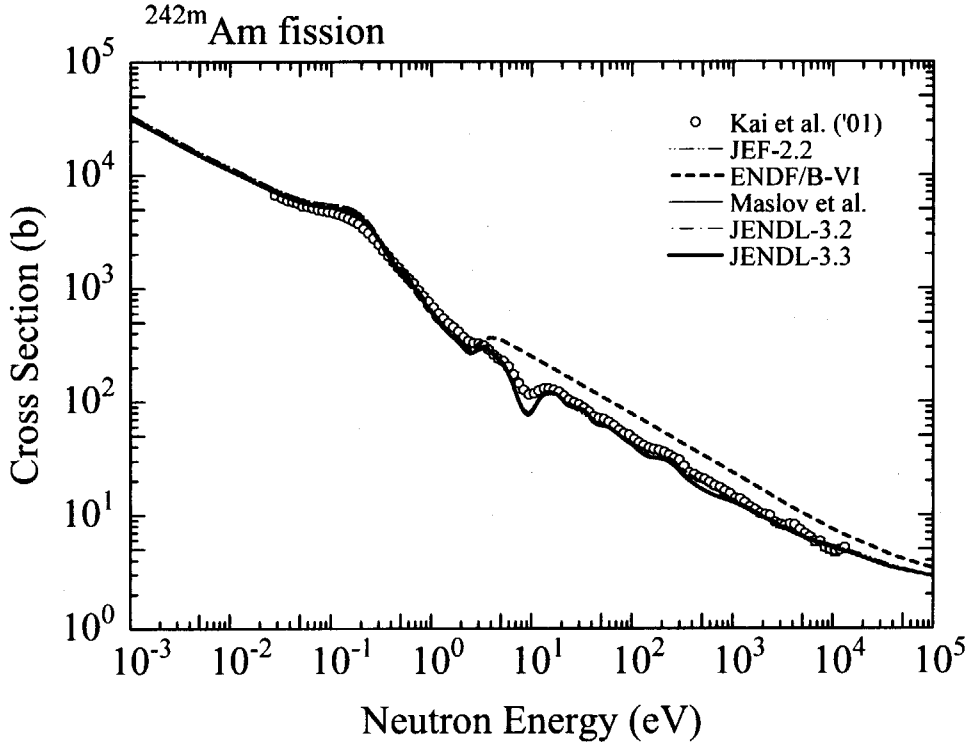

Fig. 2.6 ^{242m}Am fission cross section (comparison with KULS measurement by Kai et al.[Ka01a]

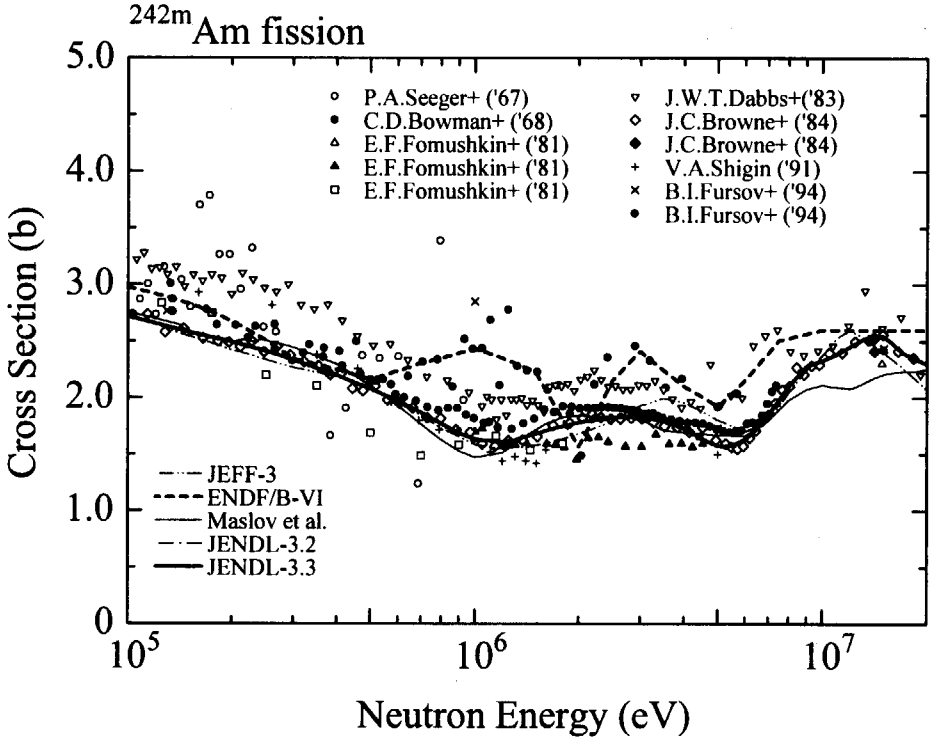

Fig. 2.7 ^{242m}Am fission cross section (100 keV – 20 MeV)
Experimental data: Seeger+('67)[Se67], Bowman+('68)[Bo68a], Fomushkin+('81)[Fo81], Dabbs+('83)[Da83], Browne+('84)[Br84], Shigin('91)[Sh91], Fursov+('94)[Fu94]

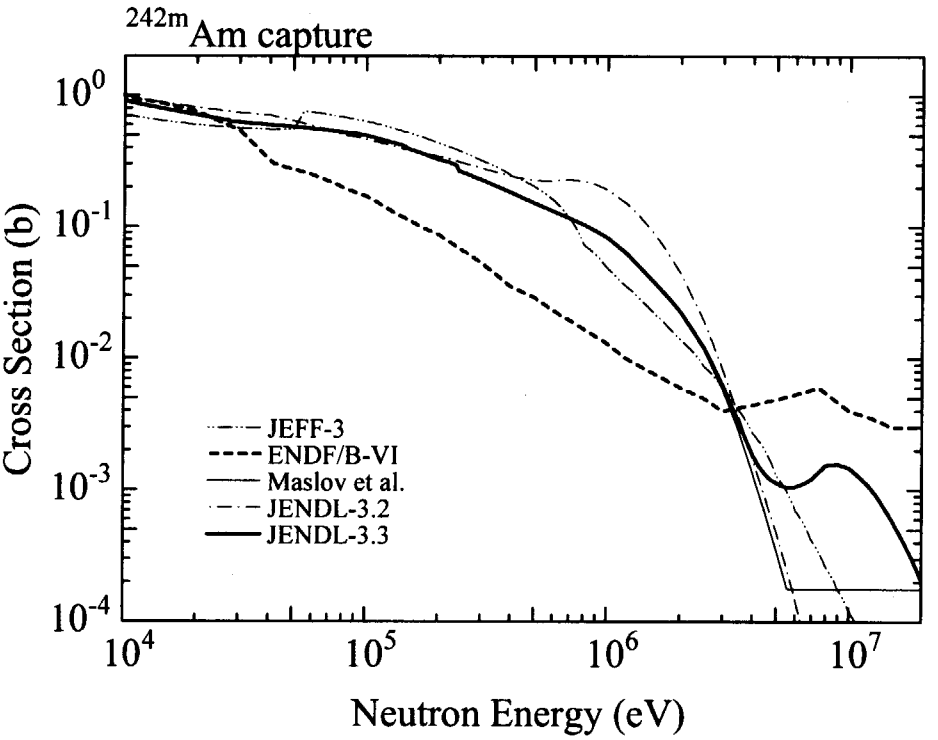

Fig. 2.8 ^{242m}Am capture cross section (10 keV – 20 MeV)

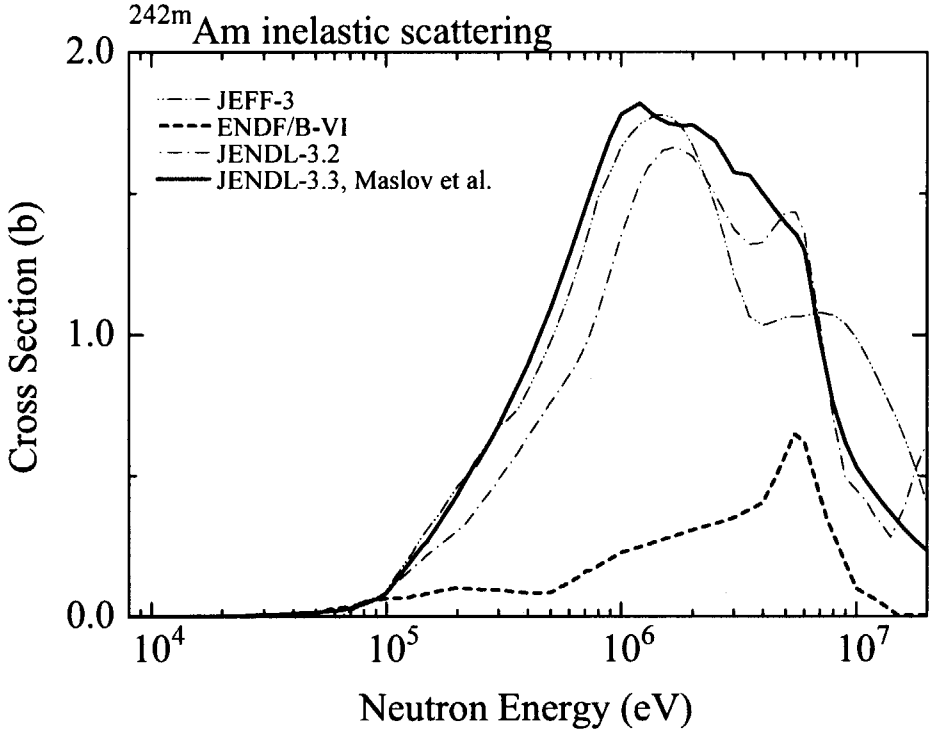

Fig. 2.9 ^{242m}Am inelastic scattering cross section

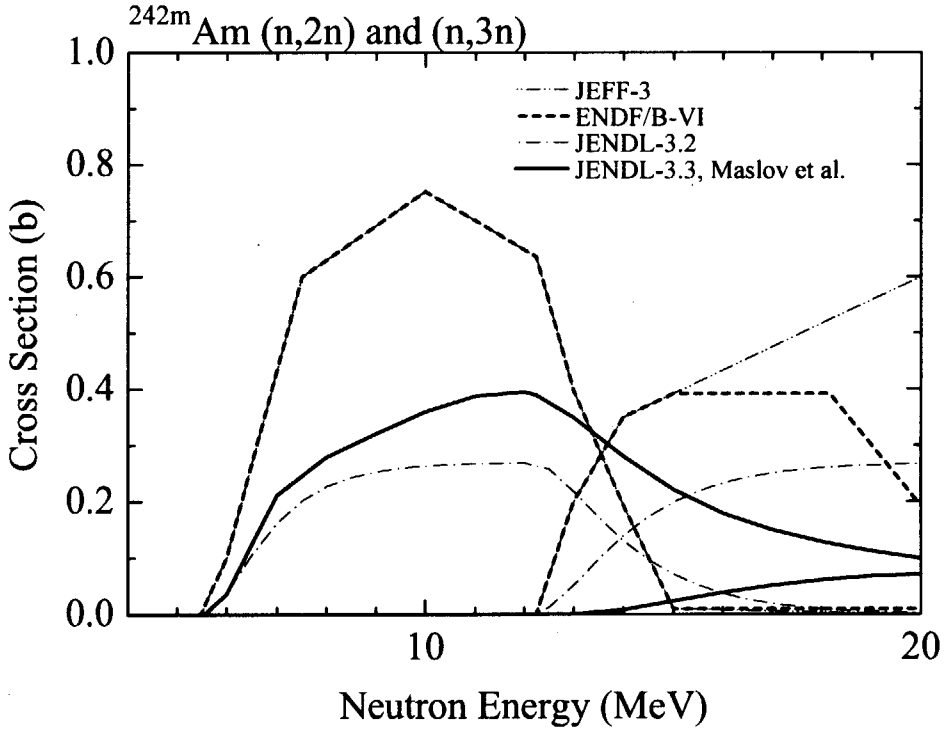

Fig. 2.10 ^{242m}Am (n,2n) and (n,3n) reaction cross sections

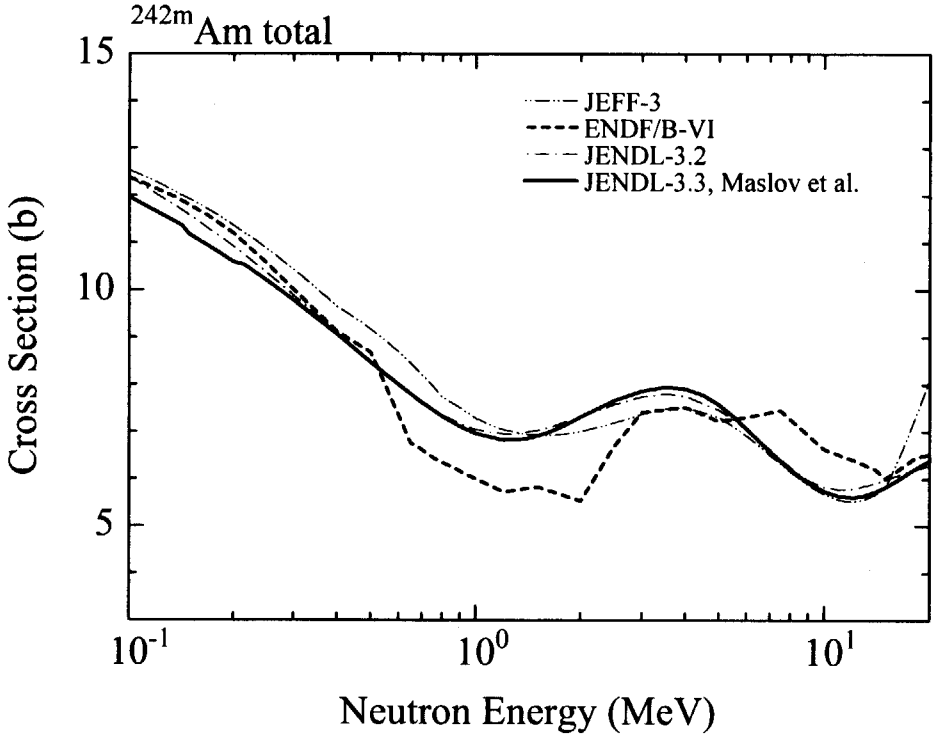

Fig. 2.11 ^{242m}Am total cross section (0.1 – 20 MeV)

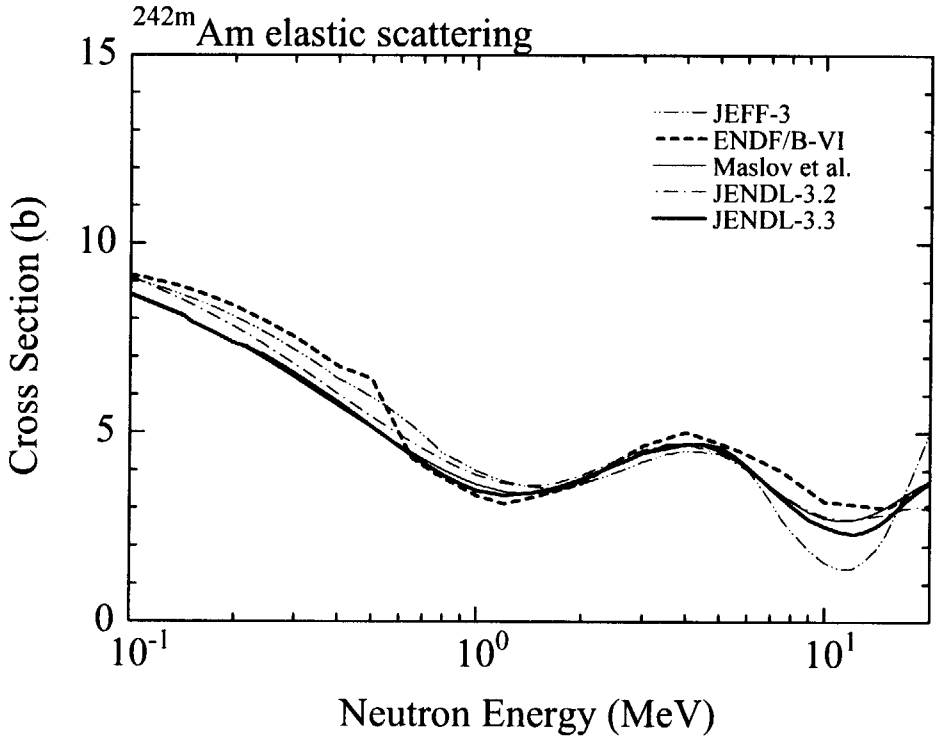

Fig. 2.12 ^{242m}Am elastic scattering cross section (0.1 – 20 MeV)

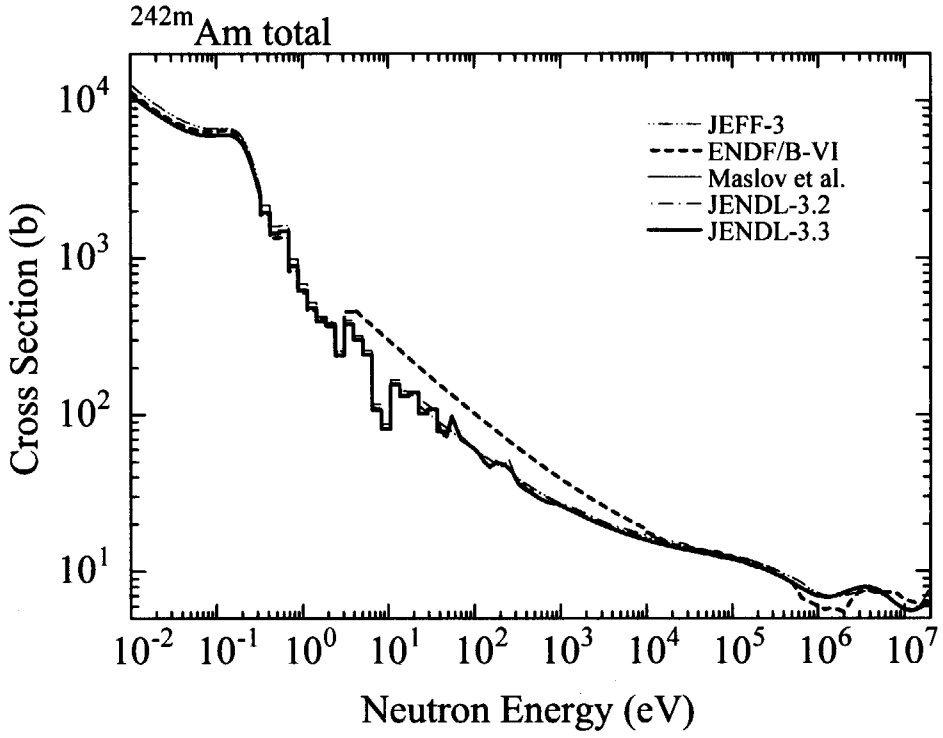

Fig. 2.13 ^{242m}Am total cross section (thermal energy – 20 MeV)

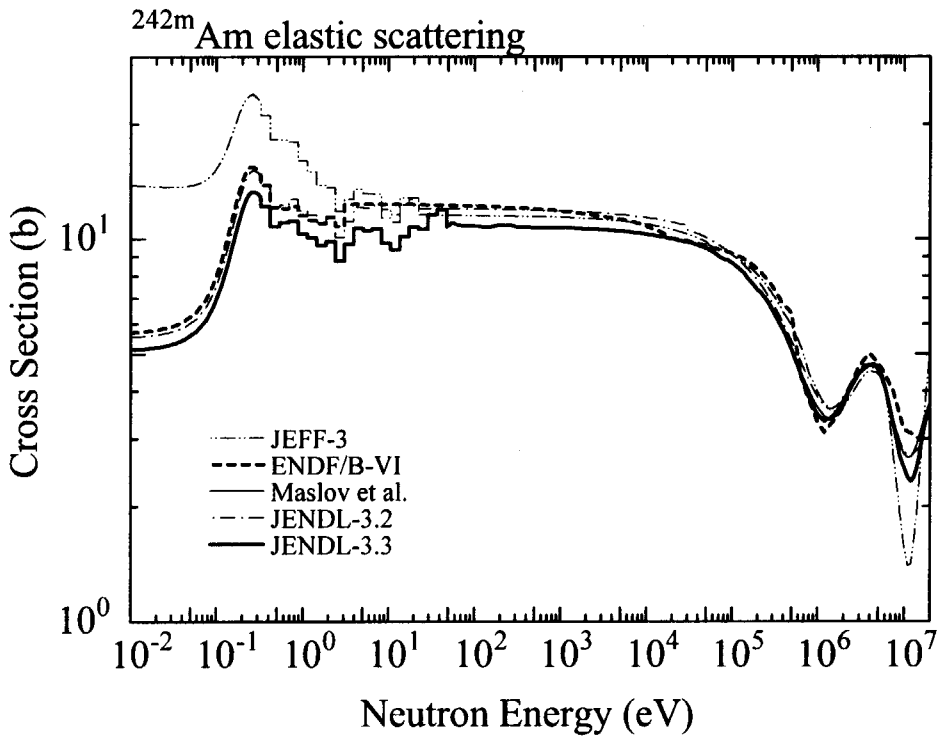

Fig. 2.14 ^{242m}Am elastic scattering cross section (thermal energy – 20 MeV)

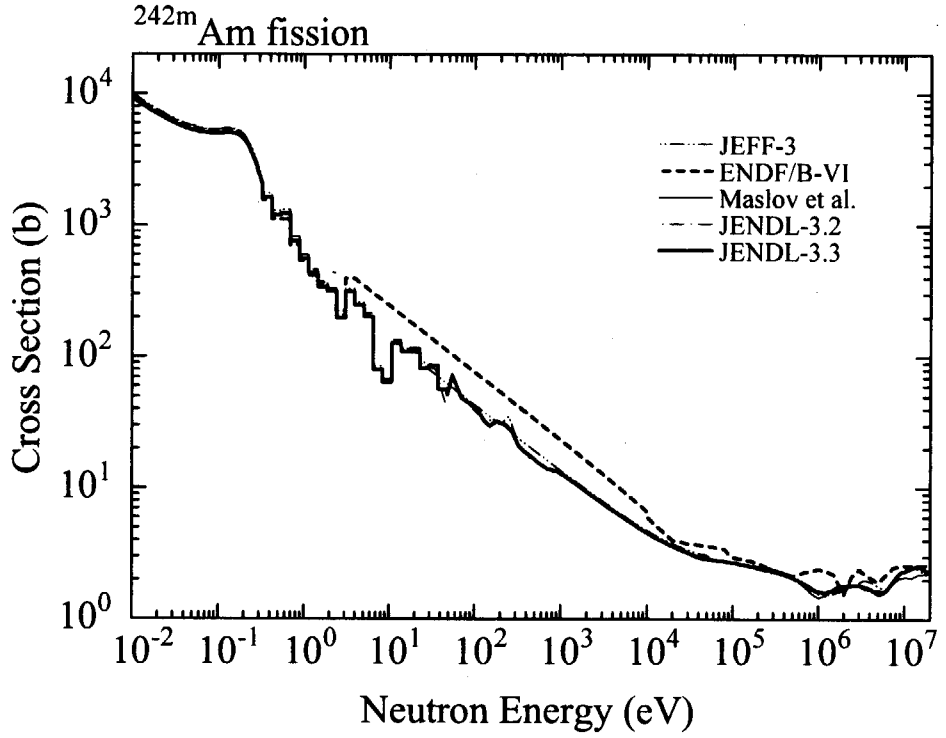

Fig. 2.15 ^{242m}Am fission cross section (thermal energy – 20 MeV)

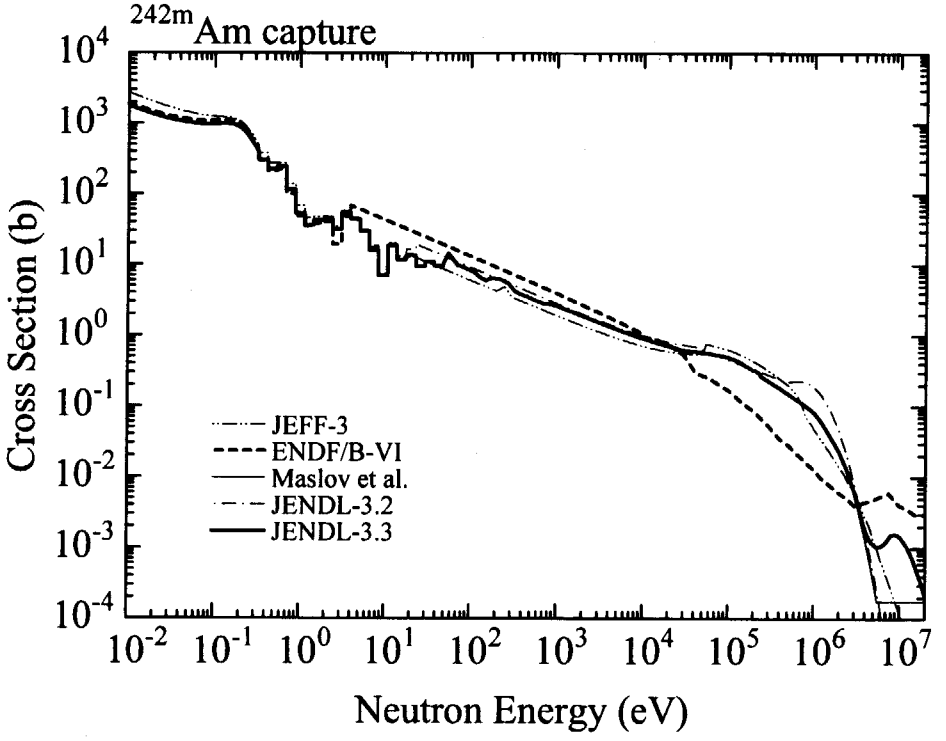

Fig. 2.16 ^{242m}Am capture cross section (thermal energy – 20 MeV)

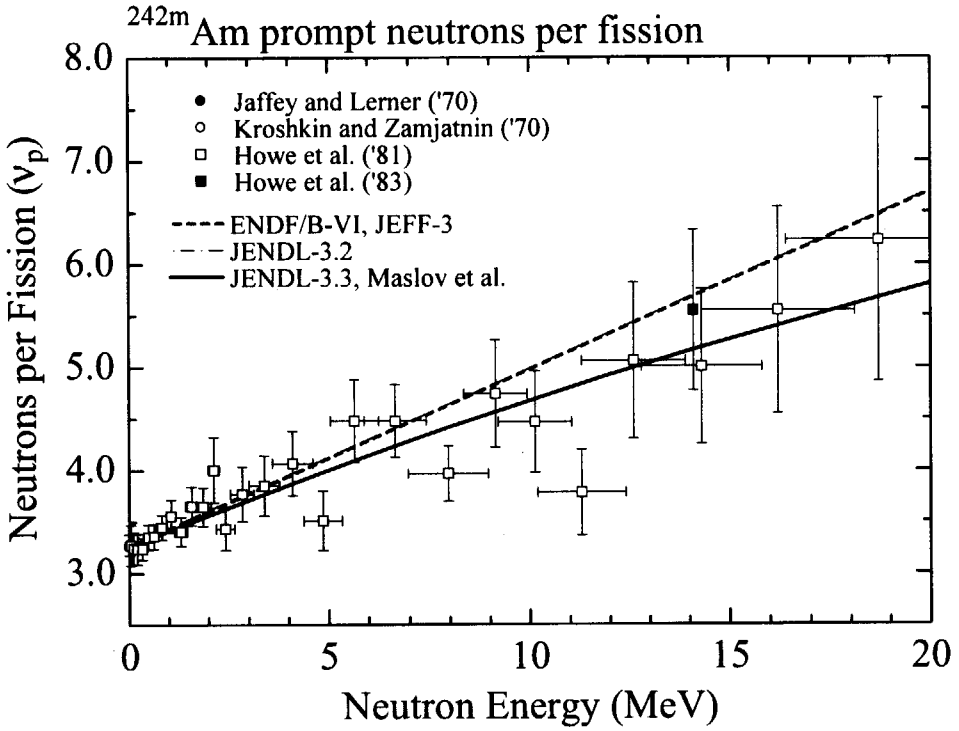

Fig. 2.17 ^{242m}Am prompt neutrons per fission
Experimental data: Jaffy and Lerner('70)[Ja70], Kroshkin and Zamjatnin('70)[Kr70], Howe et al.('81)[Ho81], Howe et al.('83)[Ho83]

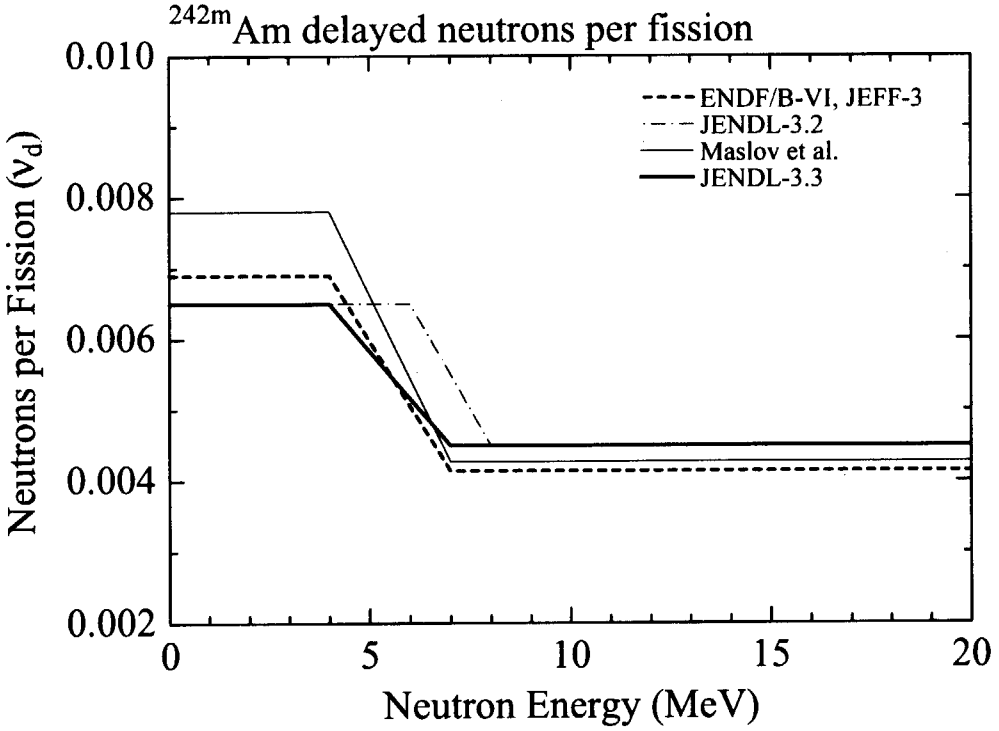

Fig. 2.18 ^{242m}Am delayed neutrons per fission

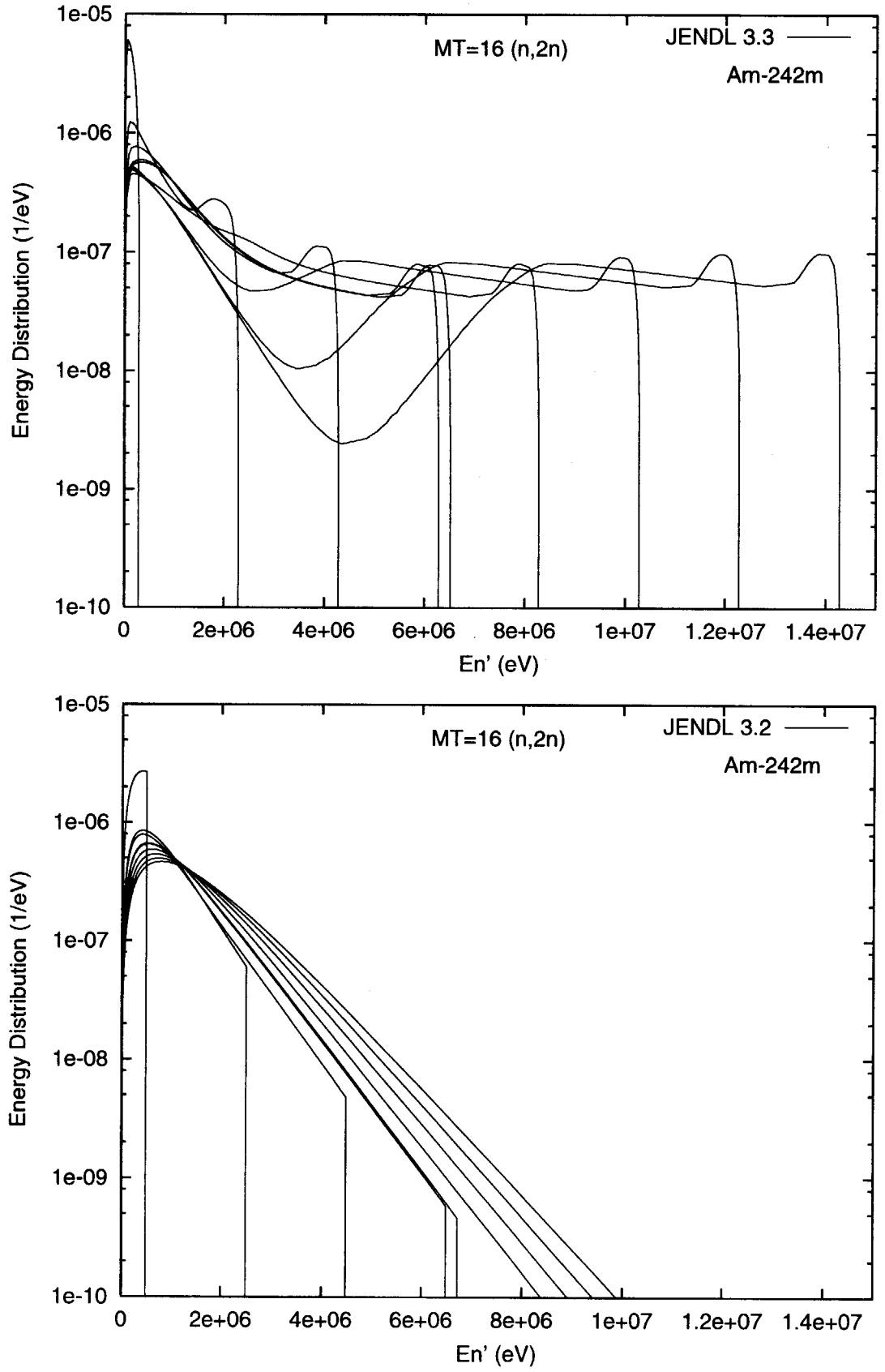

Fig. 2.19(a) ^{242m}Am (n,2n) neutron spectra

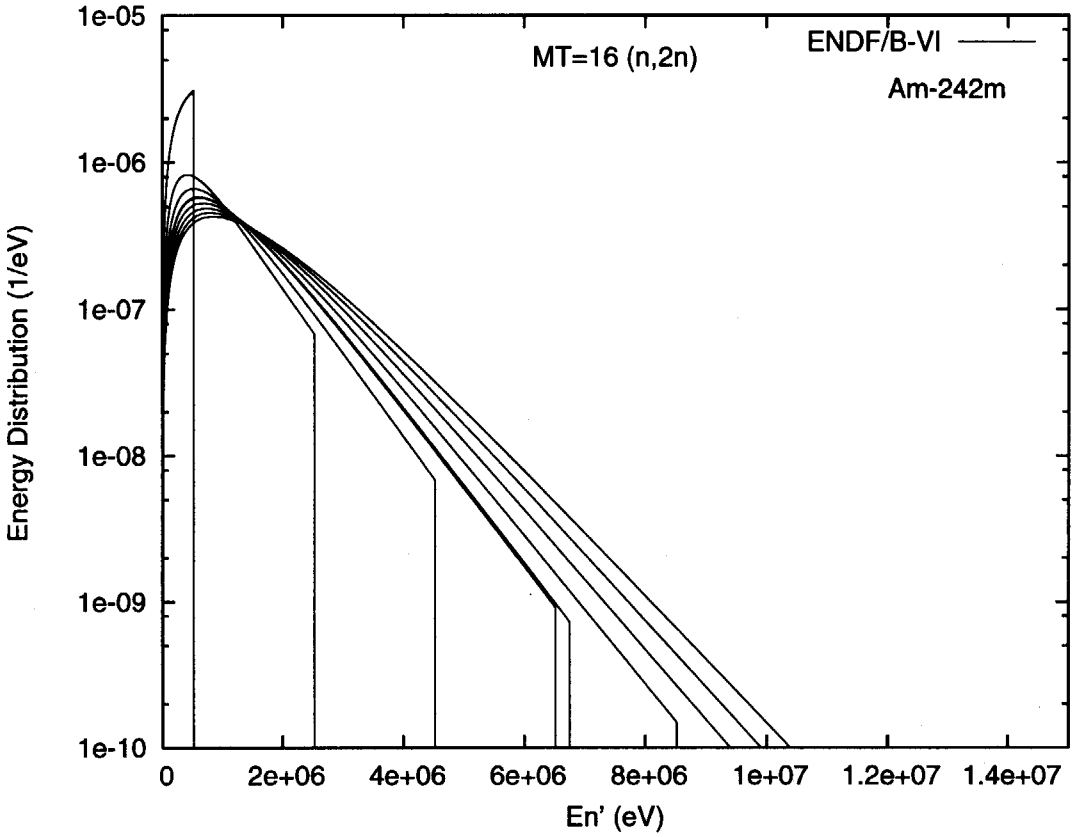

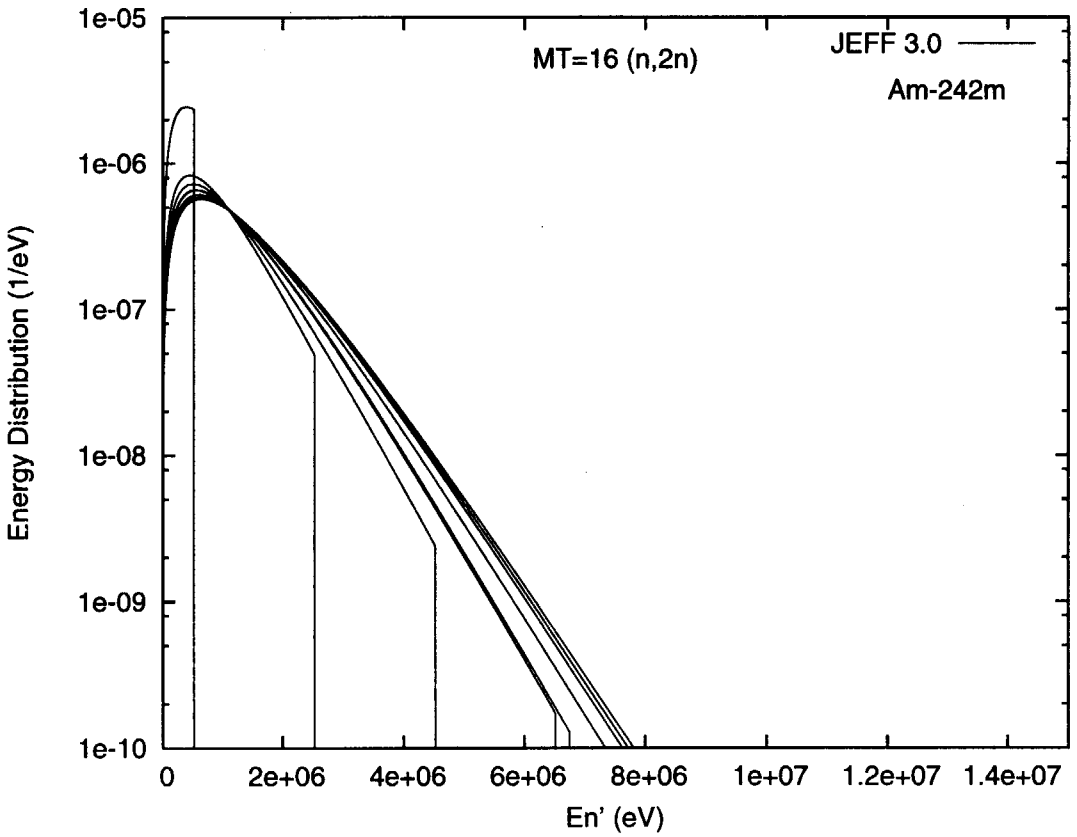

Fig. 2.19(b) ^{242m}Am (n,2n) neutron spectra

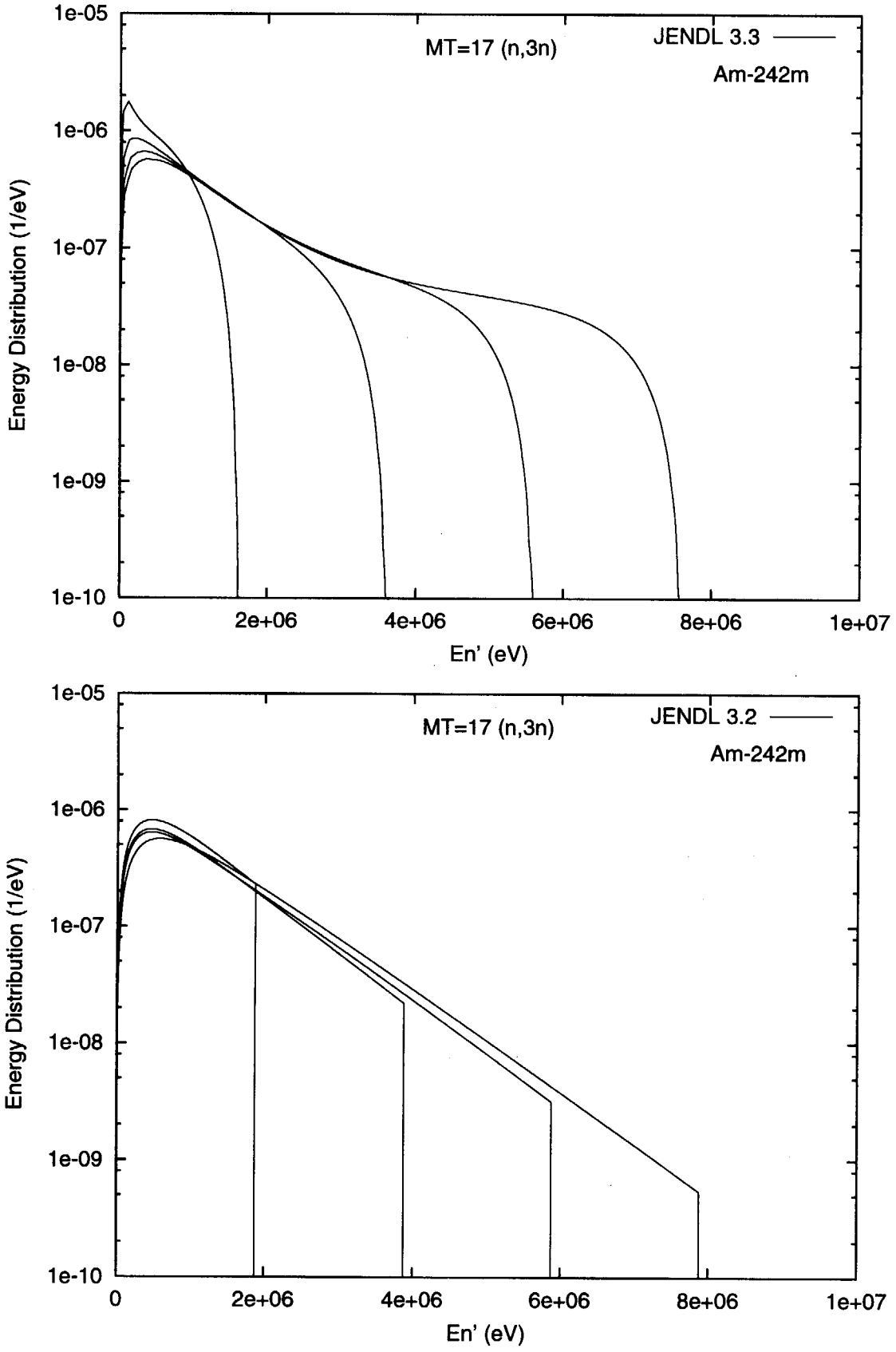

Fig. 2.20(a) ^{242m}Am (n,3n) neutron spectra

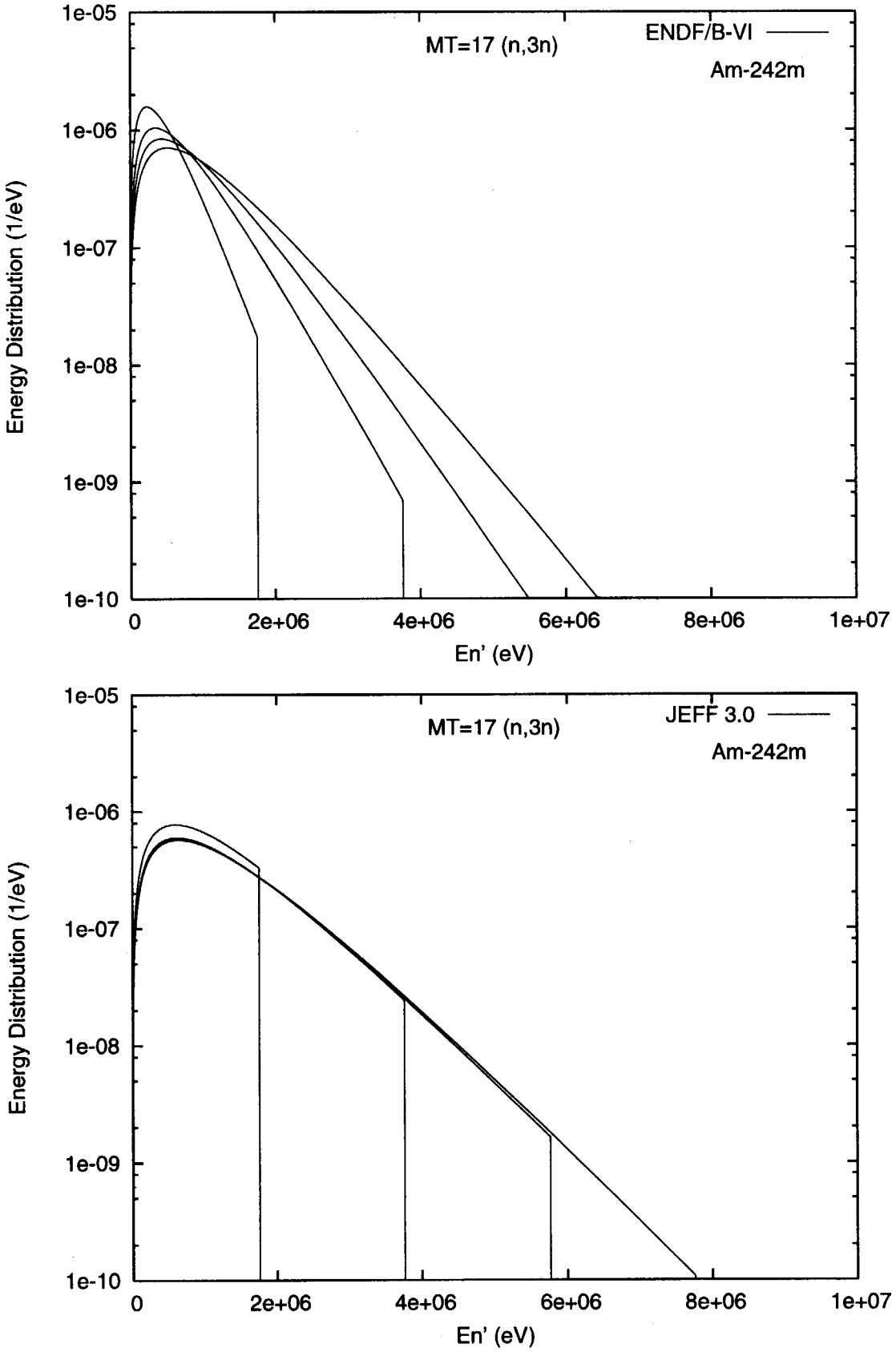

Fig. 2.20(b) ^{242m}Am (n,3n) neutron spectra

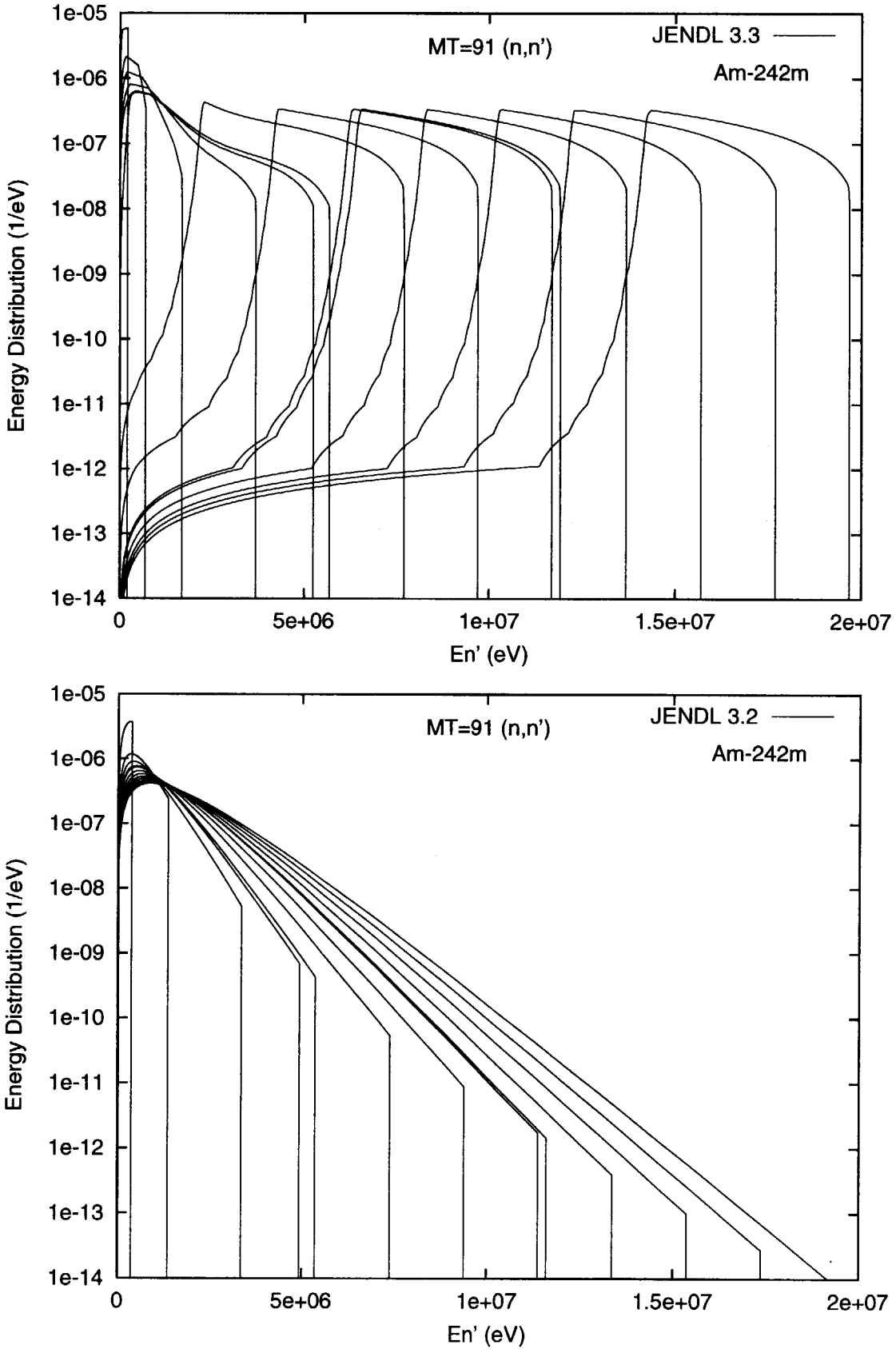

Fig. 2.21(a) ^{242m}Am (n,n') neutron spectra

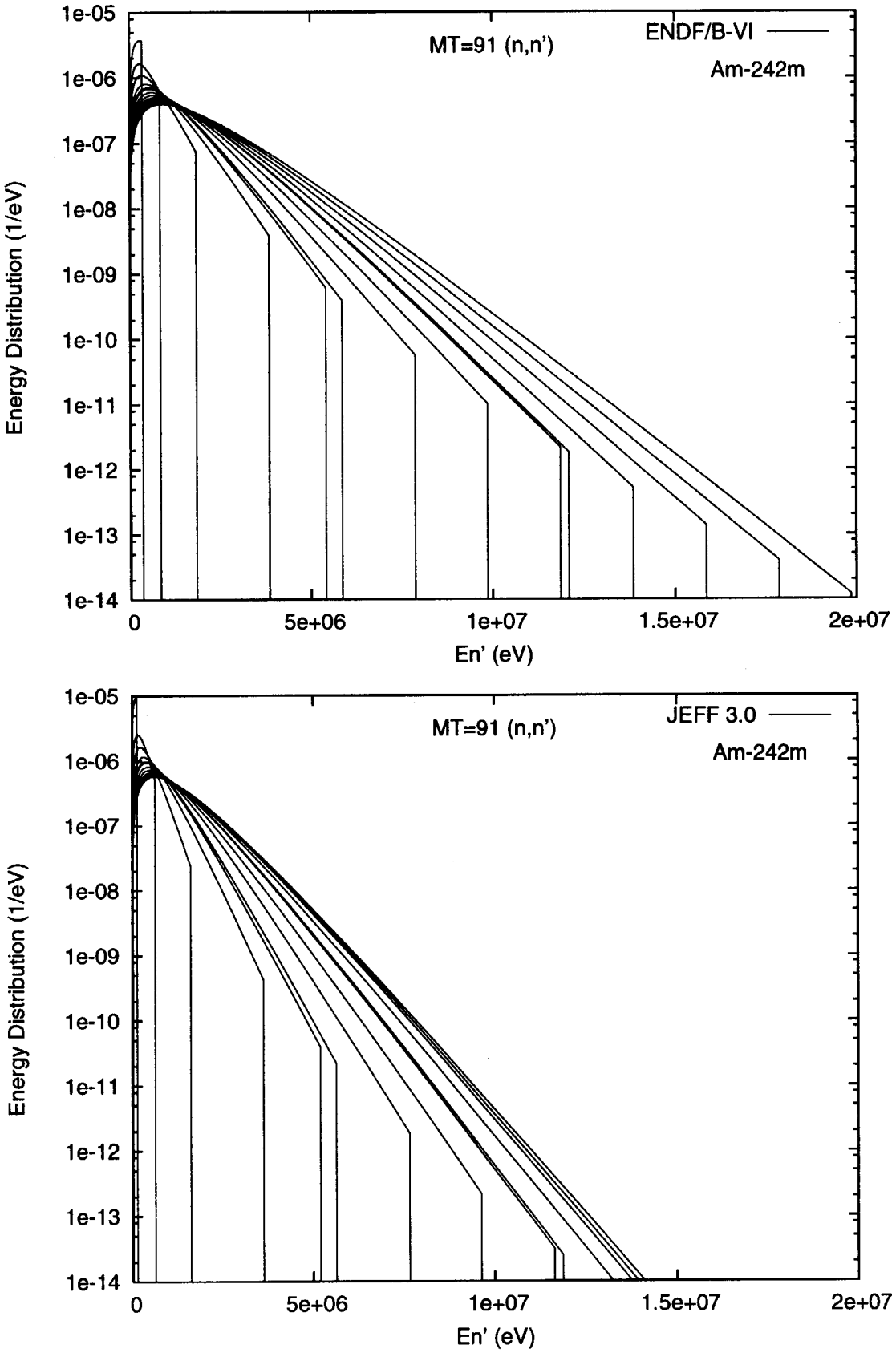

Fig. 2.21(b) ^{242m}Am (n,n') neutron spectra

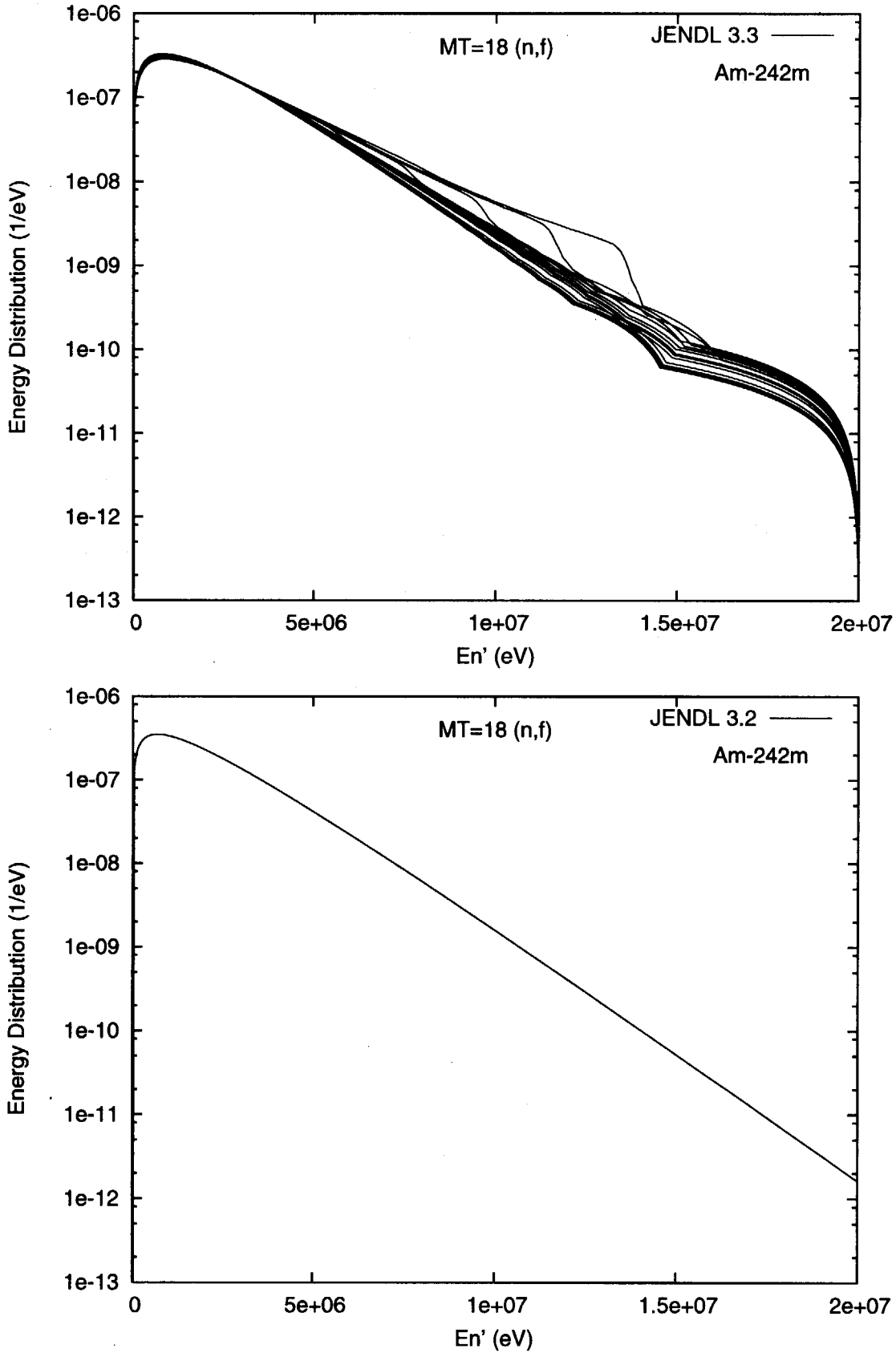

Fig. 2.22(a) ^{242m}Am fission neutron spectra

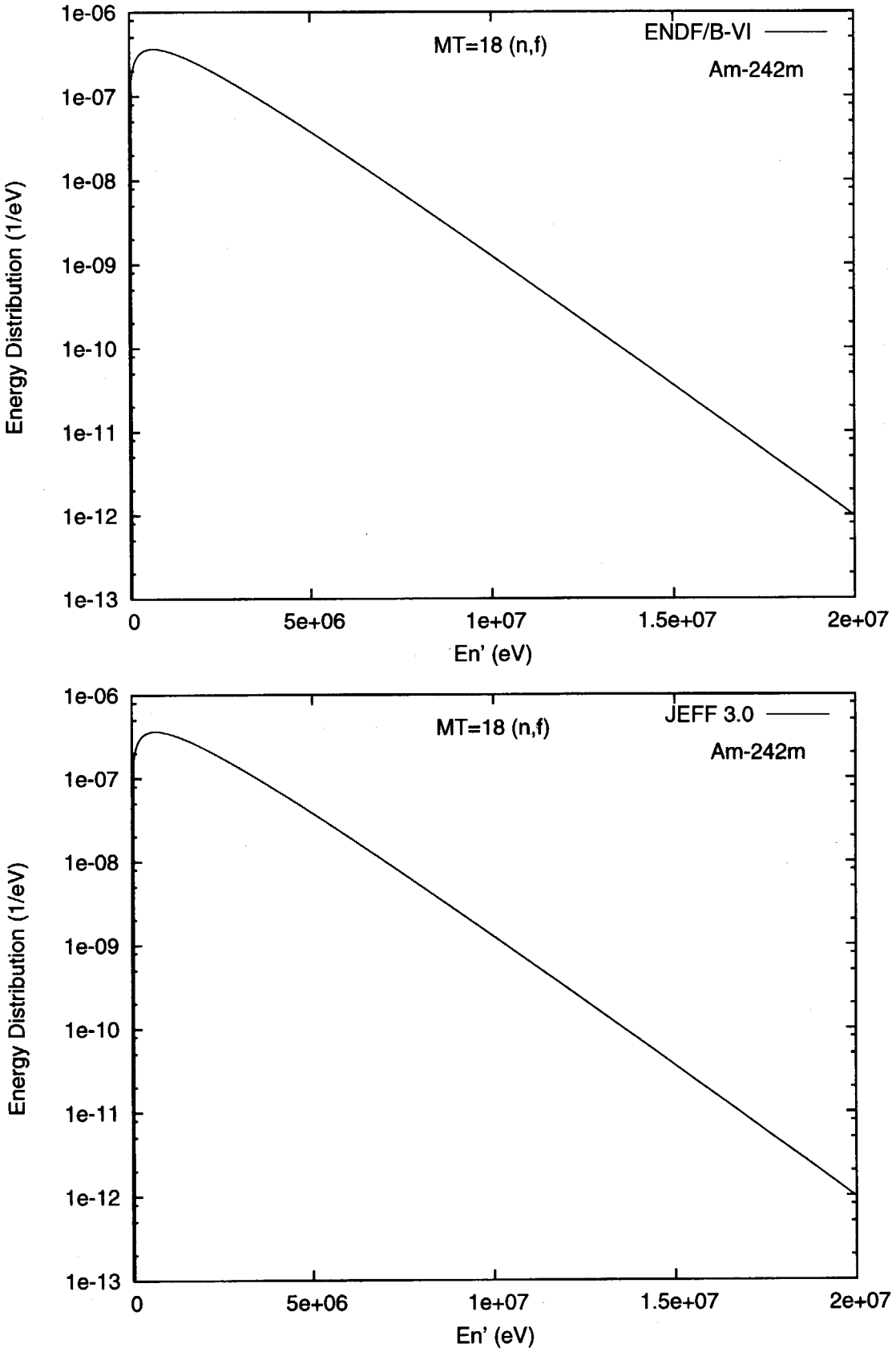

Fig. 2.22(b) ^{242m}Am fission neutron spectra

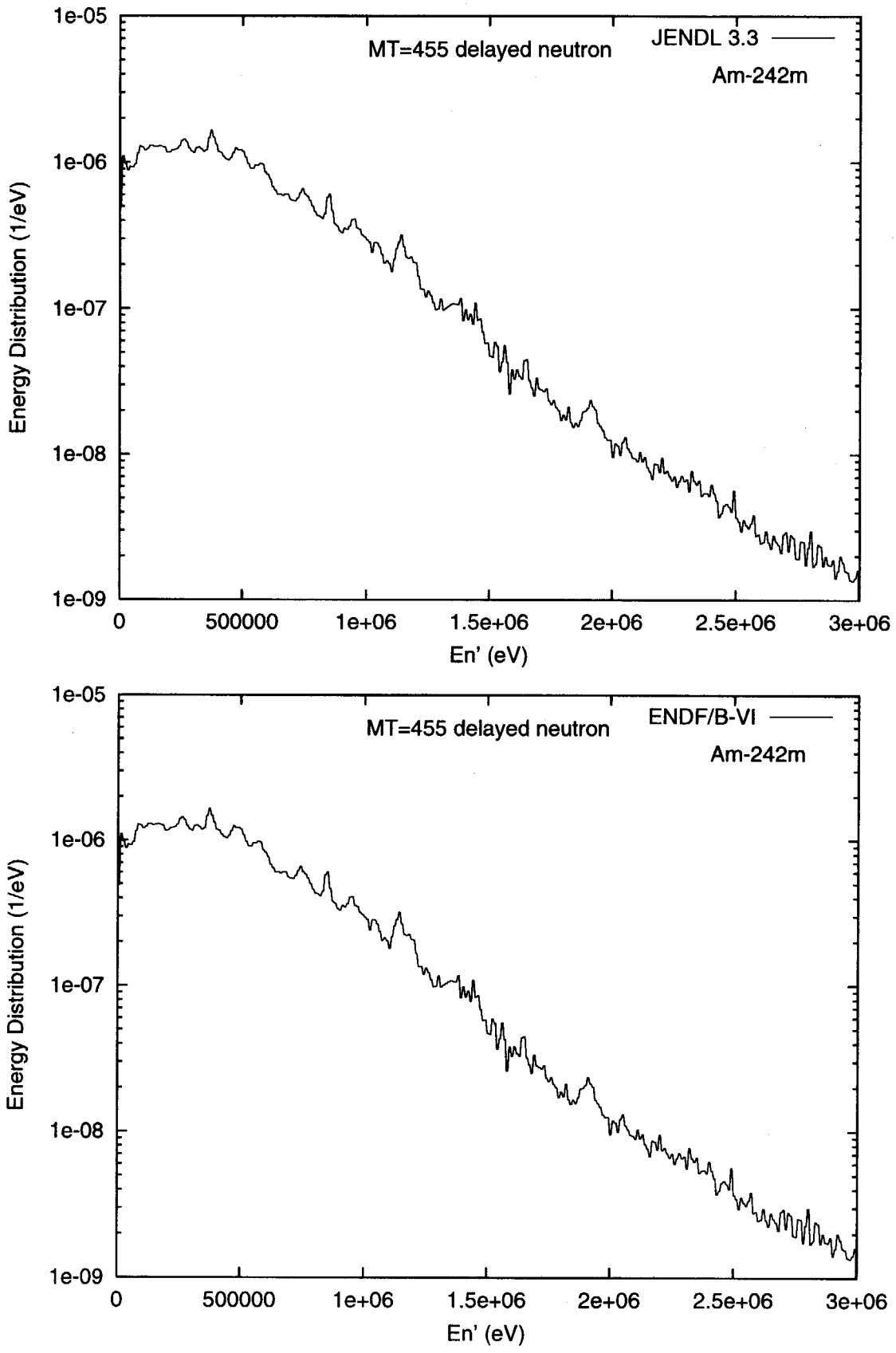

Fig. 2.23(a) ^{242m}Am delayed neutron spectra

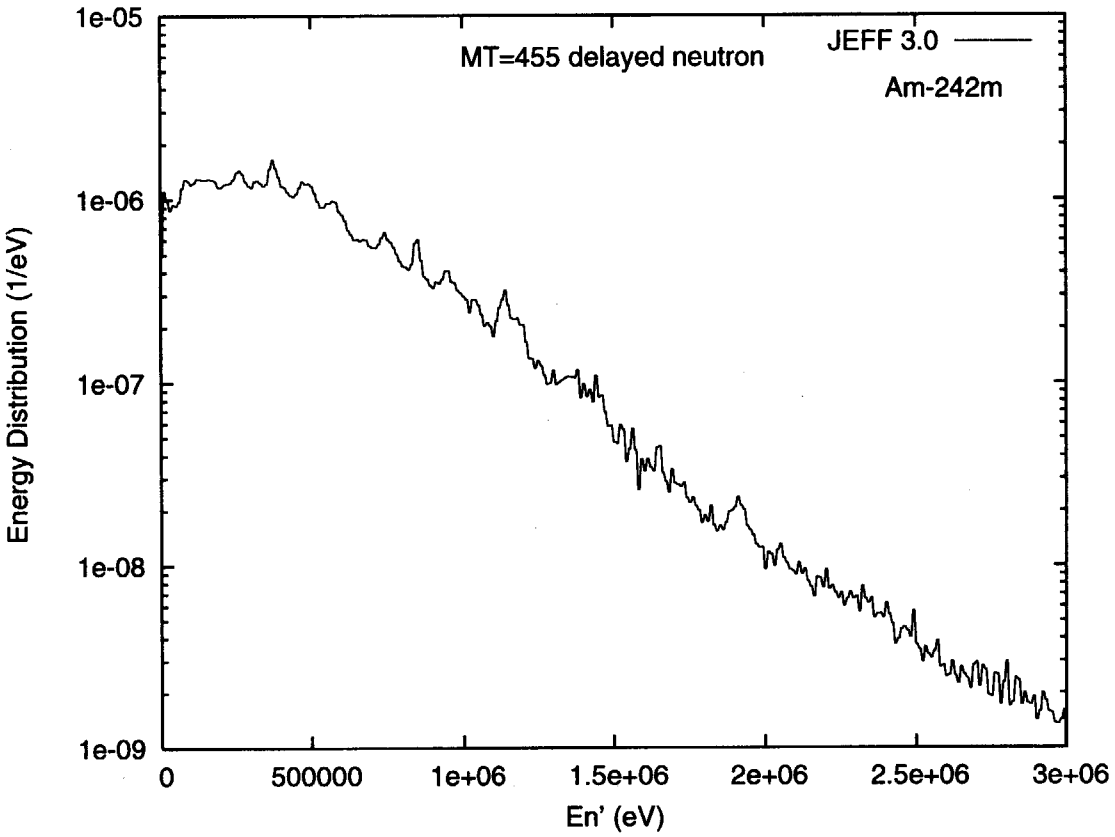

Fig. 2.23(b) ^{242m}Am delayed neutron spectra

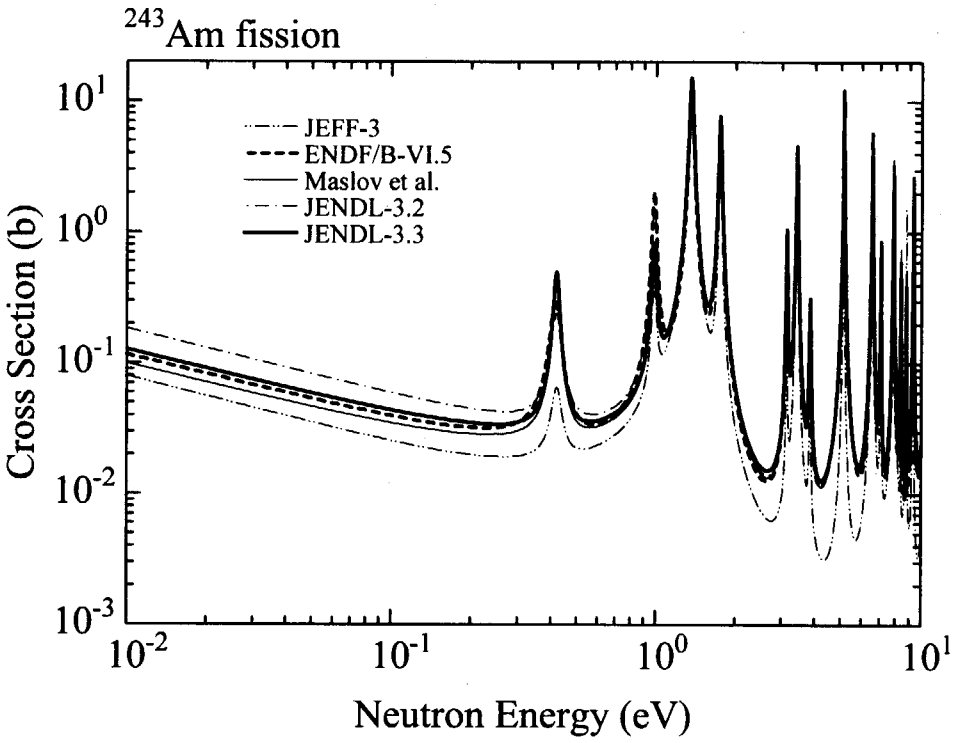

Fig. 3.1(a) ^{243}Am fission cross section (0.01 – 10 eV)

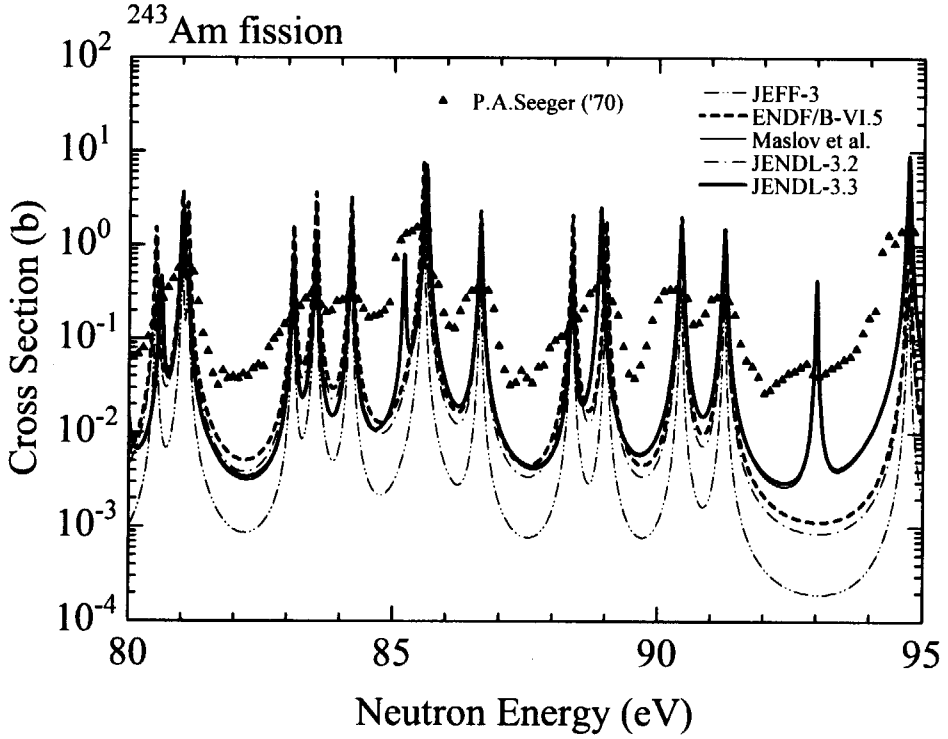

Fig. 3.1(b) ^{243}Am fission cross section (80 – 90 eV)
Experimental data: Seeger('70)[Se70]

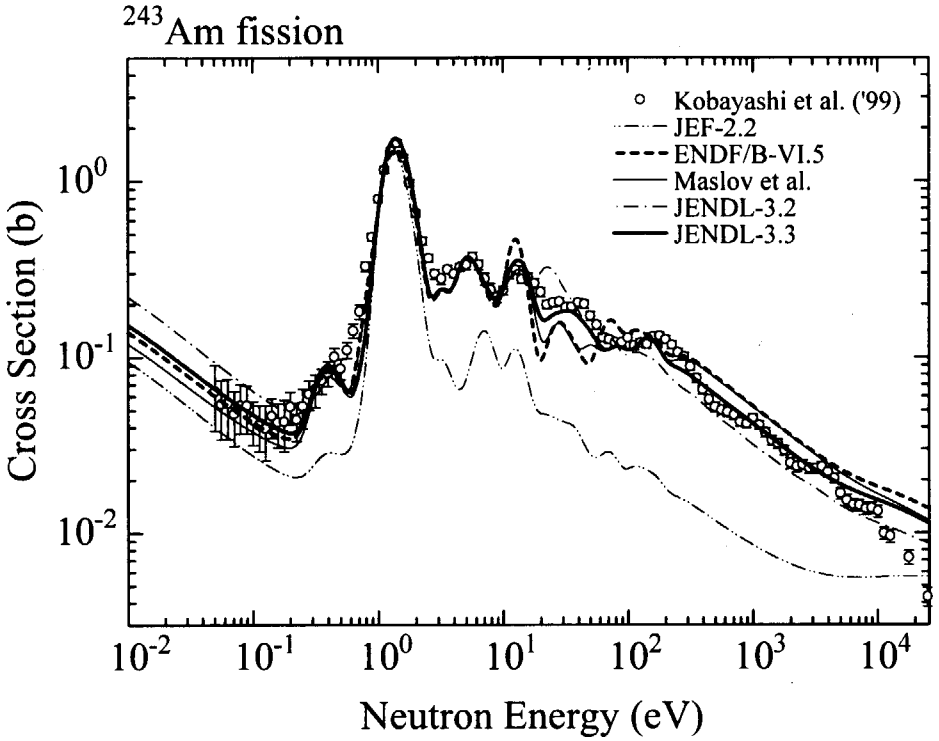

Fig. 3.2 ^{243}Am fission cross section
(comparison with KULS measurement performed by Kobayashi et al. [Ko99])

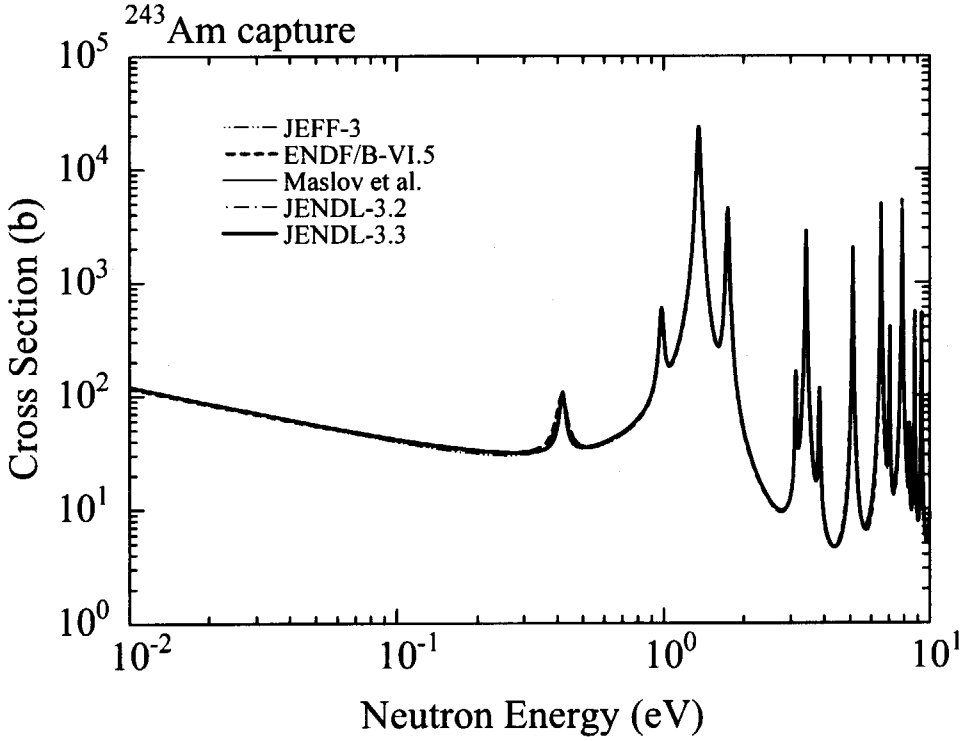

Fig. 3.3 ^{243}Am capture cross section (0.01 – 10 eV)

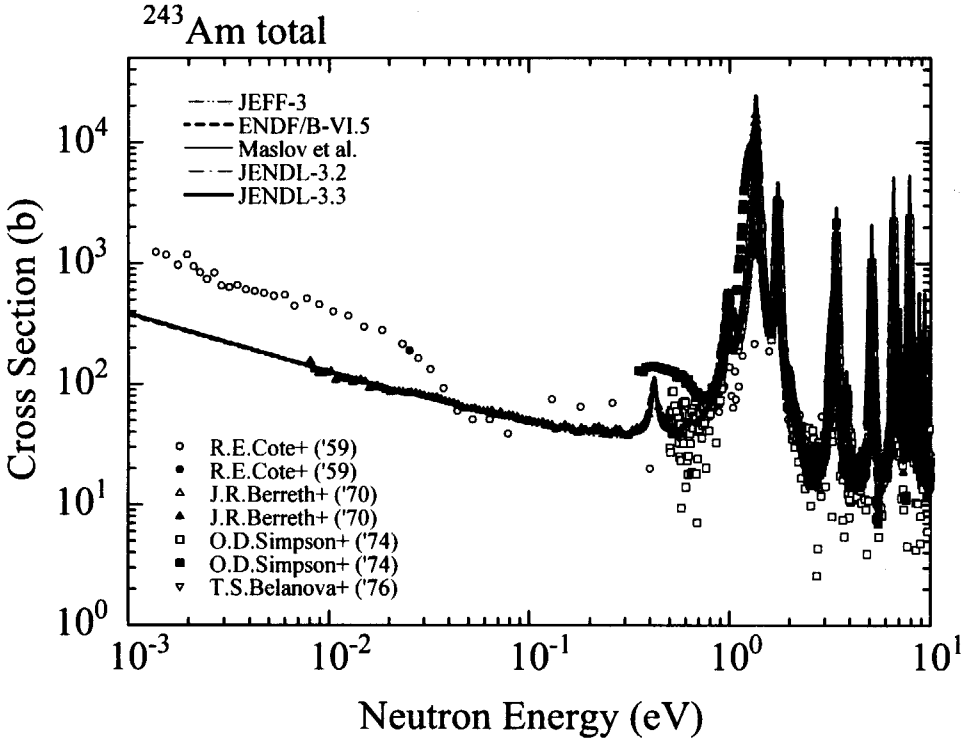

Fig. 3.4(a) ^{243}Am total cross section (0.01 – 10 eV)
Experimental data: Cote+('59)[Co59a], Berreth+('70)[Be70],
Simpson+('74)[Si74a], Belanova+('76)[Be76]

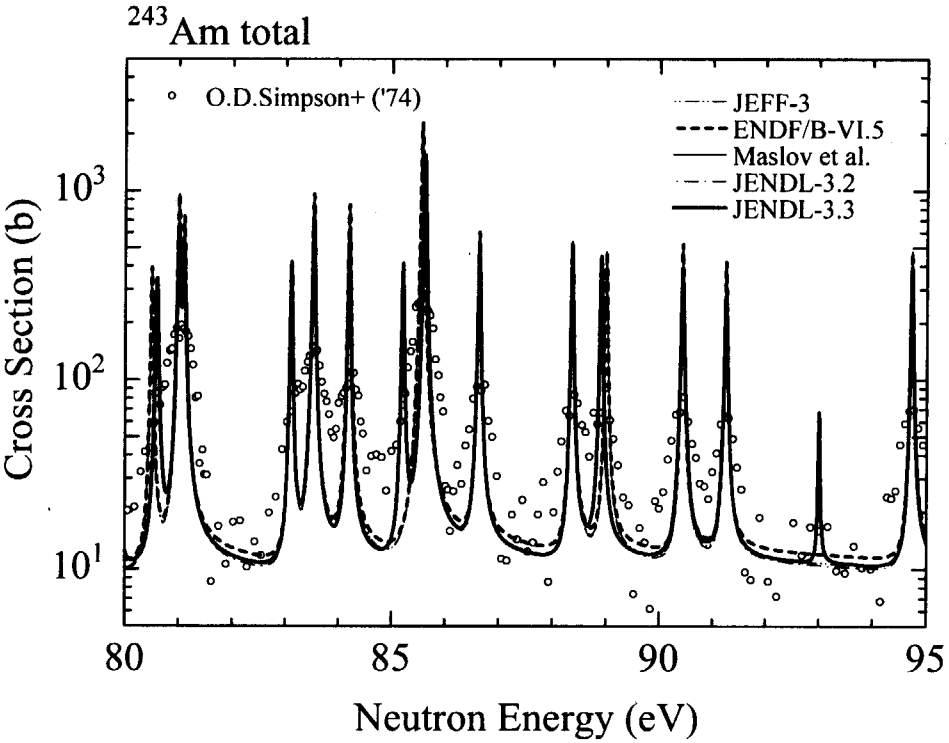

Fig. 3.4(b) ^{243}Am total cross section (80 – 95 eV)
Experimental data: Simpson+('74)[Si74a]

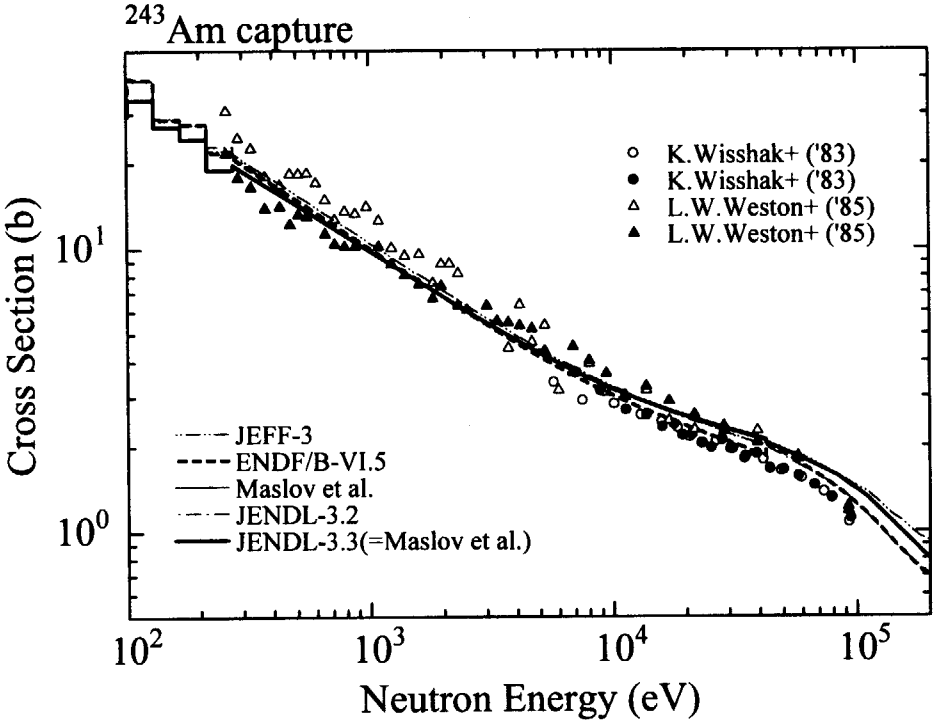

Fig. 3.5 ^{243}Am capture cross section (100 eV – 200 keV)
Experimental data: Wisshak+('83)[Wi83], Weston+('85)[We85]

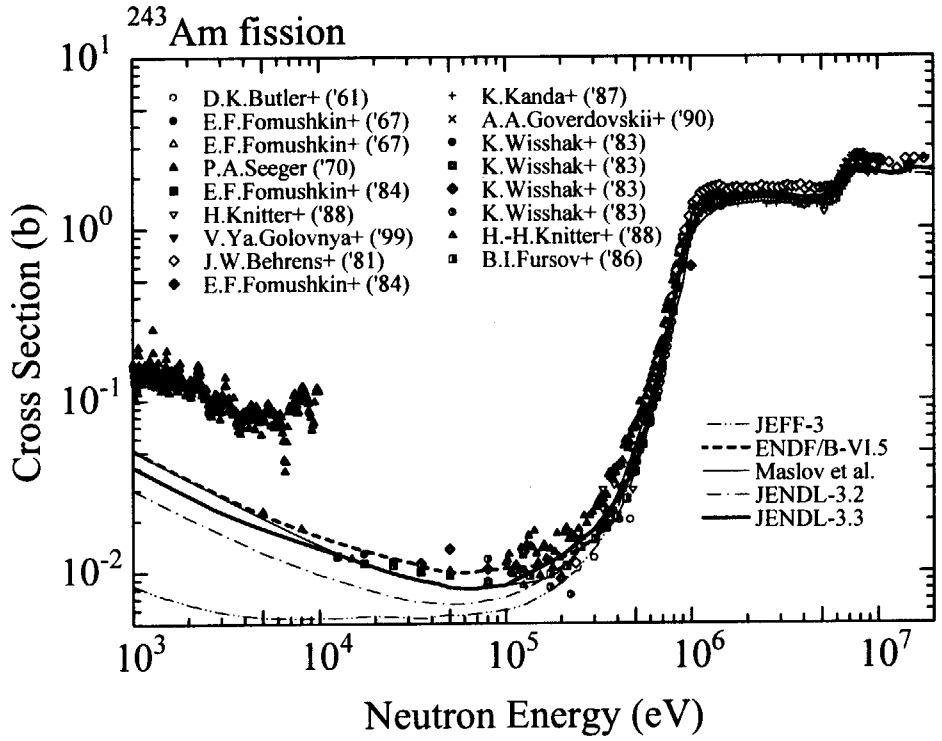

Fig. 3.6(a) ^{243}Am fission cross section (1 keV – 20 MeV)
Experimental data: Butler+('61)[Bu61], Fomushkin+('67)[Fo67], Seeger('70)[Se70], Knitter+('88)[Kn88], Golovnya+('99)[Go99], Behrens+('81)[Be81], Fomushkin+('84)[Fo84], Kanda+('87)[Ka87], Goverdovskii+('90)[Go90], Wisshak+('83)[Wi83], Fursov+('86)[Fu86]

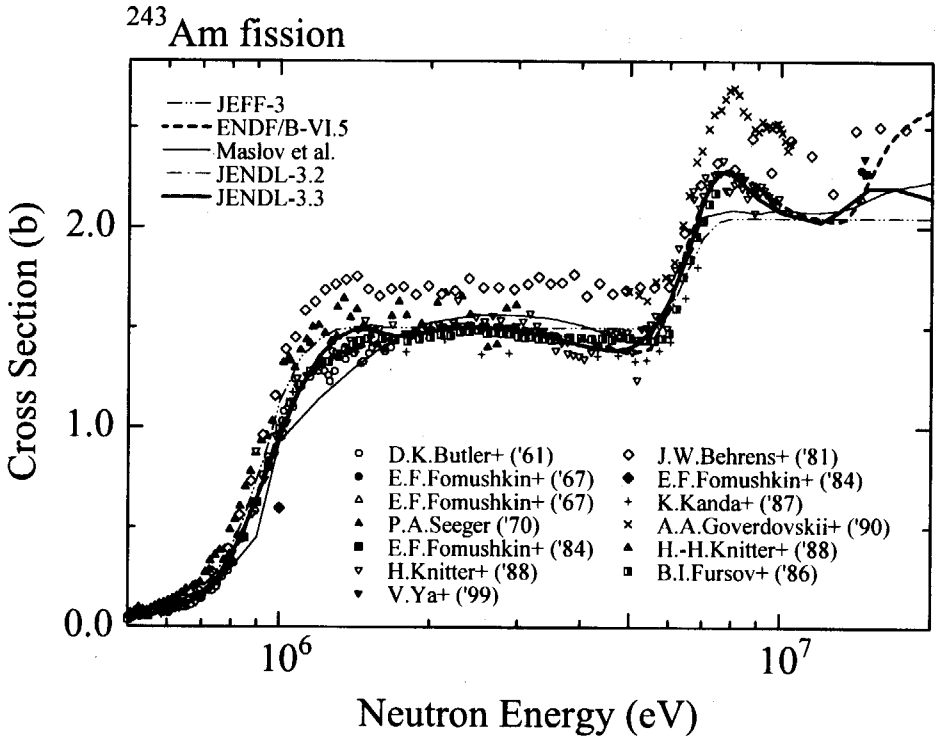

Fig. 3.6(b) ^{243}Am fission cross section (1 keV – 20 MeV)
Experimental data: see Fig. 3.6(a)

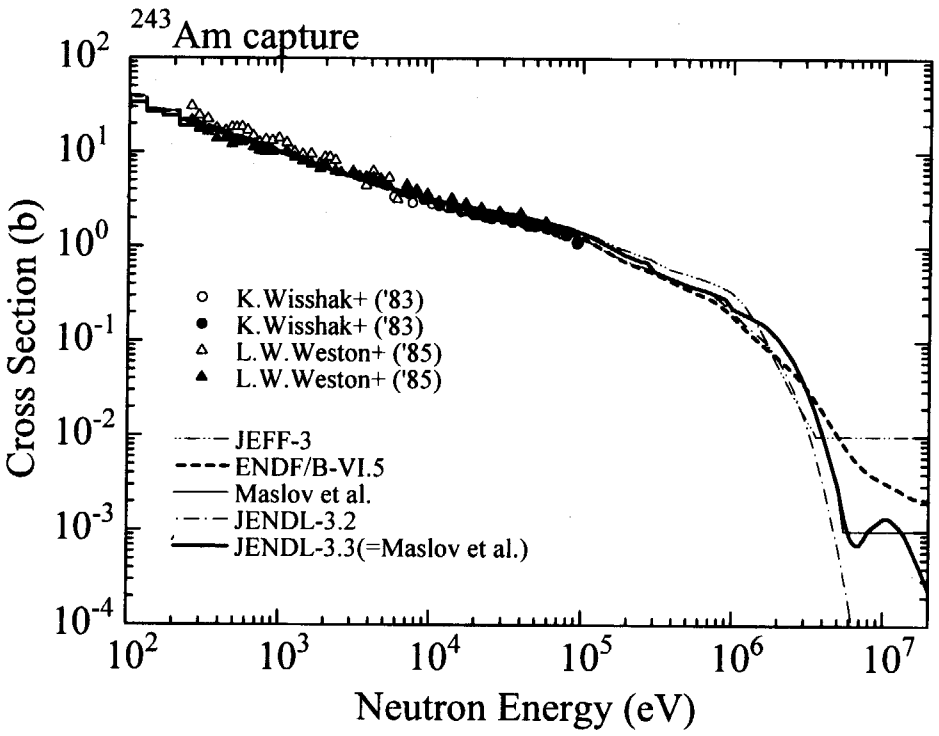

Fig. 3.7 ^{243}Am capture cross section (100 eV – 20 MeV)
Experimental data: Wisshak+('83)[Wi83], Weston+('85)[We85]

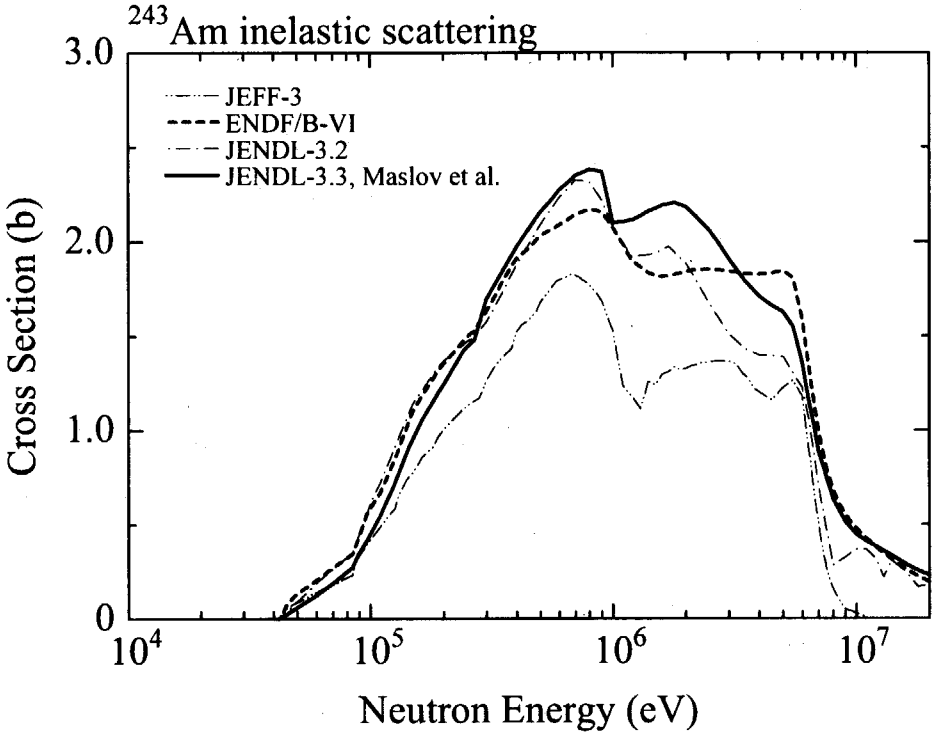

Fig. 3.8 ^{243}Am inelastic scattering cross section

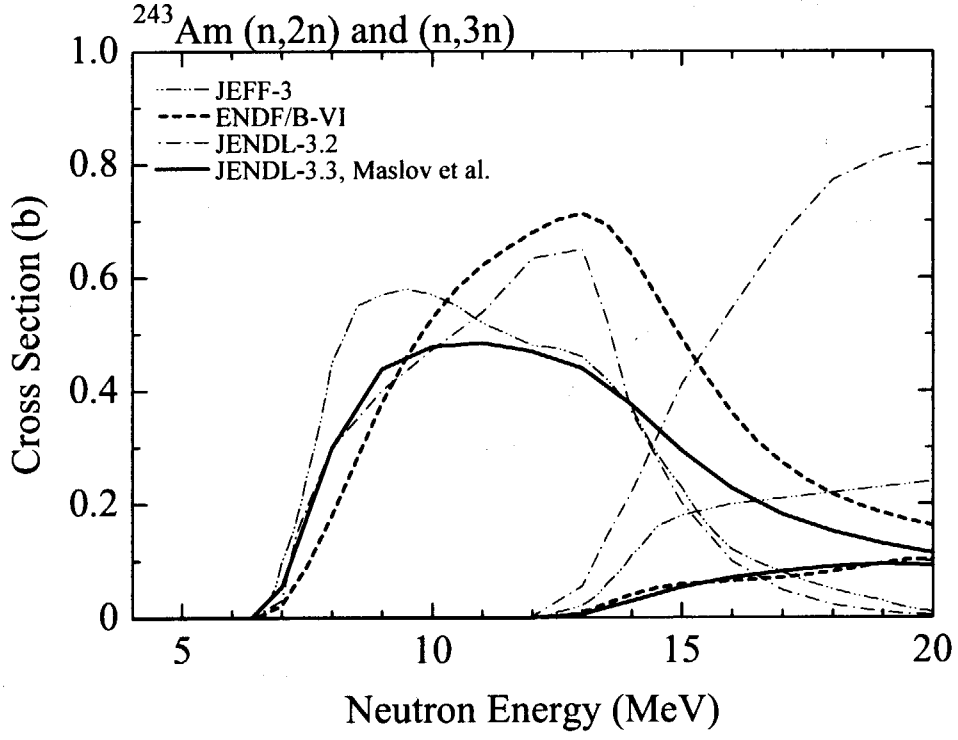

Fig. 3.9 ^{243}Am (n,2n) and (n,3n) reaction cross sections

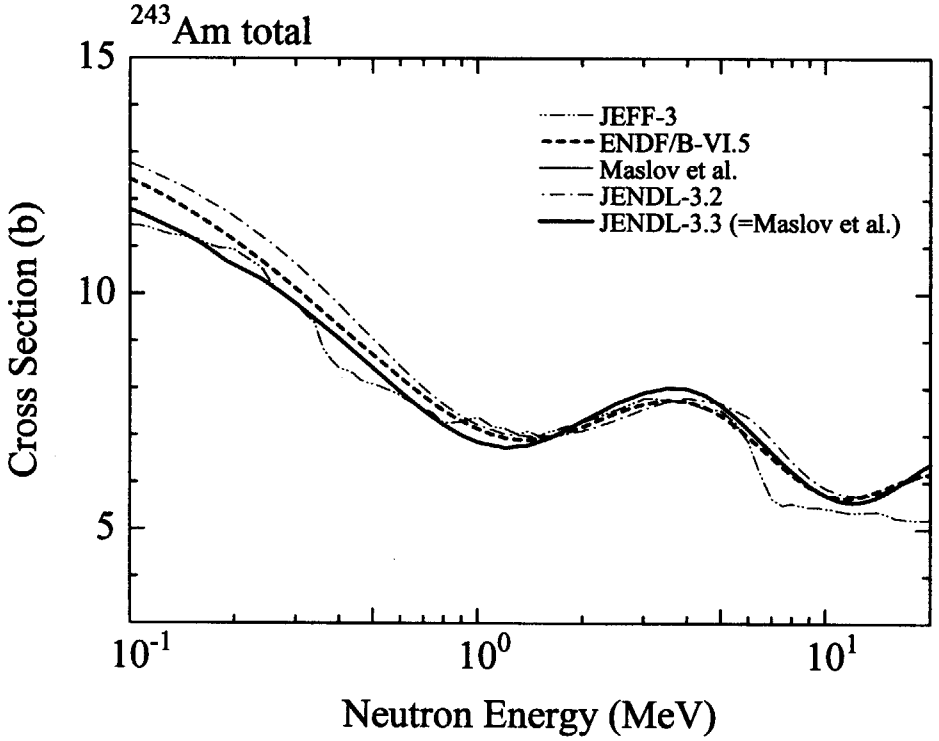

Fig. 3.10 ^{243}Am total cross section (0.1 – 20 MeV)

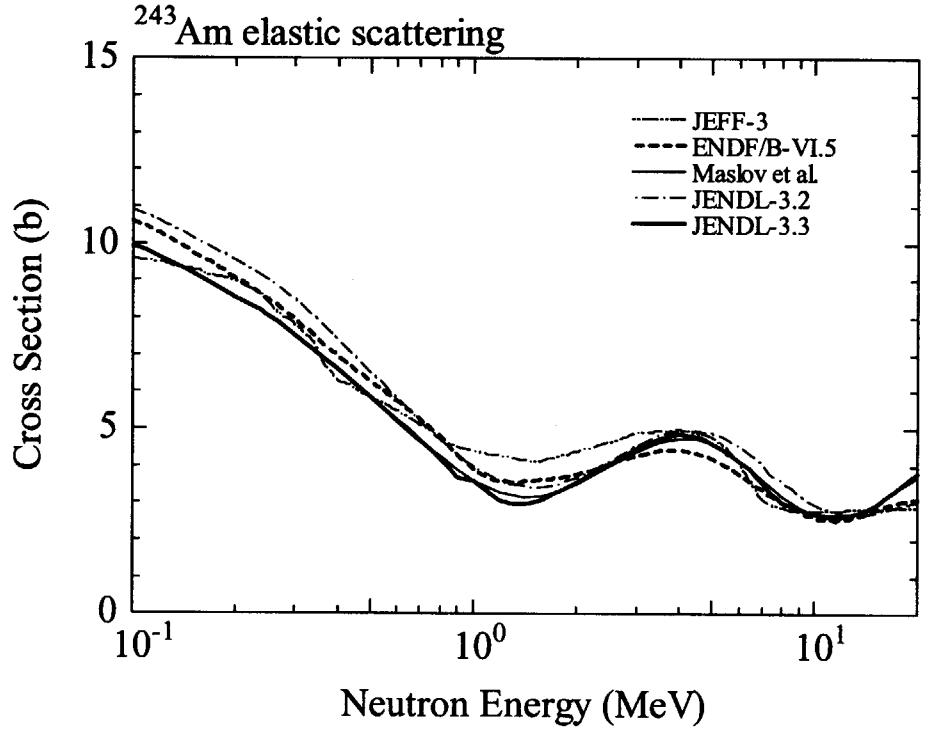

Fig. 3.11 ^{243}Am elastic scattering cross section (0.1 – 20 MeV)

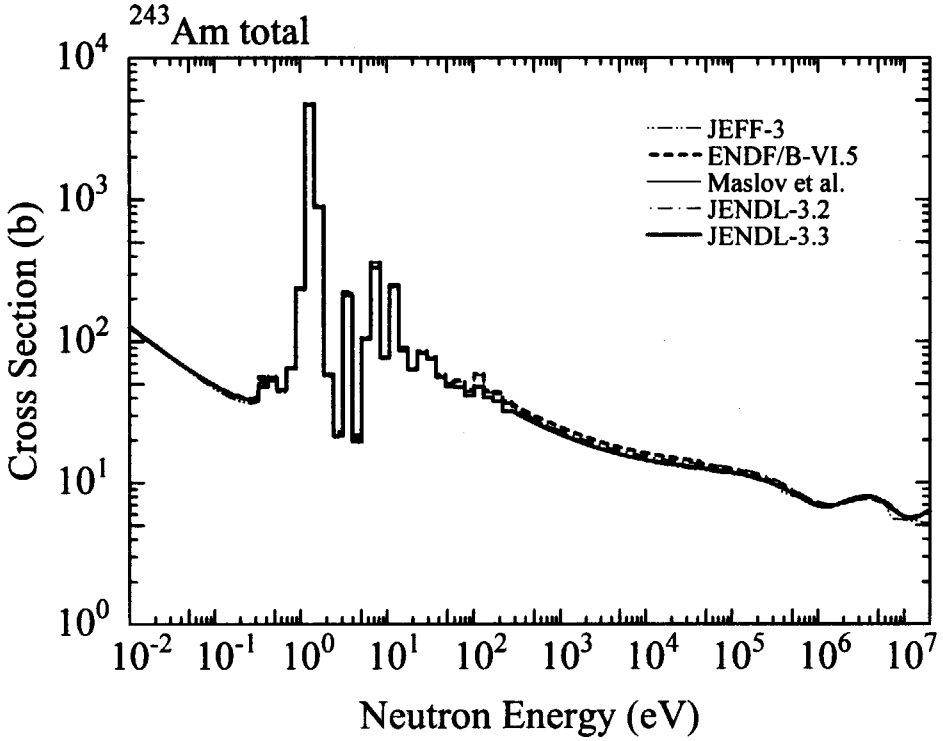

Fig. 3.12 ^{243}Am total cross section (thermal energy – 20 MeV)

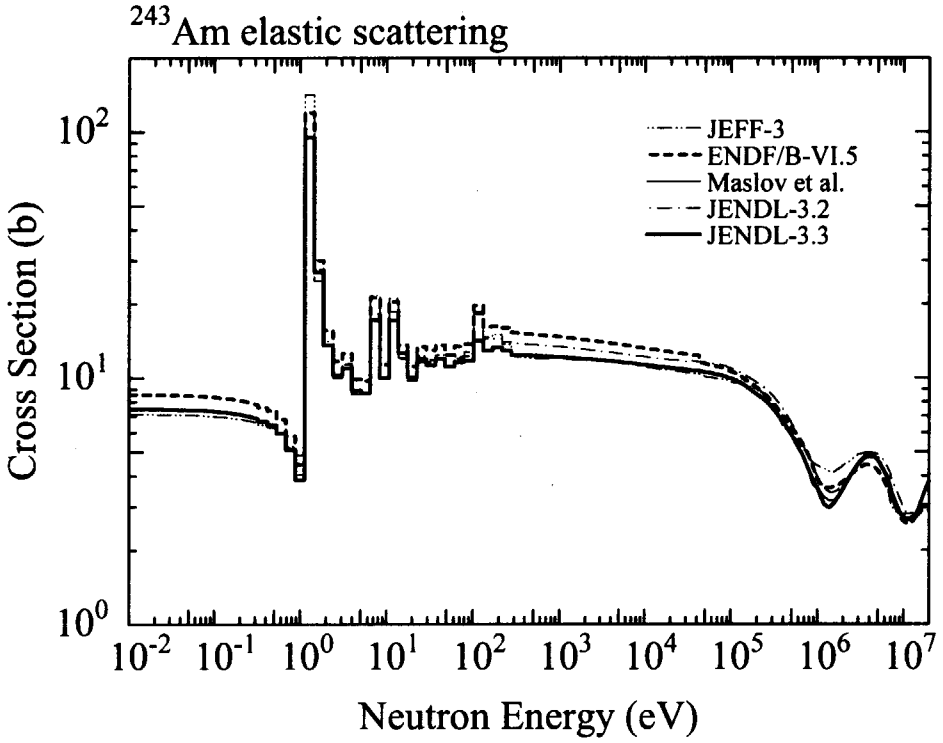

Fig. 3.13 ^{243}Am elastic scattering cross section (thermal energy – 20 MeV)

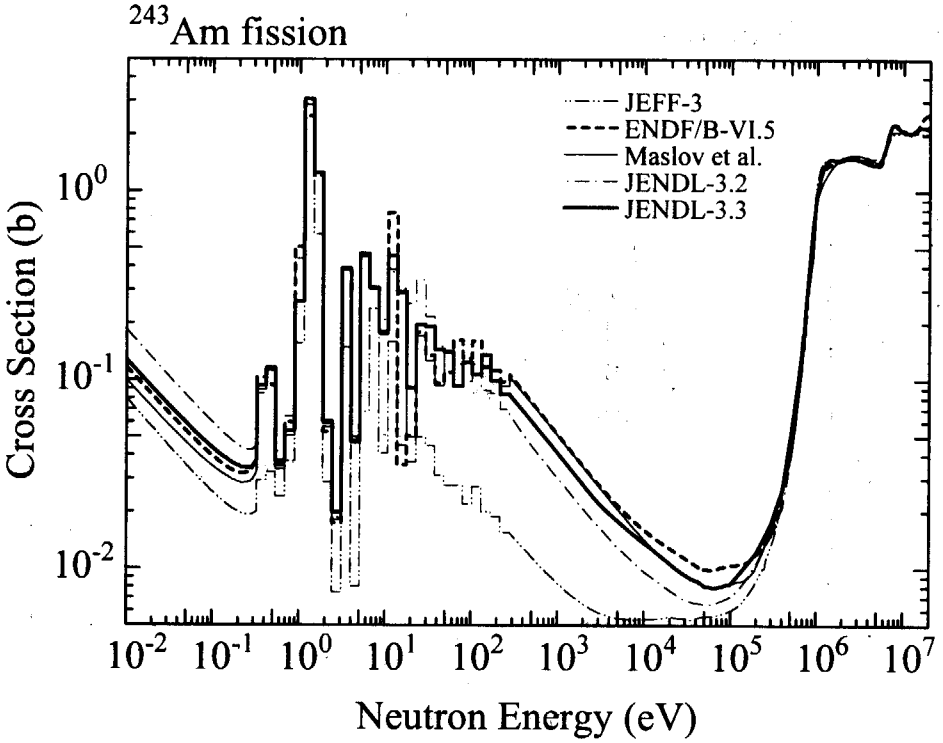

Fig. 3.14 ^{243}Am fission cross section (thermal energy – 20 MeV)

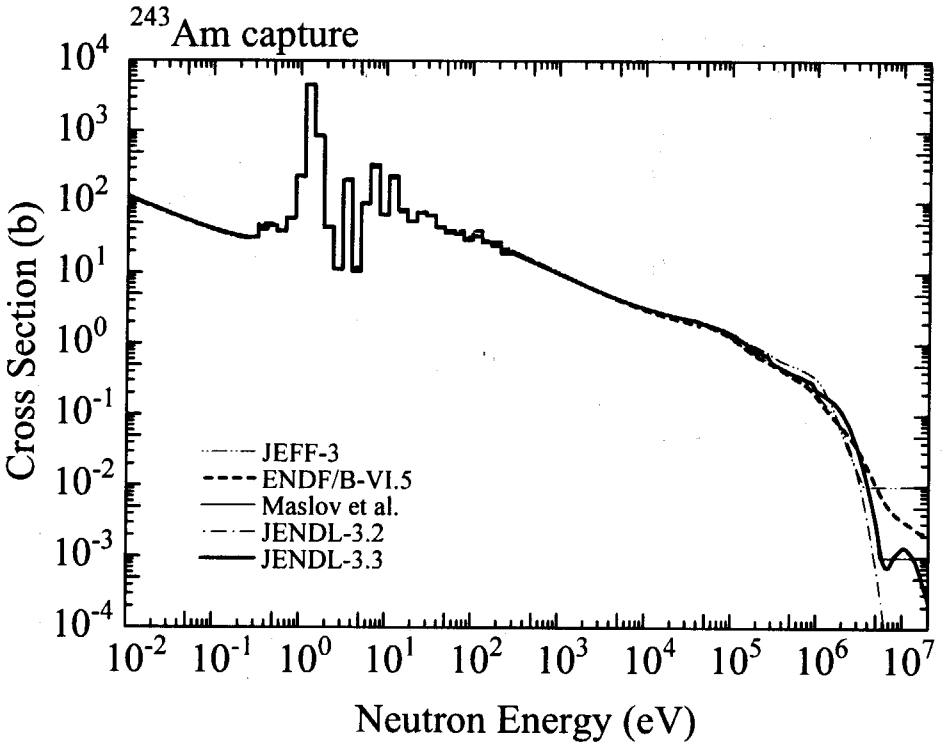

Fig. 3.15 ^{243}Am capture cross section (thermal energy – 20 MeV)

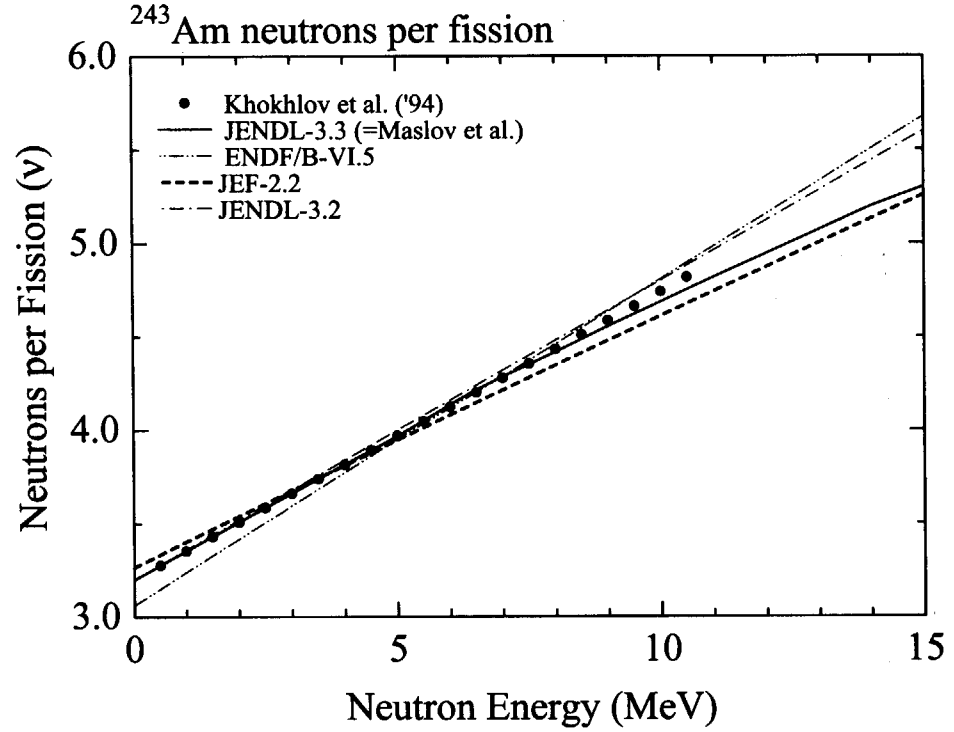

Fig. 3.16 ^{243}Am prompt neutrons per fission
Experimental data: Khokhlov et al.('94)[Kh94]

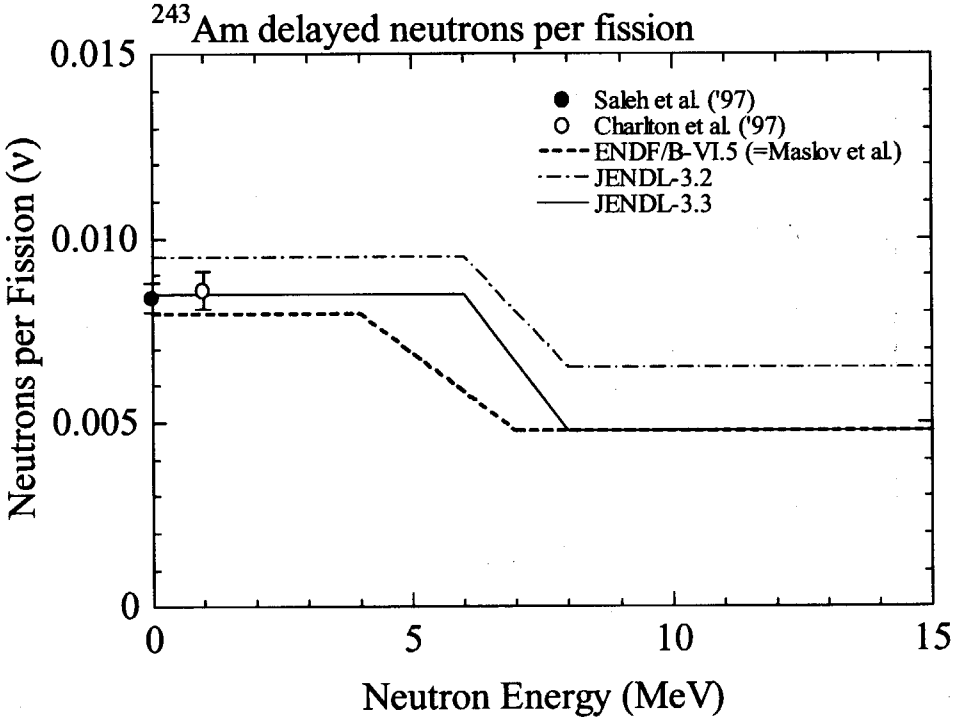

Fig. 3.17 ^{243}Am delayed neutrons per fission
Experimental data: Saleh et al.('97)[Sa97], Charlton et al.('97)[Ch97]

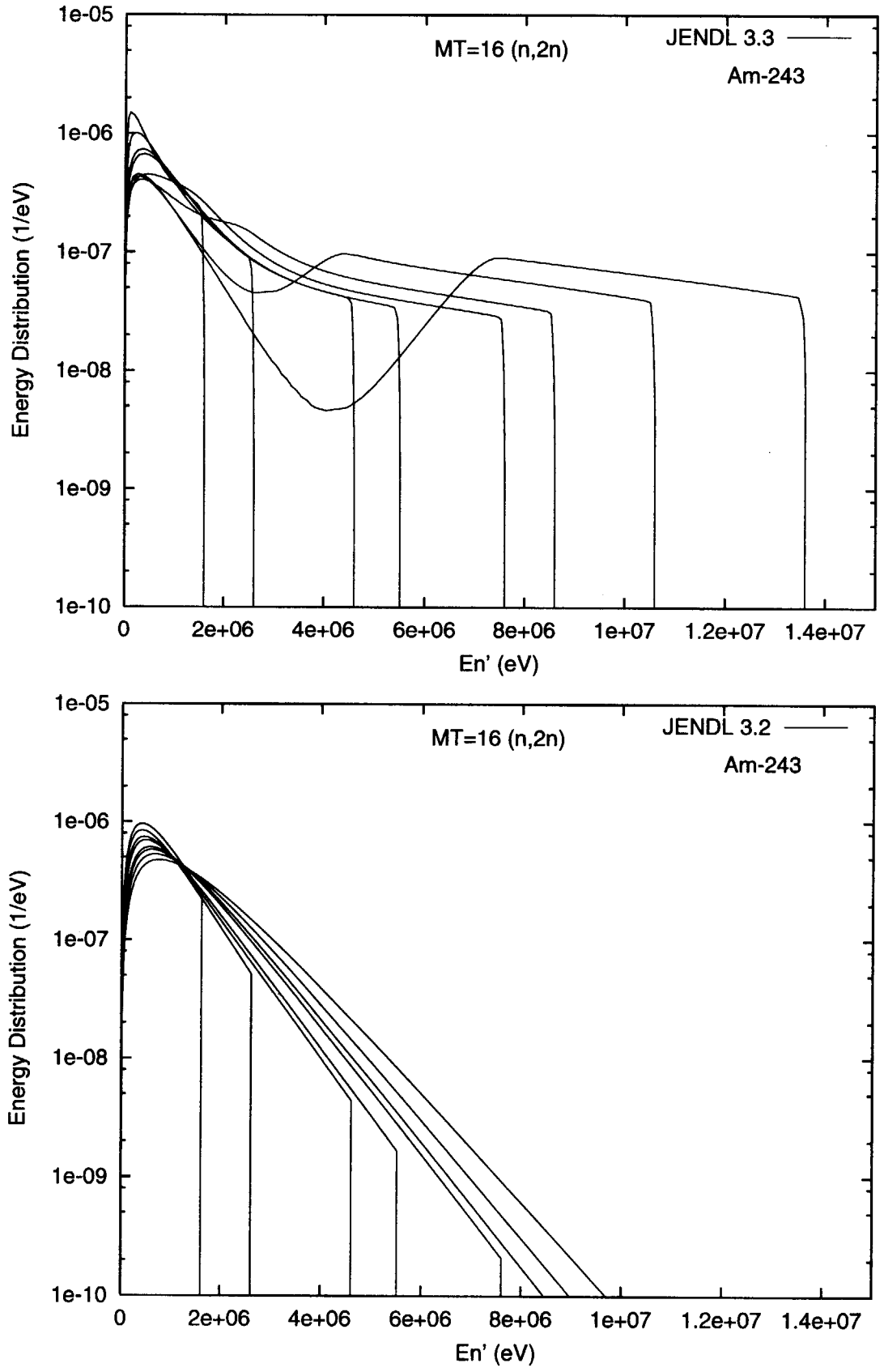

Fig. 3.18(a) ^{243}Am (n,2n) neutron spectra

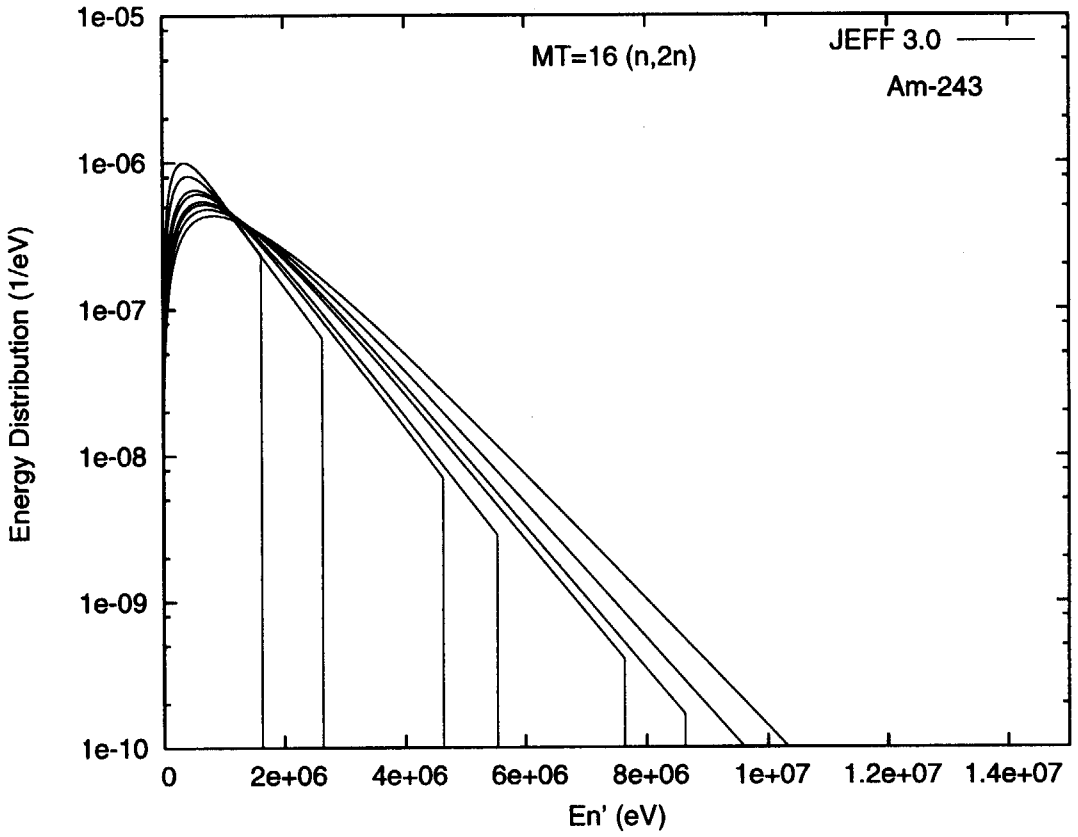

Fig. 3.18(b) ^{243}Am (n,2n) neutron spectra

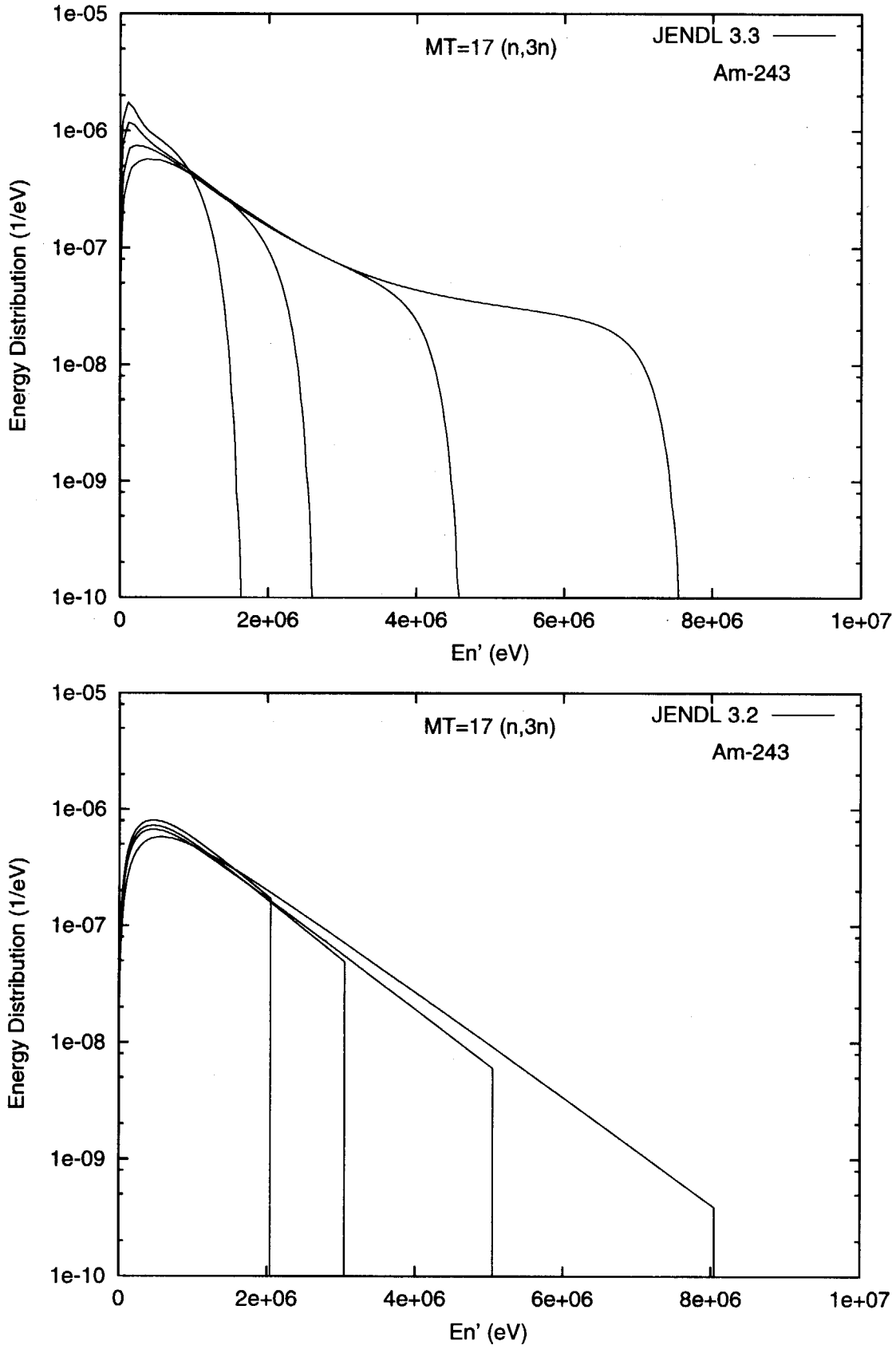

Fig. 3.19(a) ^{243}Am (n,3n) neutron spectra

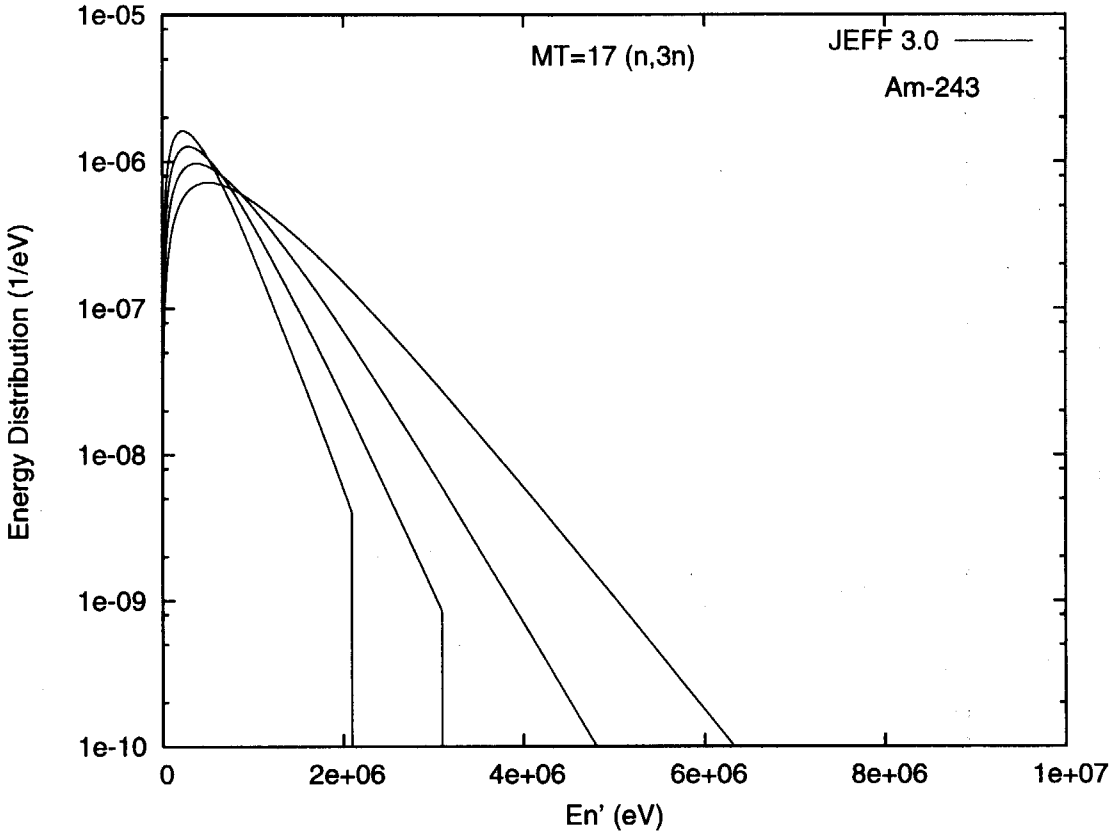

Fig. 3.19(b) ^{243}Am (n,3n) neutron spectra

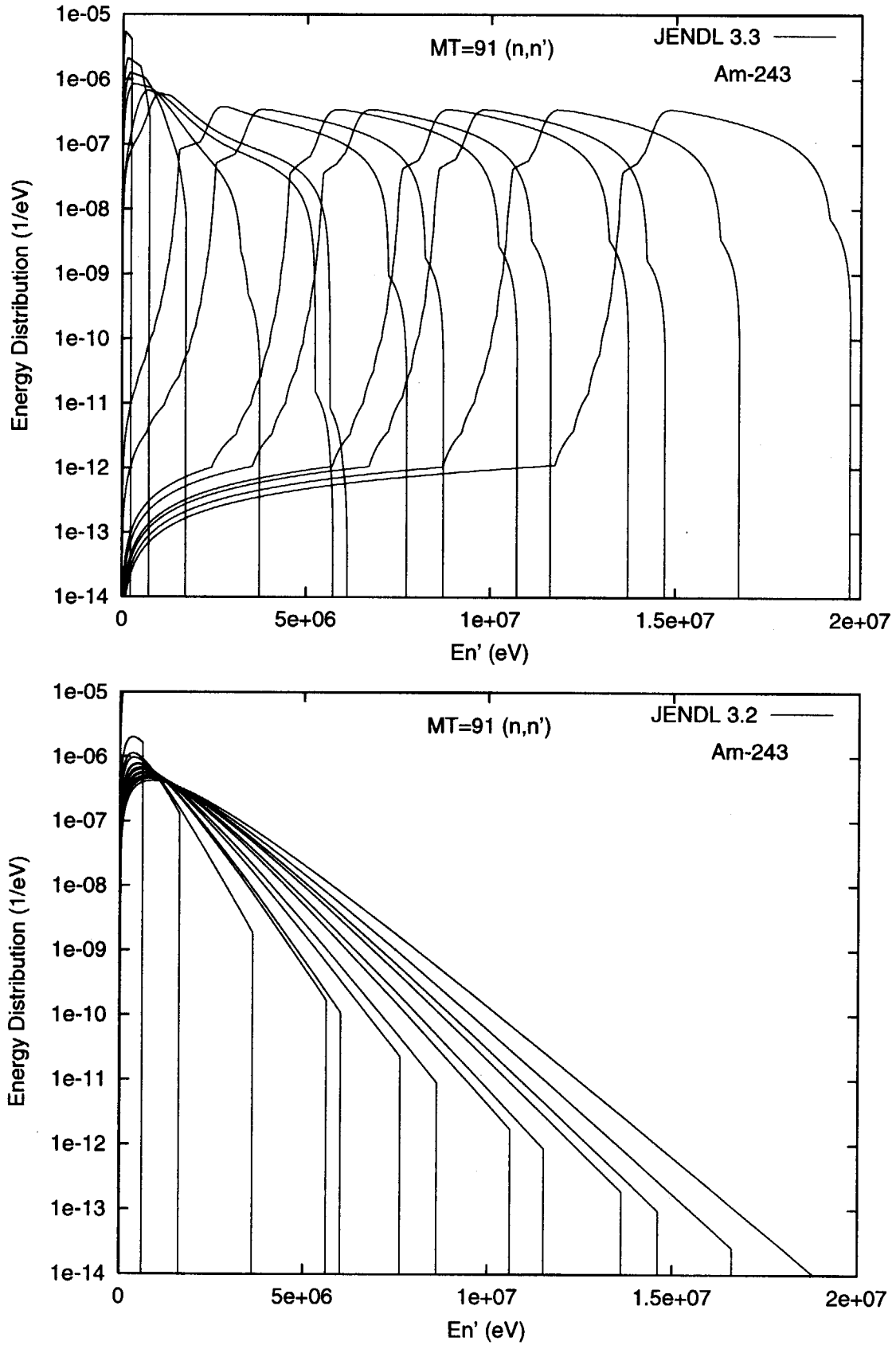

Fig. 3.20(a) ^{243}Am (n,n') neutron spectra

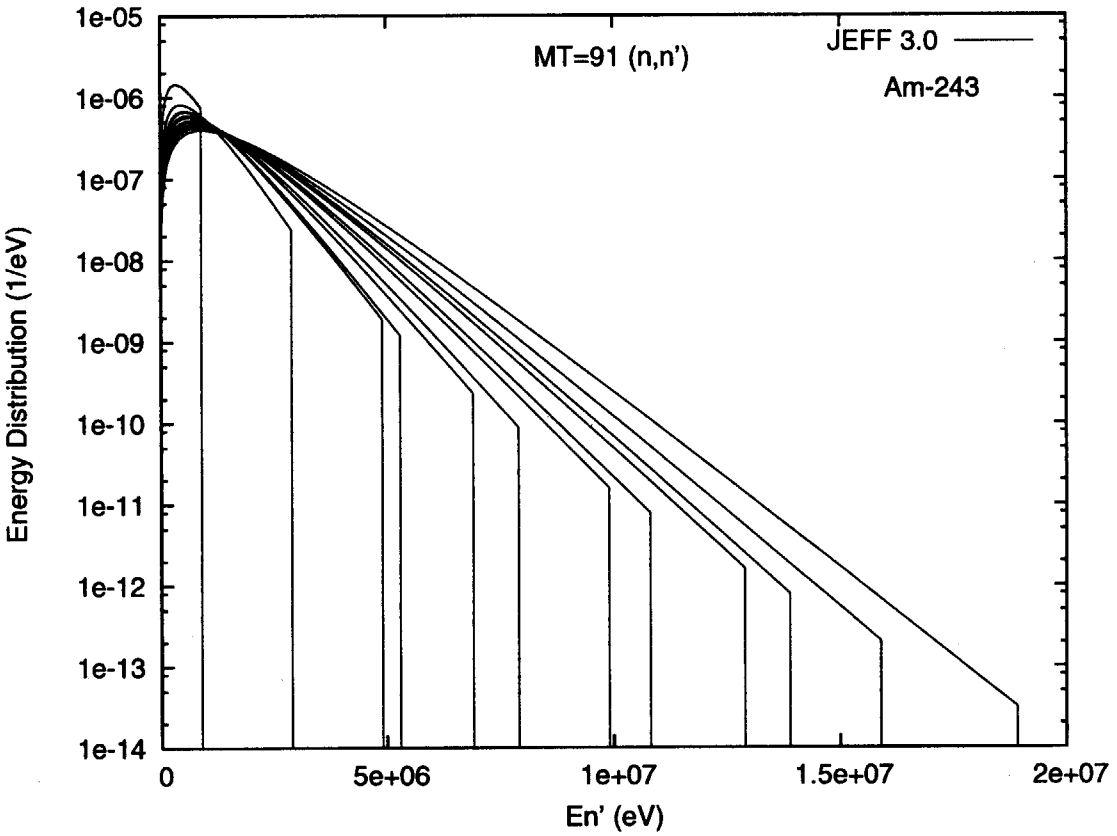

Fig. 3.20(b) ^{243}Am (n,n') neutron spectra

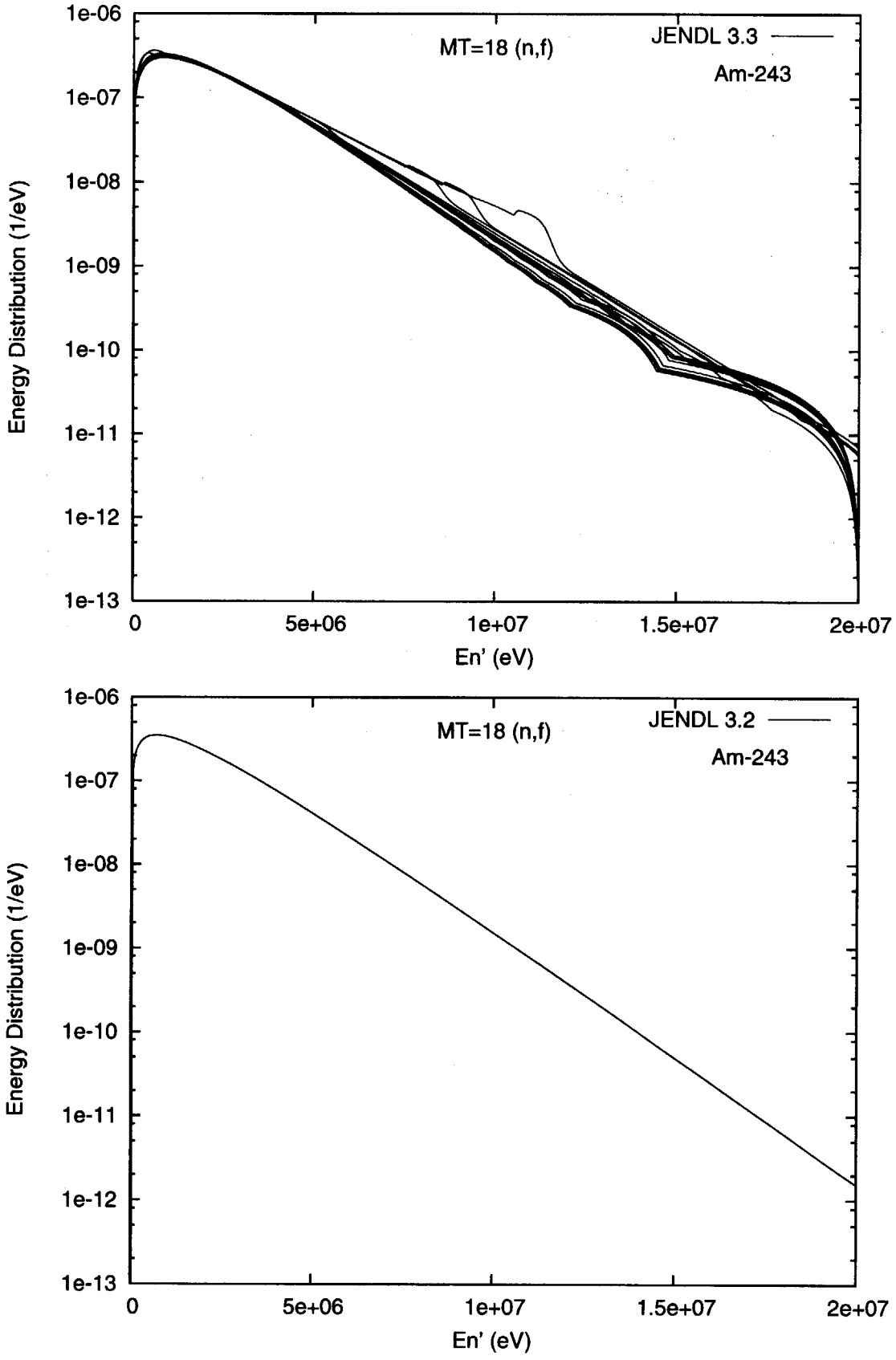

Fig. 3.21(a) ^{243}Am fission neutron spectra

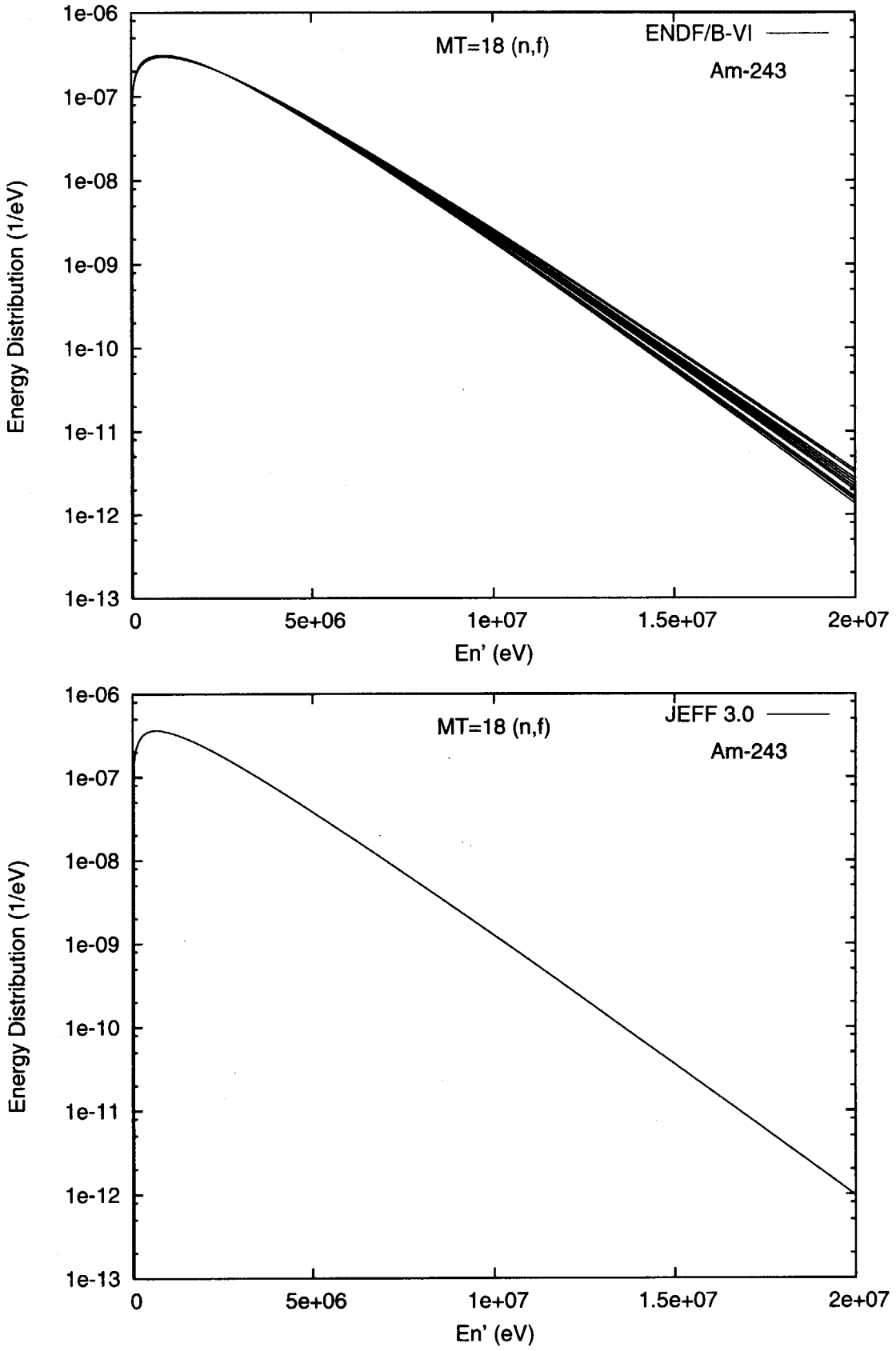

Fig. 3.21(b) ^{243}Am fission neutron spectra

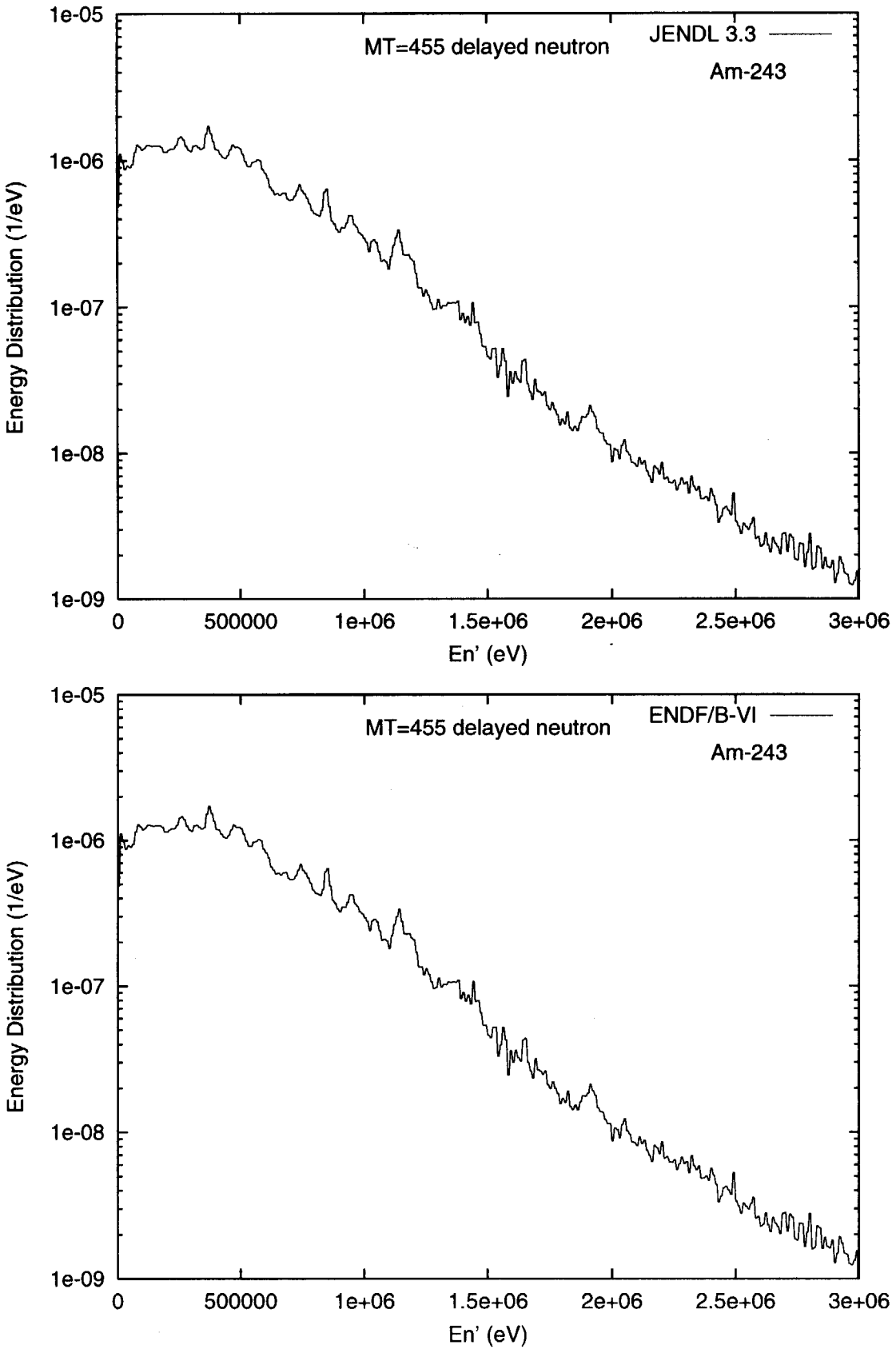

Fig. 3.22 ^{243}Am delayed neutron spectra

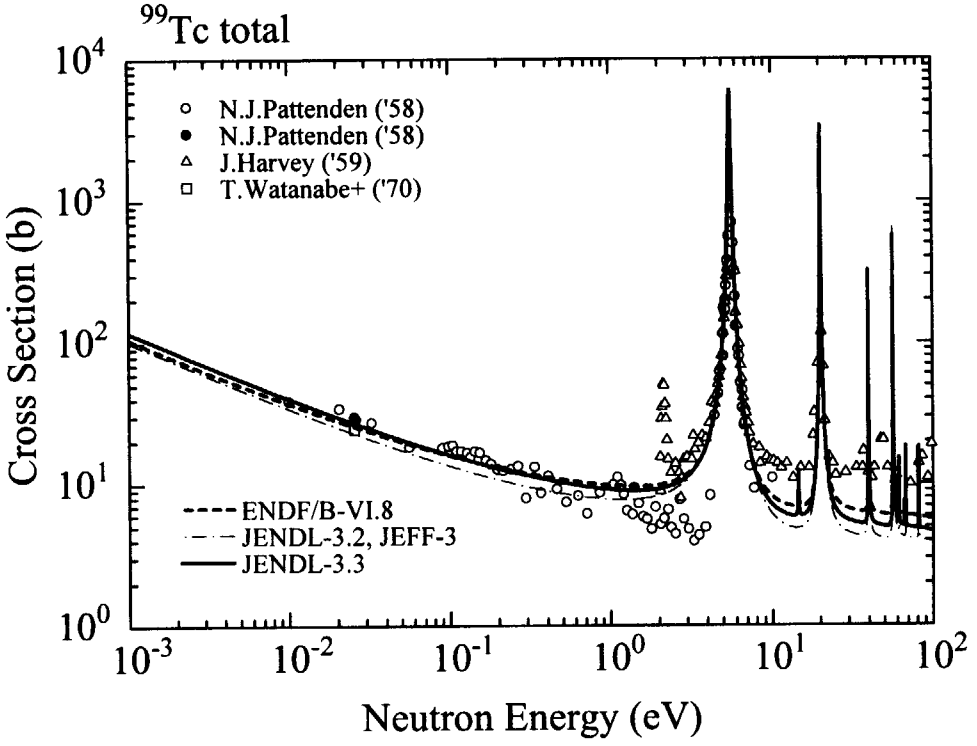

Fig. 4.1 ^{99}Tc total cross section (below 100 eV)
Experimental data: Pattenden ('58)[Pa58], Harvey ('59)[Ha59], Watanabe+(70)[Wa70]

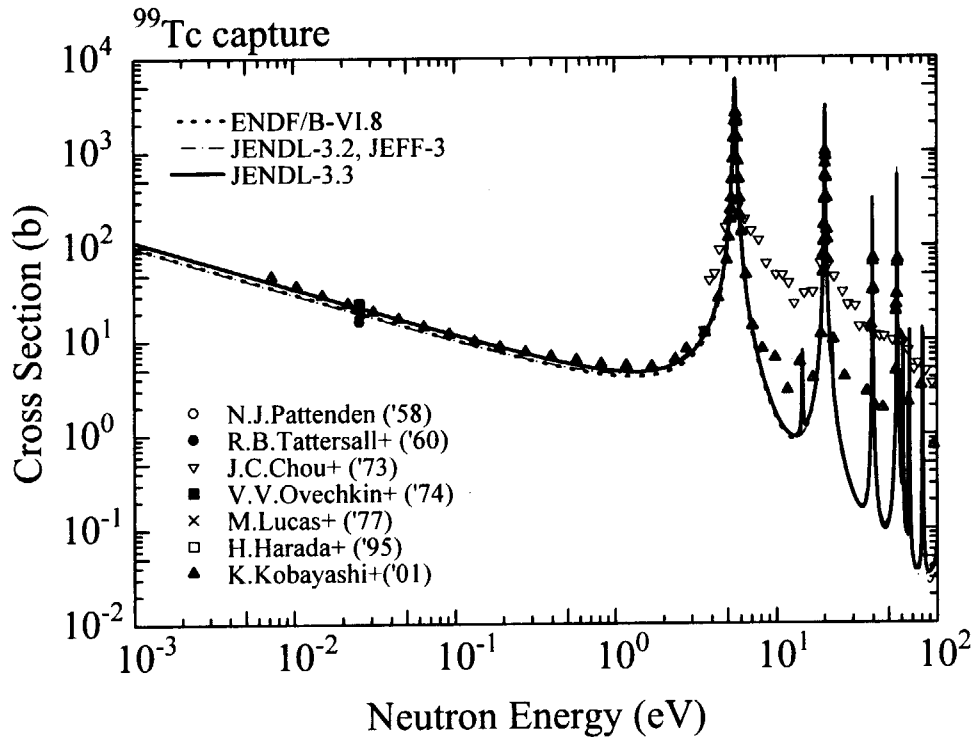

Fig. 4.2 ^{99}Tc capture cross section (below 100 eV)
Experimental data: Pattenden ('58)[Pa58], Tattersall+('60)[Ta60], Chou+('73)[Ch73], Ovechkin+('74)[Ov74], Lucas+('77)[Lu77],Harada+('95)[Ha95],Kobayashi+('01)[Ko01]

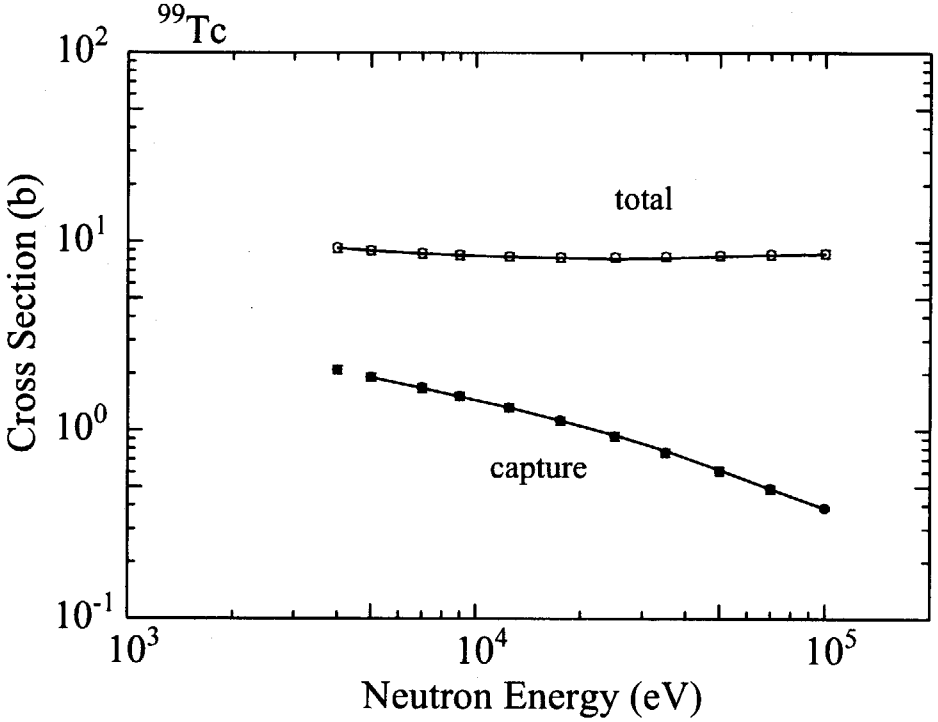

Fig. 4.3 ^{99}Tc cross sections in the unresolved resonance region

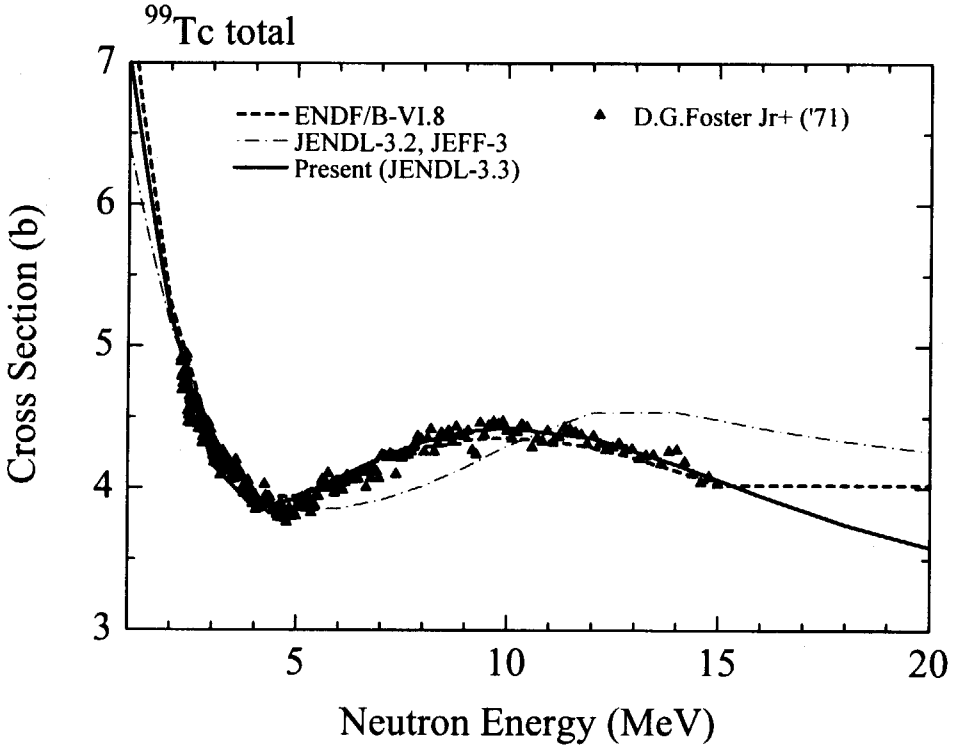

Fig. 4.4 ^{99}Tc total cross section in the MeV region
Experimental data: Foster Jr.+('71)[Fo71]

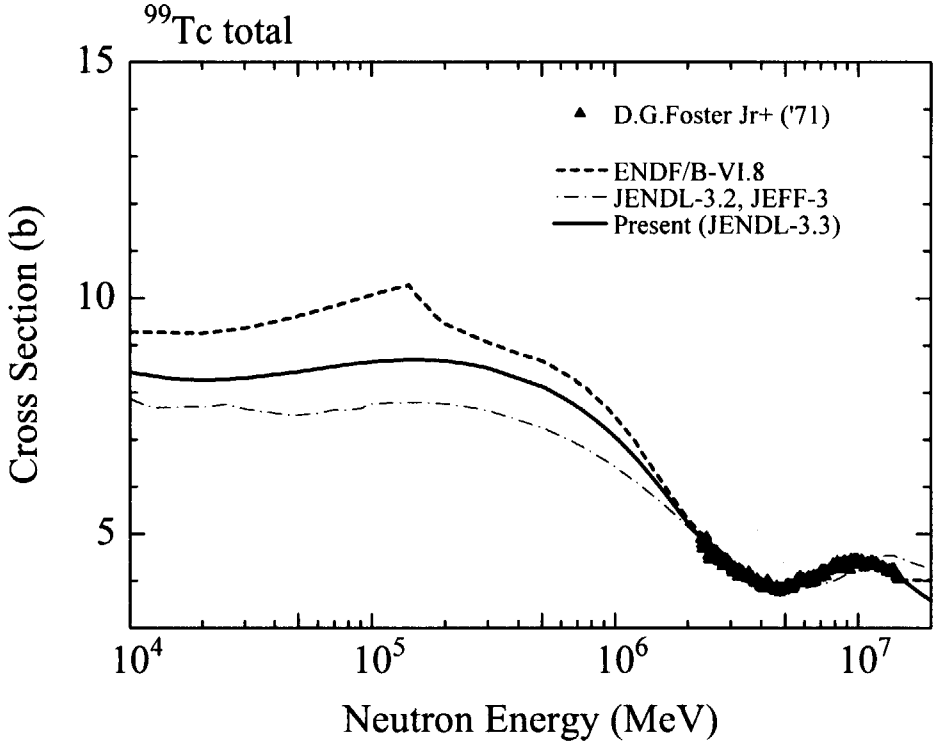

Fig. 4.5 ^{99}Tc total cross section (above 10 keV)
Experimental data: Foster Jr.+('71)[Fo71]

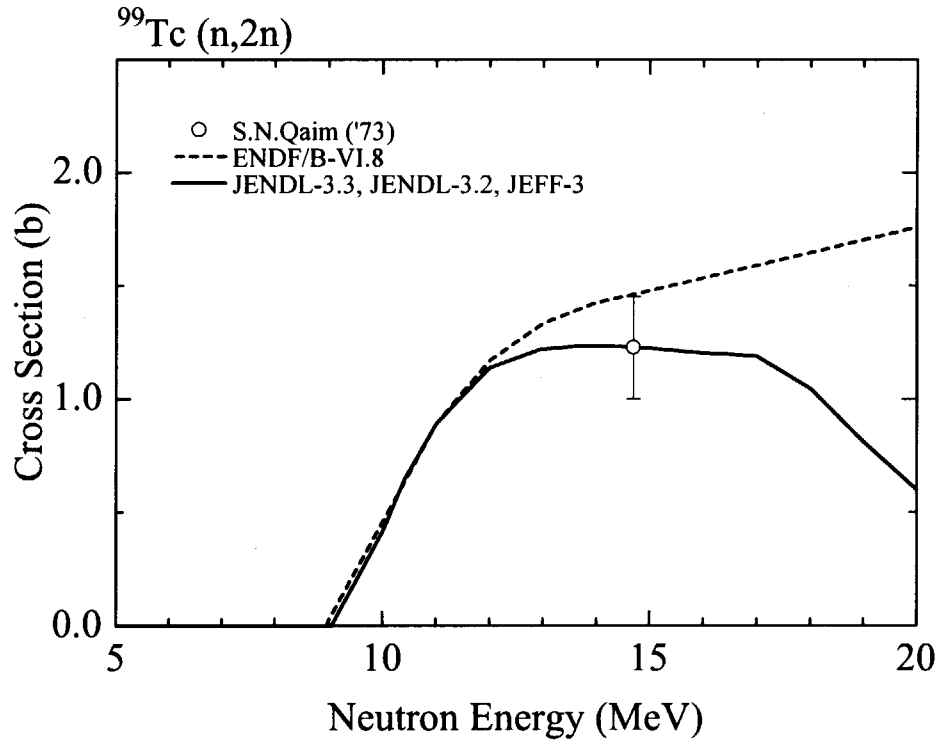

Fig. 4.6 ^{99}Tc (n,2n) reaction cross section
Experimental data: Qaim ('73)[Qa73]

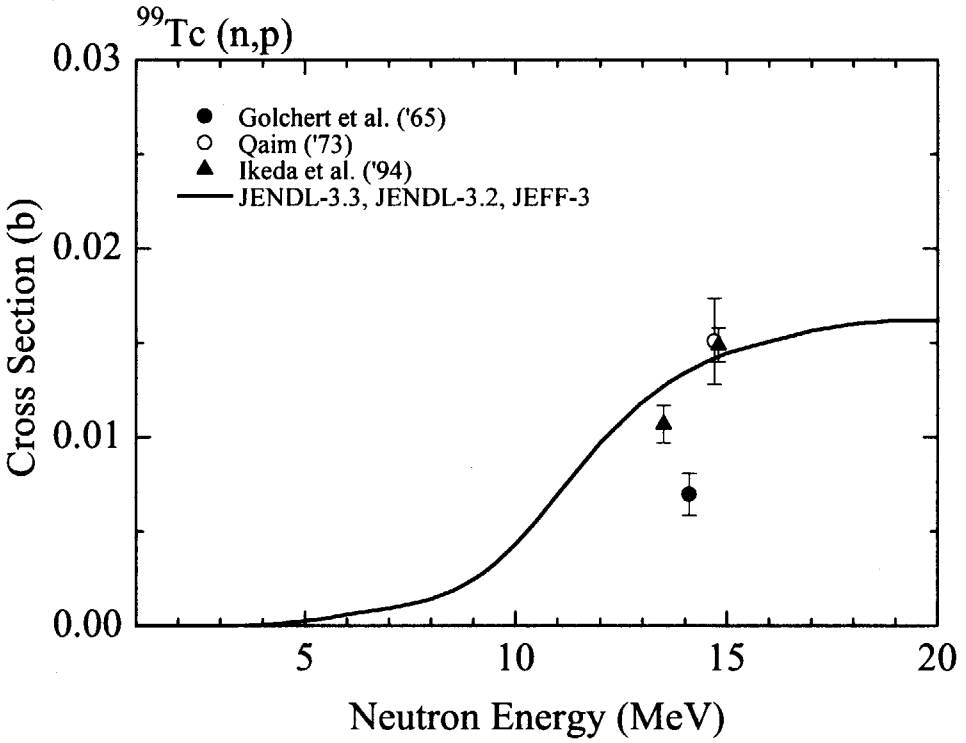

Fig. 4.7 ^{99}Tc(n,p) reaction cross section
Experimental data: Golchert et al.('65)[Go65], Qaim('73)[Qa73], Ikeda et al.('94)[Ik94]

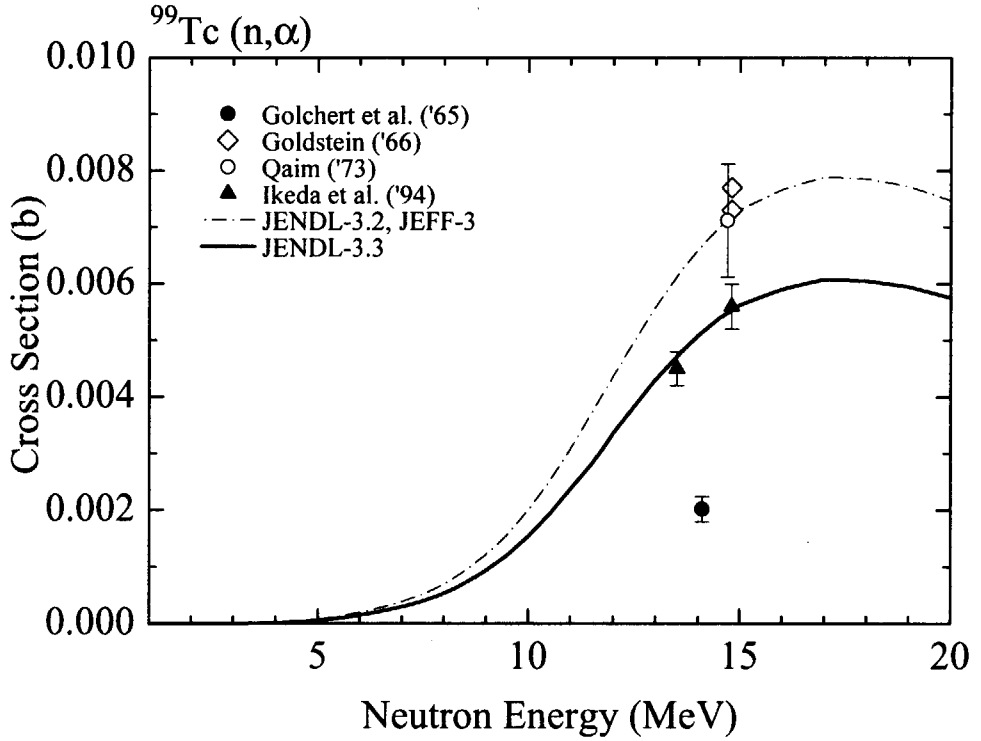

Fig. 4.8 ^{99}Tc(n,α) reaction cross section
Experimental data: Golchert et al.('65)[Go65], Goldstein('66)[Go66],
Qaim('73)[Qa73], Ikeda et al.('94)[Ik94]

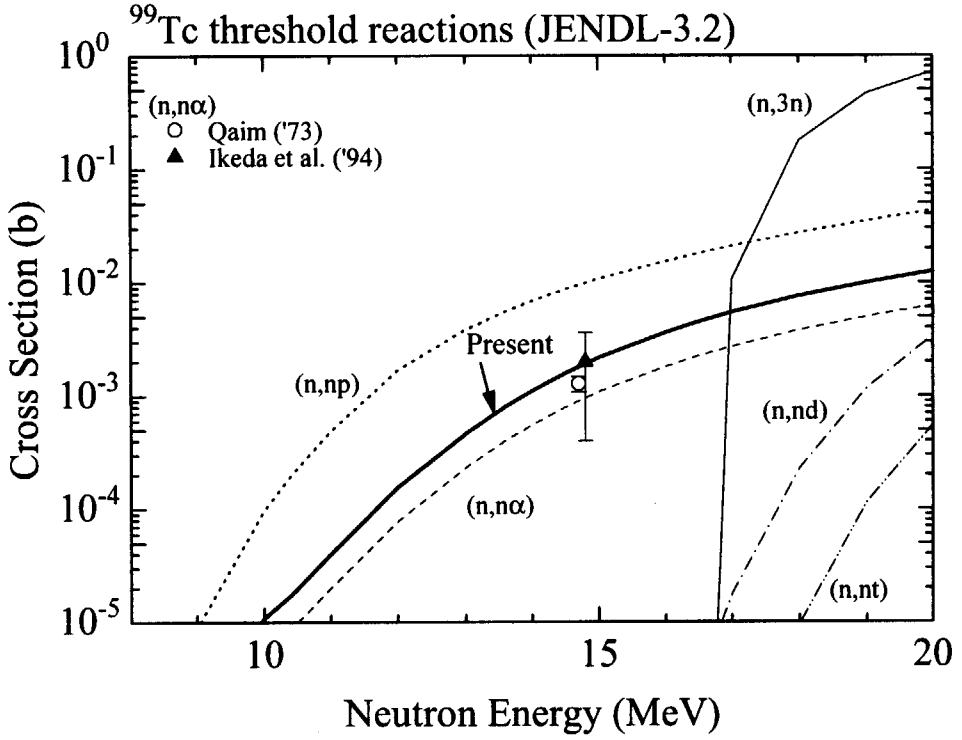

Fig. 4.9 ^{99}Tc(n,3n), (n,np), (n,nα), (n,nd) and (n,nt) reaction cross sections
Experimental data: Qaim('73)[Qa73], Ikeda et al.('94)[Ik94]

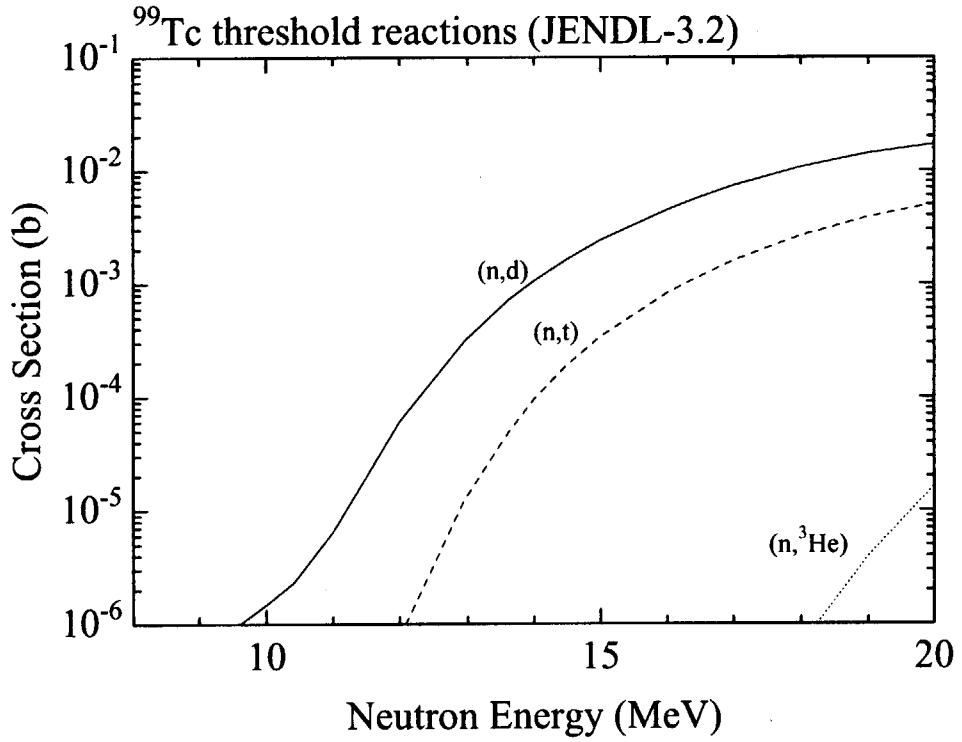

Fig. 4.10 ^{99}Tc(n,d), (n,t) and (n,^{3}He) reaction cross sections

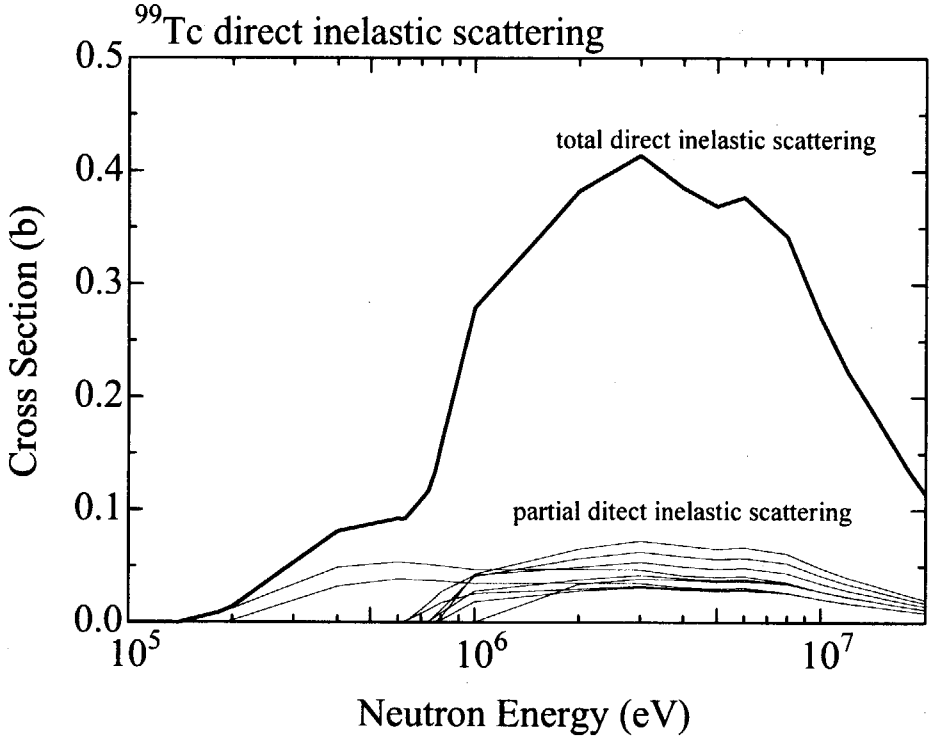

Fig. 4.11 ^{99}Tc direct inelastic scattering cross sections

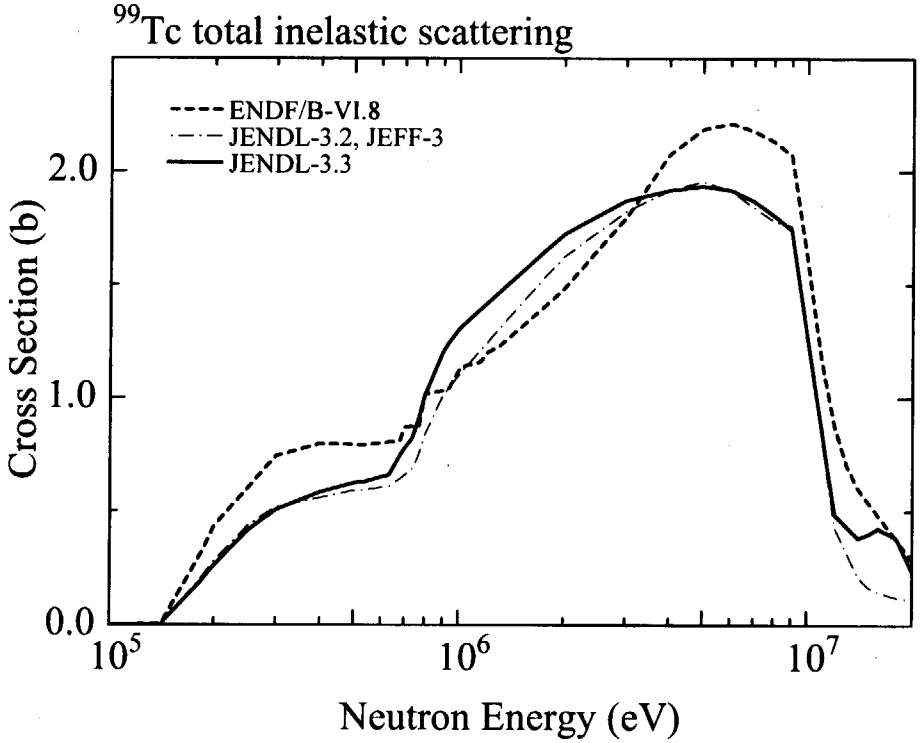

Fig. 4.12 ^{99}Tc total inelastic scattering cross sections

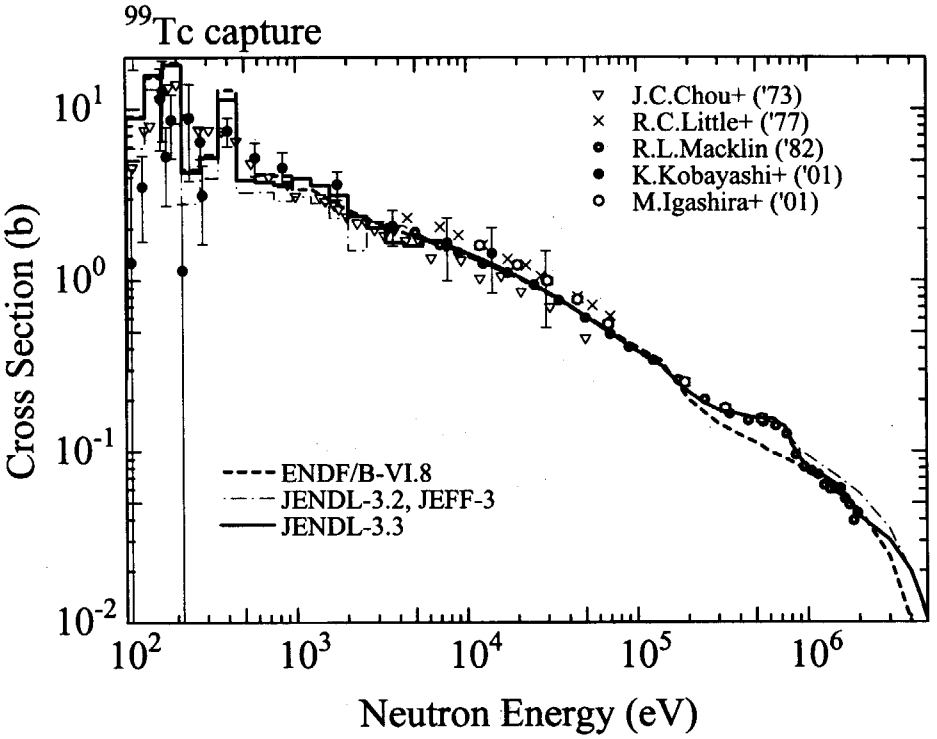

Fig. 4.13 ^{99}Tc capture cross section (100 eV – 5 MeV)
Experimental data: Chou+('73)[Ch73], Little+('77)[Li77], Macklin ('82)[Ma82], Kobayashi+('01)[Ko01], Igashira+('01)[Ig01]

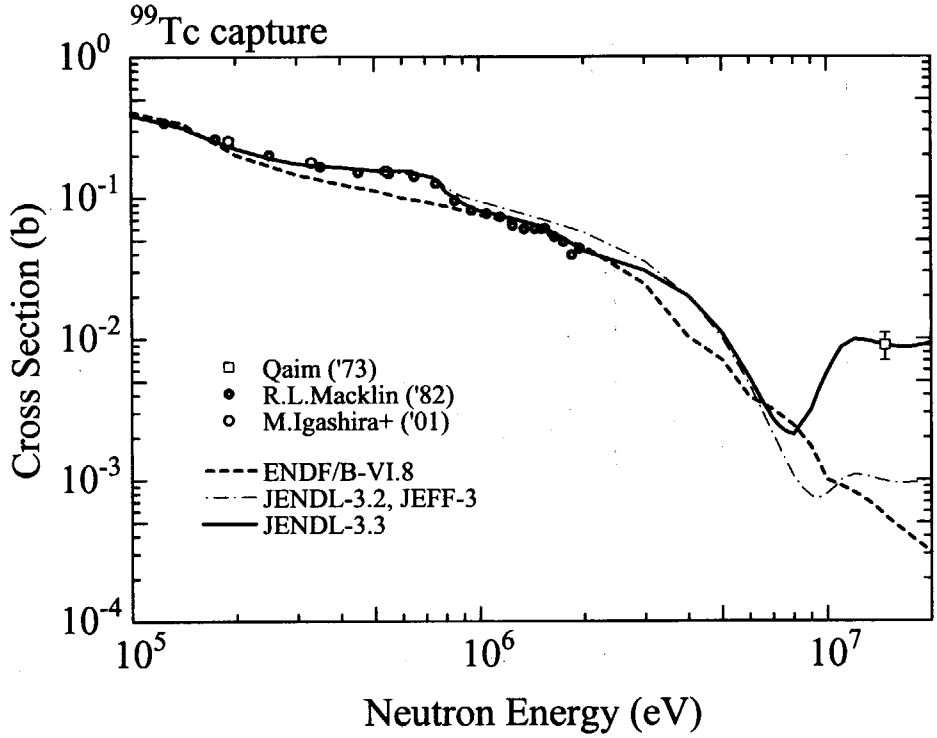

Fig. 4.14 ^{99}Tc capture cross section (100 keV – 20 MeV)
Experimental data: see Fig. 4.13.

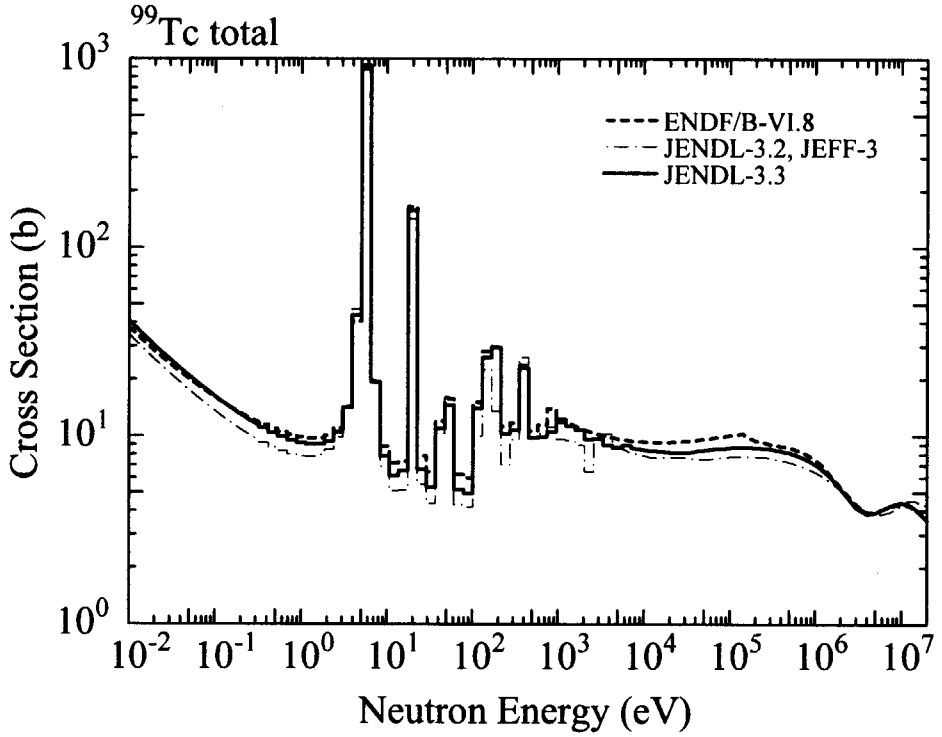

Fig. 4.15 ^{99}Tc total cross section (thermal – 20 MeV)

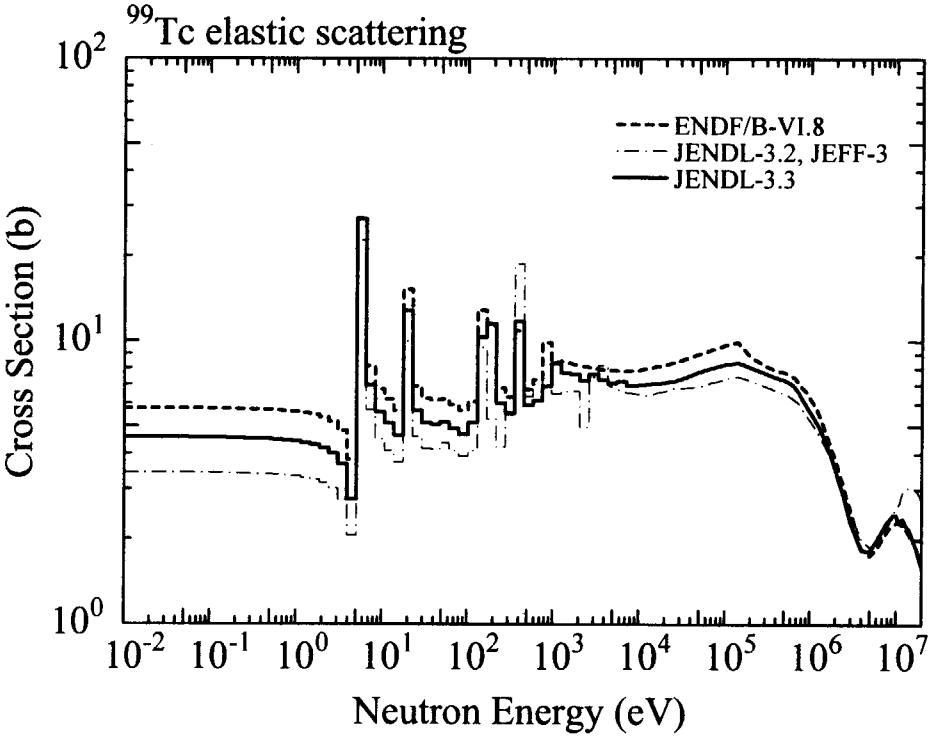

Fig. 4.16 ^{99}Tc elastic scattering cross section (thermal – 20 MeV)

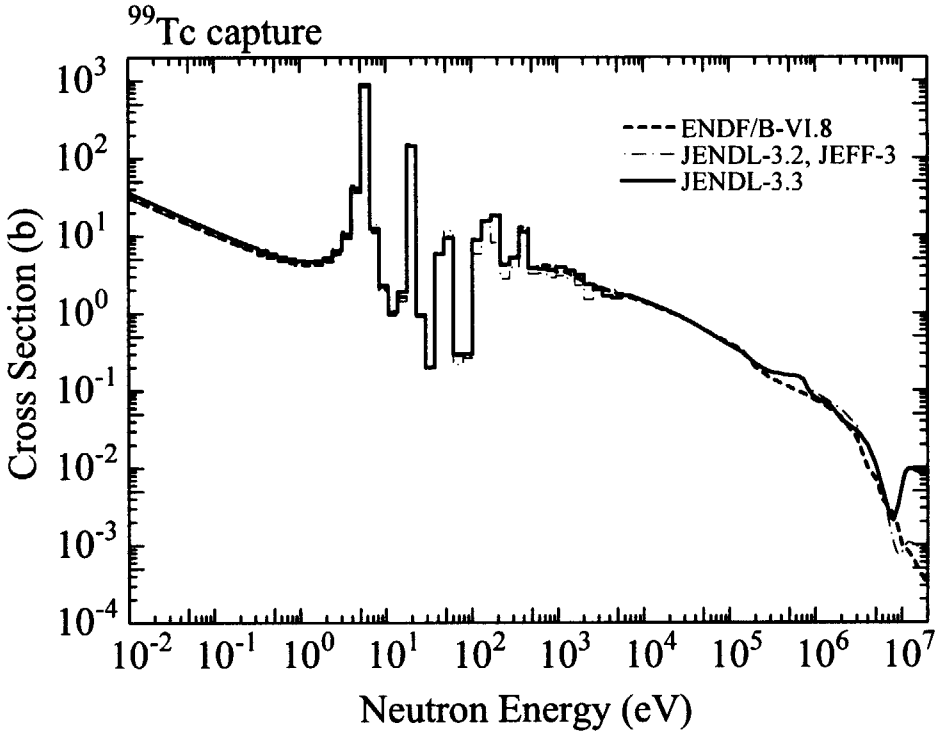

Fig. 4.17 ^{99}Tc capture cross section (thermal – 20 MeV)

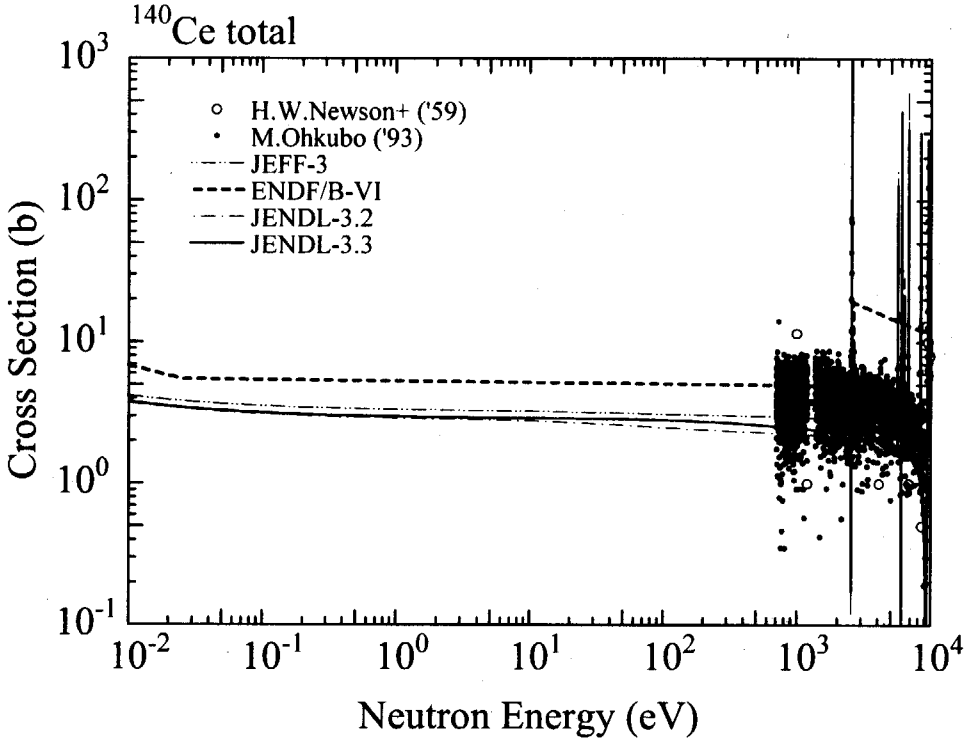

Fig. 5.1(a) ^{140}Ce total cross section (below 10 keV)
Experimental data: Newson+('59)[Ne59], Ohkubo('93)[Oh93]

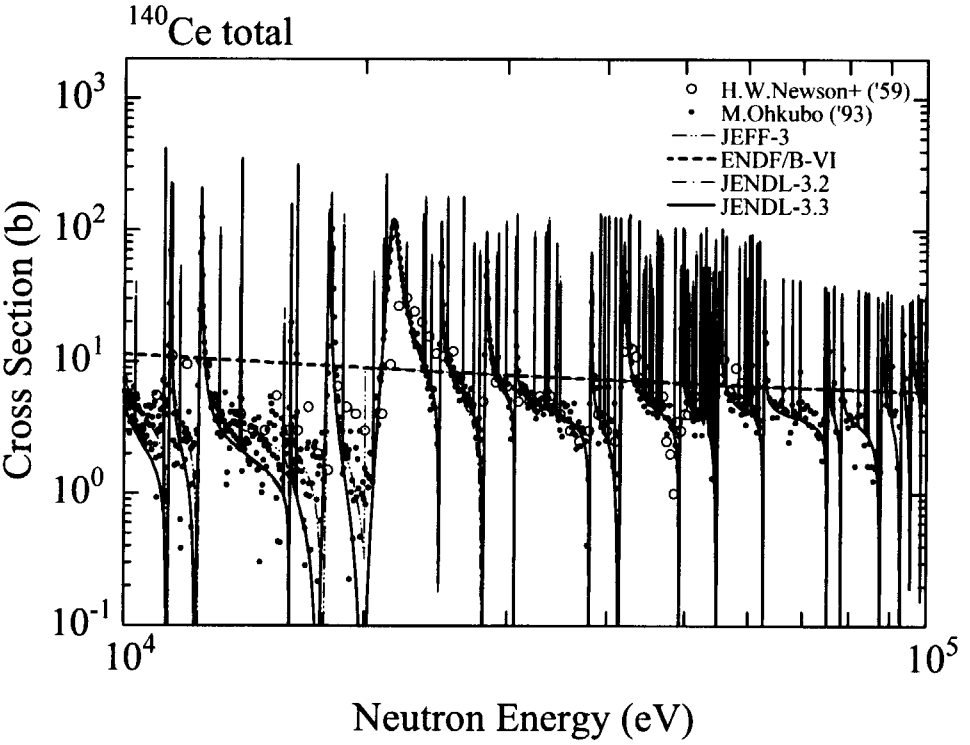

Fig. 5.1(b) ^{140}Ce total cross section (below 10 keV)
Experimental data: Newson+('59)[Ne59], Ohkubo('93)[Oh93]

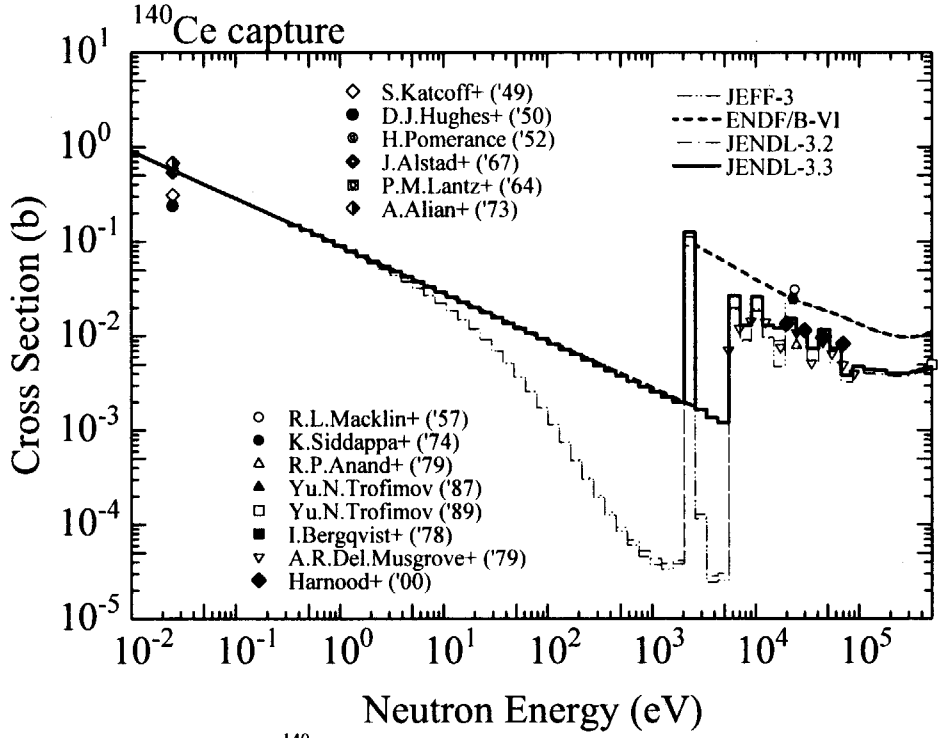

Fig. 5.2 ^{140}Ce capture cross section (below 500 keV)

Experimental data: Katcoff+('49)[Ka49], Hughes+('50)[Hu50], Pomerance('52)[Po52], Alstad+('67)[Al67], Lantz+('64)[La64], Alian+('73)[Al73], Macklin+('57)[Ma57], Siddappa+('74)[Si74b], Anand+('79)[An79], Trofimov('87)[Tr87], Trofimov('89)[Tr89], Bergqvist+('78)[Be78], Musgrove+('79)[Mu79], Harnood+('00)[Ha00]

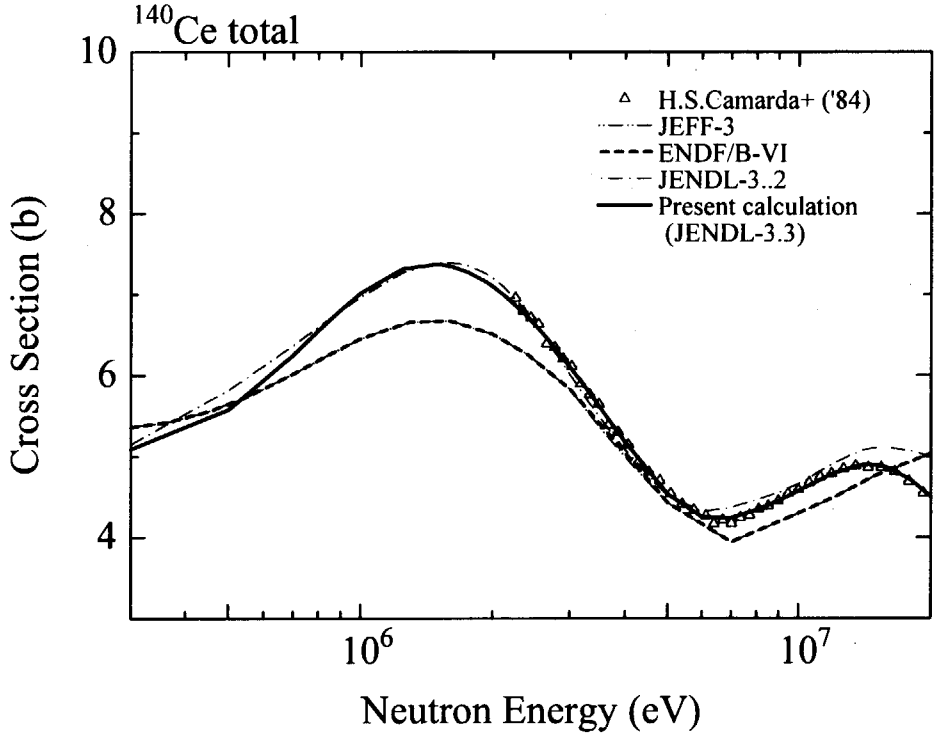

Fig. 5.3 ^{140}Ce total cross section (above 300 keV)

Experimental data: Camarda+('84)[Ca84]

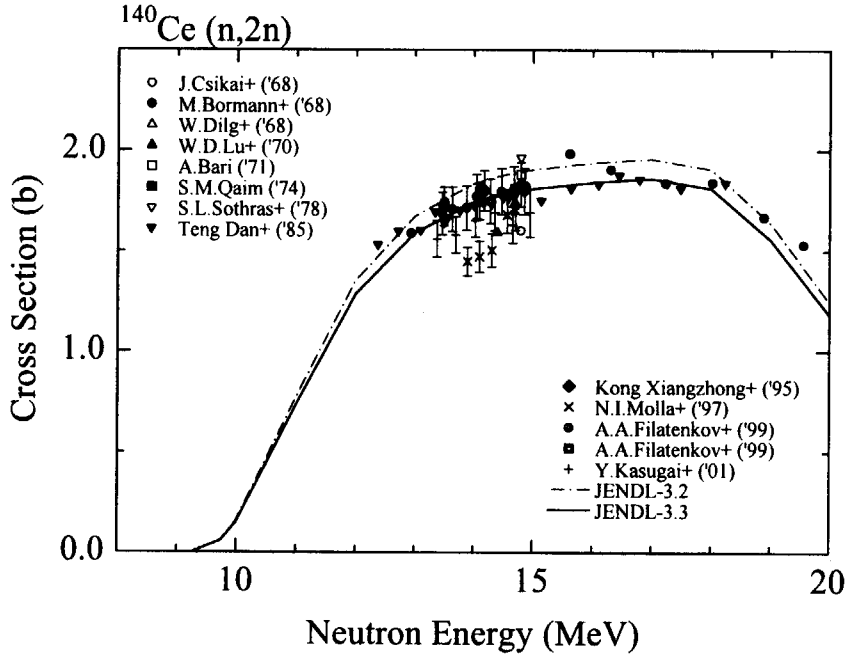

Fig. 5.4 ^{140}Ce(n,2n) reaction cross section
Experimental data: Csikai+(68)[Cs68], Bormann+('68)[Bo68b], Dilg+('68)[Di68], Lu+('70)[Lu70a], Bari+('71)[Ba71], Qaim('74)[Qa74], Sothras+('78)[So78], Teng+('85)[Te85] Kong+('95)[Ko95], Molla+('97)[Mo97], Filatenkov+('99)[Fi99],Kasugai+('01)[Ka01c]

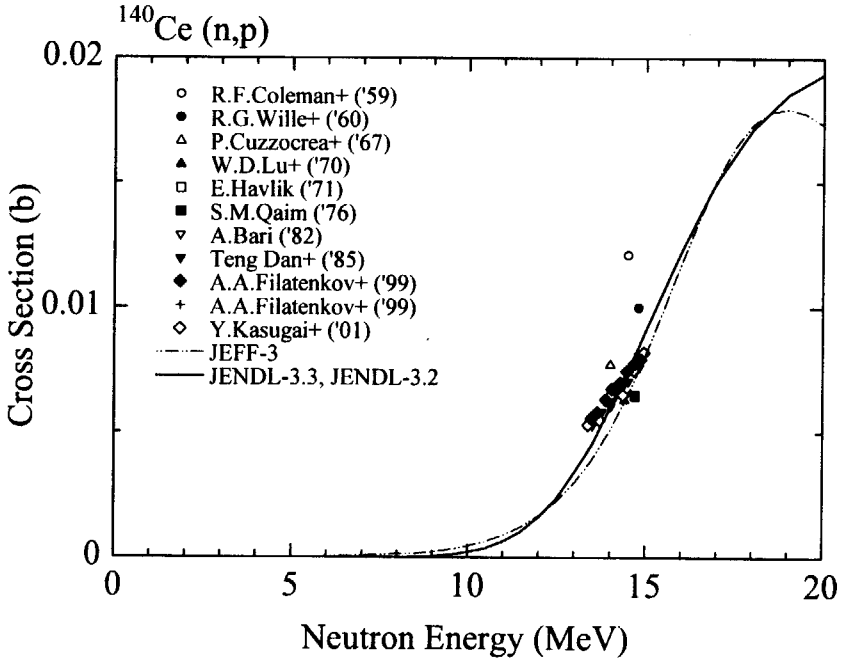

Fig. 5.5 ^{140}Ce(n,p) reaction cross section
Experimental data: Coleman+('59)[Co59b], Wille+('60)[Wi60], Cuzzocrea+('67)[Cu67], Lu+('70)[Lu70b], Havlik('71)[Ha71], Qaim('76)[Qa76], Bari('82)[Ba82], Teng+('85)[Te85], Filatenkov+('99)[Fi99],Kasugai+('01)[Ka01c]

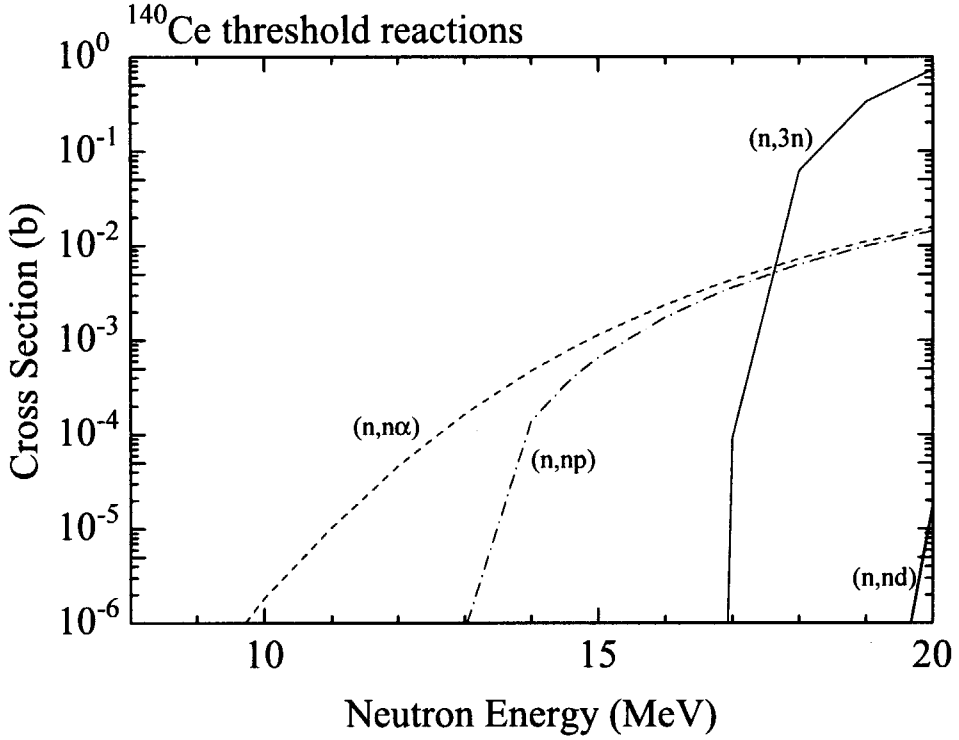

Fig. 5.6 ^{140}Ce(n,3n), (n,np), (n,nα) and (n,nd) reaction cross sections

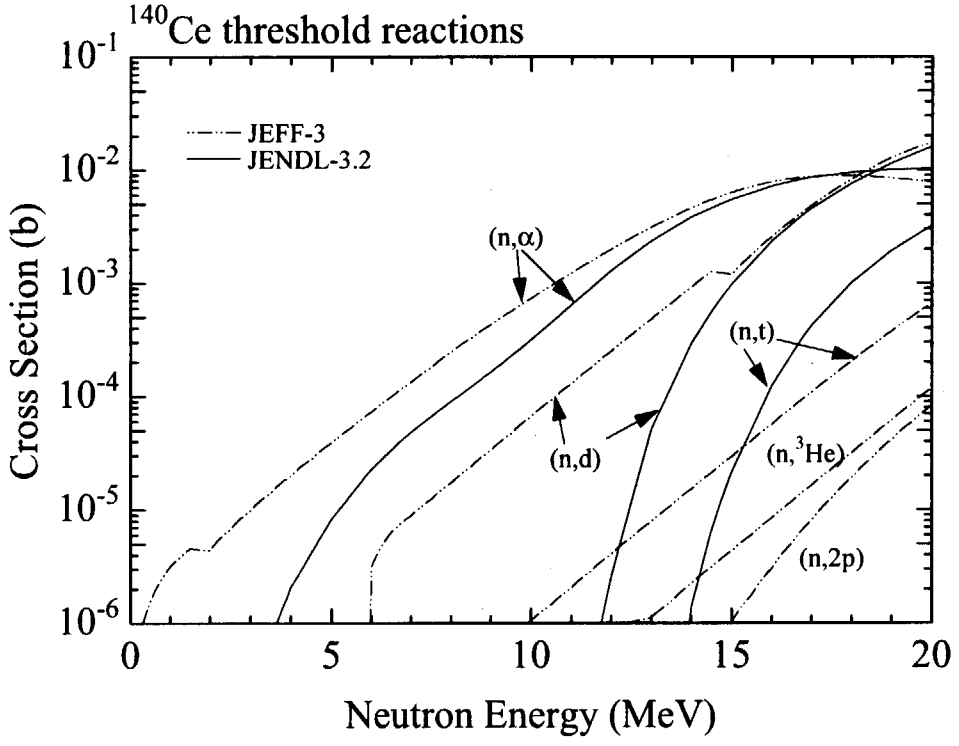

Fig. 5.7 ^{140}Ce(n,α), (n,d), (n,t), (n,^{3}He) and (n,2p) reaction cross sections

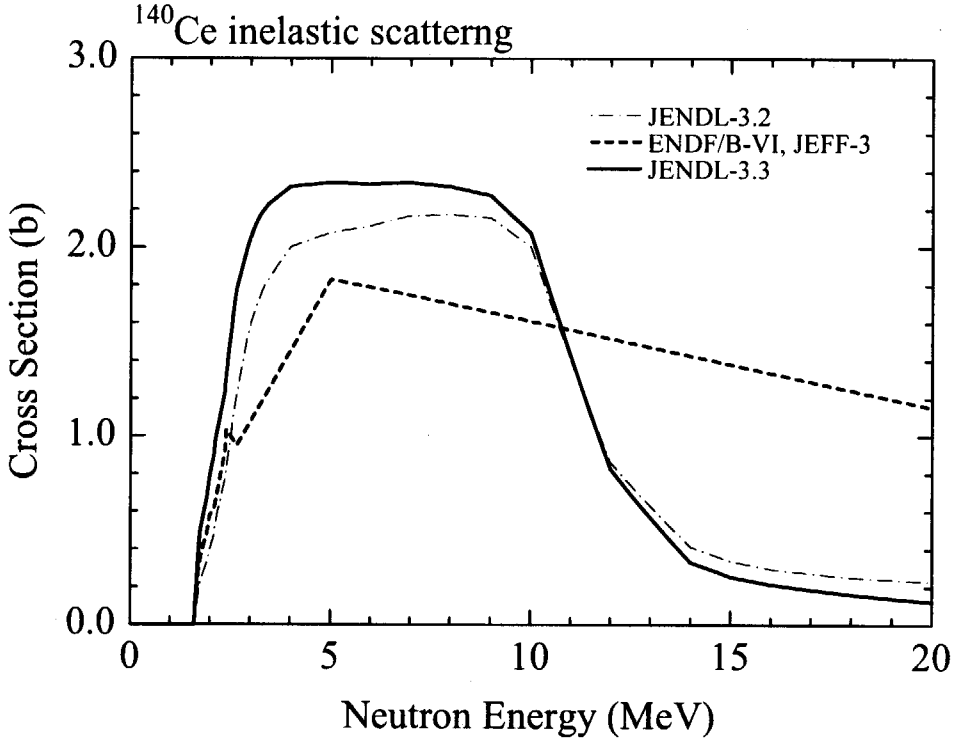

Fig. 5.8 ^{140}Ce total inelastic scattering cross section

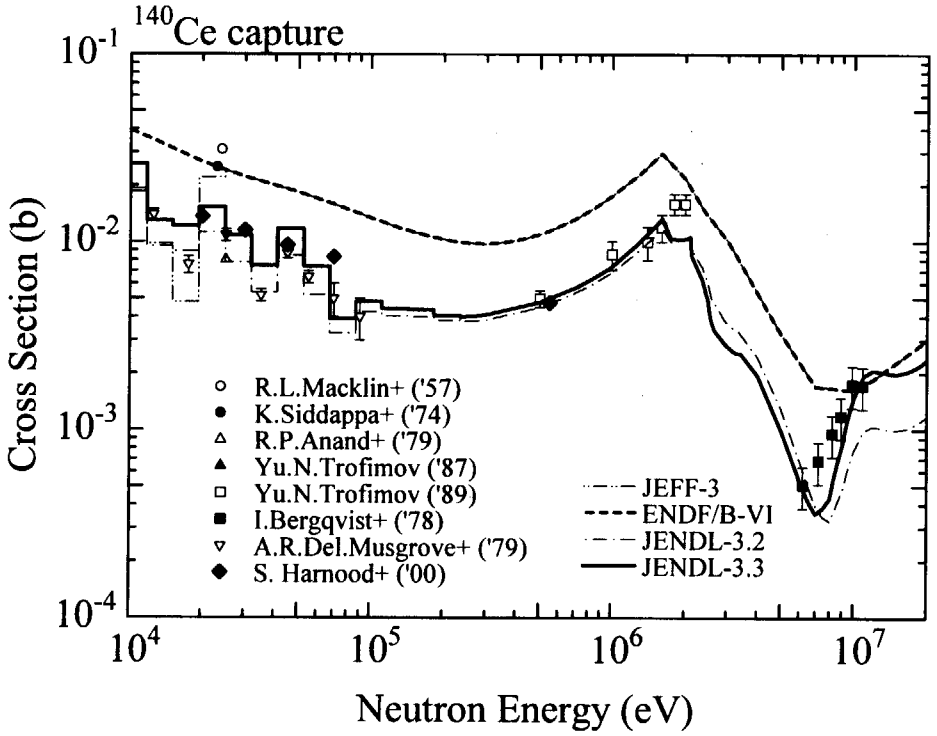

Fig. 5.9 ^{140}Ce capture cross section (above 10 keV)
Experimental data: Macklin+('57)[Ma57], Siddappa+('74)[Si74b], Anand+('79)[An79], Trofimov('87)[Tr87], Trofimov('89)[Tr89], Bergqvist+('78)[Be78], Musgrove+('79)[Mu79], Harnood+('00)[Ha00]

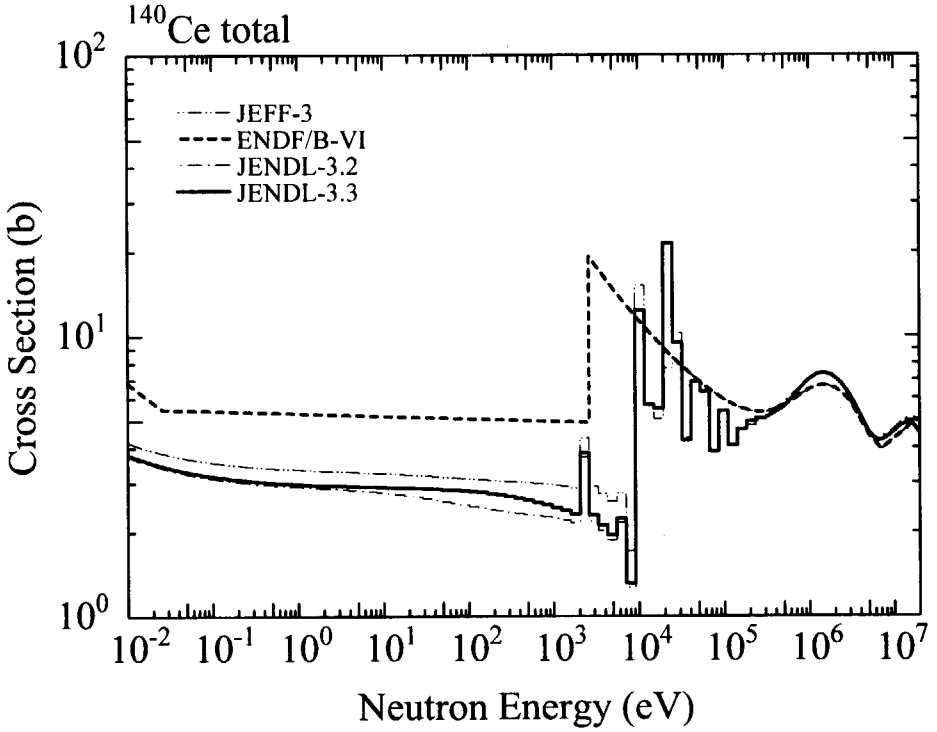

Fig. 5.10 ^{140}Ce total cross section (thermal energy – 20 MeV)

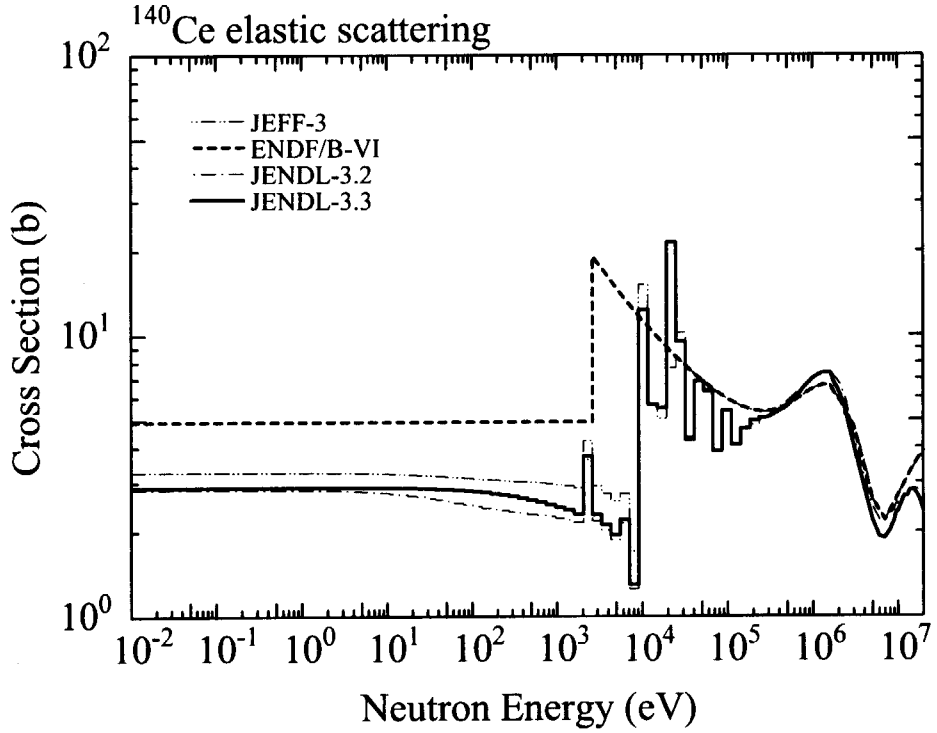

Fig. 5.11 ^{140}Ce elastic scattering cross section (thermal energy – 20 MeV)

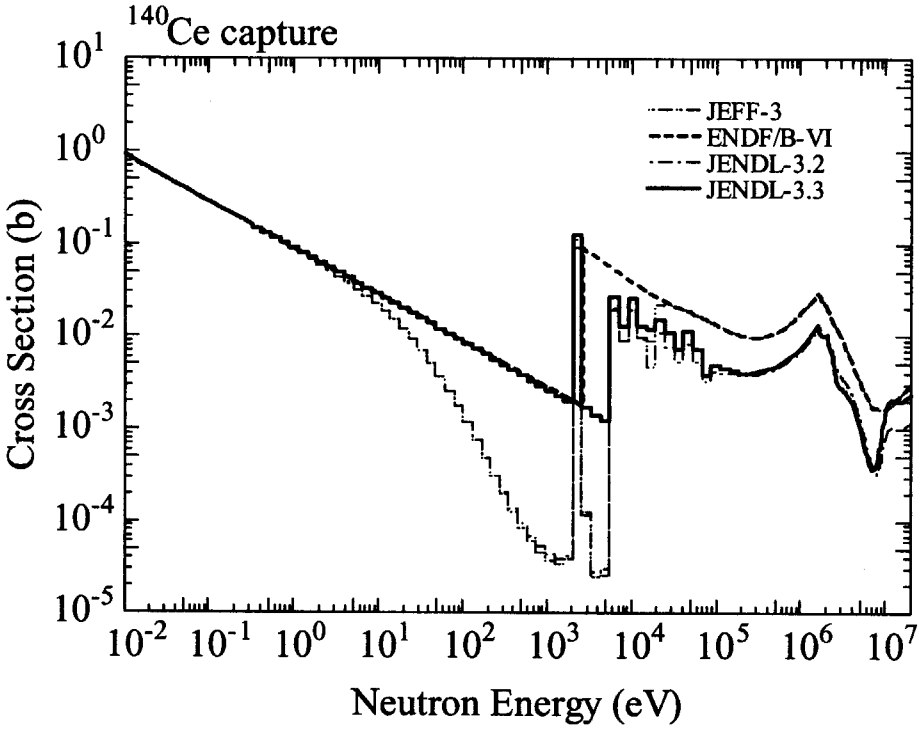

Fig. 5.12 ^{140}Ce capture cross section (thermal energy – 20 MeV)

国際単位系（SI）と換算表

表1　SI基本単位および補助単位

量	名称	記号
長さ	メートル	m
質量	キログラム	kg
時間	秒	s
電流	アンペア	A
熱力学温度	ケルビン	K
物質量	モル	mol
光度	カンデラ	cd
平面角	ラジアン	rad
立体角	ステラジアン	sr

表2　SIと併用される単位

名称	記号
分，時，日	min，h，d
度，分，秒	°，′，″
リットル	l，L
トン	t
電子ボルト	eV
原子質量単位	u

1 eV=1.60218×10^{-19}J

1 u=1.66054×10^{-27}kg

表3　固有の名称をもつSI組立単位

量	名称	記号	他のSI単位による表現
周波数	ヘルツ	Hz	s^{-1}
力	ニュートン	N	$m\cdot kg/s^2$
圧力，応力	パスカル	Pa	N/m^2
エネルギー，仕事，熱量	ジュール	J	N·m
工率，放射束	ワット	W	J/s
電気量，電荷	クーロン	C	A·s
電位，電圧，起電力	ボルト	V	W/A
静電容量	ファラド	F	C/V
電気抵抗	オーム	Ω	V/A
コンダクタンス	ジーメンス	S	A/V
磁束	ウェーバ	Wb	V·s
磁束密度	テスラ	T	Wb/m^2
インダクタンス	ヘンリー	H	Wb/A
セルシウス温度	セルシウス度	℃	
光束	ルーメン	lm	cd·sr
照度	ルクス	lx	lm/m^2
放射能	ベクレル	Bq	s^{-1}
吸収線量	グレイ	Gy	J/kg
線量等量	シーベルト	Sv	J/kg

表4　SIと共に暫定的に維持される単位

名称	記号
オングストローム	Å
バーン	b
バール	bar
ガル	Gal
キュリー	Ci
レントゲン	R
ラド	rad
レム	rem

1 Å=0.1nm=10^{-10}m

1 b=100fm^2=10^{-28}m^2

1 bar=0.1MPa=10^{5}Pa

1 Gal=1cm/s^2=10^{-2}m/s^2

1 Ci=3.7×10^{10}Bq

1 R=2.58×10^{-4}C/kg

1 rad=1cGy=10^{-2}Gy

1 rem=1cSv=10^{-2}Sv

表5　SI接頭語

倍数	接頭語	記号
10^{18}	エクサ	E
10^{15}	ペタ	P
10^{12}	テラ	T
10^{9}	ギガ	G
10^{6}	メガ	M
10^{3}	キロ	k
10^{2}	ヘクト	h
10^{1}	デカ	da
10^{-1}	デシ	d
10^{-2}	センチ	c
10^{-3}	ミリ	m
10^{-6}	マイクロ	μ
10^{-9}	ナノ	n
10^{-12}	ピコ	p
10^{-15}	フェムト	f
10^{-18}	アト	a

（注）

1．表1－5は「国際単位系」第5版，国際度量衡局1985年刊行による。ただし，1 eVおよび1 uの値はCODATAの1986年推奨値によった。

2．表4には海里，ノット，アール，ヘクタールも含まれているが日常の単位なのでここでは省略した。

3．barは，JISでは流体の圧力を表わす場合に限り表2のカテゴリーに分類されている。

4．EC閣僚理事会指令ではbar，barnおよび「血圧の単位」mmHgを表2のカテゴリーに入れている。

換算表

力

N(=10^{5}dyn)	kgf	lbf
1	0.101972	0.224809
9.80665	1	2.20462
4.44822	0.453592	1

粘度　1 Pa·s(N·s/m^2)=10 P(ポアズ)(g/(cm·s))

動粘度　1m^2/s=10^{4}St(ストークス)(cm^2/s)

圧力

MPa(=10bar)	kgf/cm^2	atm	mmHg(Torr)	lbf/in^2(psi)
1	10.1972	9.86923	7.50062×10^3	145.038
0.0980665	1	0.967841	735.559	14.2233
0.101325	1.03323	1	760	14.6959
1.33322×10^{-4}	1.35951×10^{-3}	1.31579×10^{-3}	1	1.93368×10^{-2}
6.89476×10^{-3}	7.03070×10^{-2}	6.80460×10^{-2}	51.7149	1

エネルギー・仕事・熱量

J(=10^7 erg)	kgf·m	kW·h	cal(計量法)	Btu	ft·lbf	eV
1	0.101972	2.77778×10^{-7}	0.238889	9.47813×10^{-4}	0.737562	6.24150×10^{18}
9.80665	1	2.72407×10^{-6}	2.34270	9.29487×10^{-3}	7.23301	6.12082×10^{19}
3.6×10^6	3.67098×10^5	1	8.59999×10^5	3412.13	2.65522×10^6	2.24694×10^{25}
4.18605	0.426858	1.16279×10^{-6}	1	3.96759×10^{-3}	3.08747	2.61272×10^{19}
1055.06	107.586	2.93072×10^{-4}	252.042	1	778.172	6.58515×10^{21}
1.35582	0.138255	3.76616×10^{-7}	0.323890	1.28506×10^{-3}	1	8.46233×10^{18}
1.60218×10^{-19}	1.63377×10^{-20}	4.45050×10^{-26}	3.82743×10^{-20}	1.51857×10^{-22}	1.18171×10^{-19}	1

1 cal= 4.18605J（計量法）

= 4.184J（熱化学）

= 4.1855J（15℃）

= 4.1868J（国際蒸気表）

仕事率　1 PS(仏馬力)

= 75 kgf·m/s

= 735.499W

放射能

Bq	Ci
1	2.70270×10^{-11}
3.7×10^{10}	1

吸収線量

Gy	rad
1	100
0.01	1

照射線量

C/kg	R
1	3876
2.58×10^{-4}	1

線量当量

Sv	rem
1	100
0.01	1

（86年12月26日現在）

Re-evaluation of Neutron Nuclear Data for ^{242m}Am, ^{243}Am, ^{99}Tc and ^{140}Ce